

Computer Analysis of Left Ventricular Cineangiograms

PROEFSCHRIFT

TER VERKRIJGING VAN DE GRAAD VAN DOCTOR IN DE
GENEESKUNDE
AAN DE ERASMUS UNIVERSITEIT ROTTERDAM
OP GEZAG VAN DE RECTOR MAGNIFICUS
PROF. DR. J. SPERNA WEILAND
EN
VOLGENS BESLUIT VAN HET COLLEGE VAN DEKANEN

DE OPENBARE VERDEDIGING ZAL PLAATSVINDEN OP
WOENSDAG, 14 APRIL 1982, DES NAMIDDAGS
TE 3.45 UUR

DOOR

TON ERIC HILCO HOOGHOUT
GEBOREN TE AMSTERDAM

Promotor: Prof. P.G. Hugenholtz.

Co-referenten: Prof. Dr. G. Hennemann
Prof. Dr. Ir. J. Davidse.

Publication of this thesis was supported by The Dutch Heart Foundation

To Ria,

To my parents.

CONTENTS

	page
Chapter I	Introduction 1
Chapter IIa	Overview and summary of this thesis 3
Chapter IIb	Overzicht en samenvatting van dit proefschrift 5
Chapter III	A review of the relevant literature 7
Chapter IVa	Endocardial landmark motion; a new approach to the assessment of regional left ventricular performance. Slager C.J., Hooghoudt T.E.H., Reiber J.H.C., Schuurbiens J.C.H., Verdouw P.D., Hugenholtz P.G. (submitted for publication in <i>Circulation Research</i>) 30
Chapter IVb	Left ventricular contour segmentation from anatomical landmark trajectories and its application to wall motion analysis. Slager C.J., Hooghoudt T.E.H., Reiber J.H.C., Schuurbiens J.C.H., Booman F., Meester G.T. <i>Computers in Cardiology</i> , pp. 347-350, IEEE Computer Society, Long Beach, California, 1979 50
Chapter V	Quantitative assessment of regional pump- and contractile function. Part I: The normal human heart. Hooghoudt T.E.H., Slager C.J., Reiber J.H.C., Schuurbiens J.C.H., Meester G.T., Hugenholtz P.G. (material contained in this chapter has been submitted in a modified form to <i>Am. J. Cardiol.</i>) 59
Chapter VI	Quantitative assessment of regional pump- and contractile function. Part II: Changes in regional wall motion and pump function induced by pacing in patients with coronary artery disease. Hooghoudt T.E.H., Serruys P.W., Slager C.J., Reiber J.H.C., Schuurbiens J.C.H., Meester G.T., Hugenholtz P.G. (material contained in this chapter has been submitted in a modified form to <i>Am. J. Cardiol.</i>) 82

Chapter VII	Regional contribution to ejection fraction used to assess the applicability of a new wall motion model to the detection of regional wall motion in patients with asynergy. Hooghoudt T.E.H., Slager C.J., Reiber J.H.C., Serruys P.W., Schuurbiens J.C.H., Meester G.T. Computers in Cardiology, pp. 253-256, IEEE Computer Society, Long Beach, California, 1980	90
Chapter VIII	Observer variability in the visual assessment of regional wall motion and in computer assisted analysis of regional left ventricular function. Hooghoudt T.E.H., Slager C.J., Reiber J.H.C., Brower R.W., Castellanos S., Zorn I.C.J., Hugenholtz P.G.	98
Chapter IX	Influence of intracoronary nifedipine on left ventricular function, coronary vasomotility and myocardial oxygen consumption. Serruys P.W., Hooghoudt T.E.H., Reiber J.H.C., Slager C.J., Brower R.W., Hugenholtz P.G. (submitted for publication in Am. J. Cardiol.)	111
Chapter X	Recanalization of the occluded coronary artery in patients with acute myocardial infarction: influence on left ventricular function. Hooghoudt T.E.H., Serruys P.W., Reiber J.H.C., Slager C.J., Van den Brand M. (material contained in this chapter has been submitted in a modified form to Am. J. Cardiol.)	141
	Curriculum vitae	151

ACKNOWLEDGEMENTS

Many people contributed to the development and evaluation of the automated regional left ventricular function analysis system, which is the subject of this thesis. First of all I am grateful to Prof. P.G. Hugenholtz, who enabled me to work in the stimulating atmosphere of the Thoraxcenter, supported this project and reviewed the text. Prof. Dr. G.T. Meester, who is auctor intellectualis of the system, interested me for this research project, and was a great source of support in many hours of criticism and discussion. I won't forget the help of M. van den Brand and P.W. Serruys, who as chiefs of the cardiac catheterization laboratory, enabled me to gain experience in angiocardiology, and gave all support to make the production of this thesis possible. My deepest thanks go to Ir C.J. Slager and Ir J.H.C. Reiber Ph.D., who created the hardware of the contour detector and with whose close cooperation the philosophy of the application of the system in clinical practice was developed. J.H.C. Reiber developed the software of the analysis system, while J.C.H. Schuurbijs B.Sc. analyzed many of the angiograms used in this study. The assistance and support of Miss I.C.J. Zorn, of Mr. J. Tuin, and of many other members of the technical and paramedical staff of the "cath. lab." was most appreciated. Dr. P.D. Verdouw enabled us to perform the animal experiments. A special recognition goes to A.J.W. van der Does for typing this manuscript. Most grateful I am to my wife Ria, whose continuous support in many ways, has enabled me to execute my plans. Finally I want to thank my family and friends, who as consequence of this work have had less attention than they deserved.

CHAPTER I

INTRODUCTION

The heart is in continuous and rhythmic motion. For centuries this unique property has fascinated clinicians and scientists, although their attempts to get a better insight in the mechanisms which govern heart wall motion were seriously hampered by the almost complete absence of effective measurement tools.

A dramatic change took place in the course of this century thanks to the technological revolution which changed cardiology more than any other of the biomedical sciences. The introduction of roentgen rays into medical practice enabled physicians for the first time to observe the beating heart in the intact human being. In cases of myocardial infarction, assessed by the new electrocardiographic technique, the fluoroscopy screen revealed abnormal motion of the epicardial contour. Numerous tools and methods were designed and developed to preclude the subjectivity and inaccuracy inherent with naked eye observation of heart wall motion. However, as only the epicardial contour could be determined, the information thus obtained remained limited. In 1929 Forssman introduced a catheter into his right heart. This act set the pace for the development of angiocardiology which after a hesitating start became one of the fastest growing areas in the medical field. As a consequence of the rapidly increasing number of cardiac catheterizations paralleled by an explosive growth of the amount of data obtained during each procedure, automated data processing became indispensable.

In 1967 cardiologists of Stanford University in Palo Alto, California, described their first experiences with the use of a computing device in the cardiac catheterization procedure. This example was soon followed by cardiologists and technicians of the Thoraxcenter who developed a computer system, tailored to their catheterization laboratory, which became operative in 1973 and comprised facilities to process pressure signals on line and under control of the operator. To pursue the automation of data processing in the catheterization laboratory two more systems had to be developed: a system to detect automatically coronary artery contours and an analysis system for left ventriculograms. For this automated detection of the left ventricular endocardial contour from cineangiograms, a hard-wired system was designed and constructed. It was called the 'Contouromat'.

The aim of this thesis is to describe work to evaluate and validate this tool and its applicability in clinical practice and research. The first question which

arises is whether an automated angio processing system has any benefit. Indeed in some clinics left ventriculograms continue to be judged in a purely qualitative way, although Herman et al's semiquantitative classification into normo-, hypo-, and dyskinesia is now applied in most centers. Since the angiogram contains more information than the human eye can detect by simple inspection, and the human observation often is inaccurate and inconsistent and strongly dependent upon the experience of the observer, there is much to be said for some form of standardization. The same applies to hand-drawn contours from end diastolic and end systolic cineframes which are currently employed to quantify the respective volumes. In conclusion, a well designed angioprocessing system which produces consistent and reproducible quantitative data at a rate man cannot match, may help us to manage the diagnostic problems of our patients, whose interest — in spite of all emphasis on the technical tool we use — remains the primary aim of our efforts.

CHAPTER IIa

AN OVERVIEW AND SUMMARY OF THIS THESIS.

In this thesis a computer assisted system for quantitative frame by frame analysis of left ventricular cineangiograms is described. The concept of automated detection of the left ventricular endocardial border in the contrast angiogram, as part of the computer system which assists in data processing in the cardiac catheterization laboratory, is introduced in chapter I. The summary of this thesis is contained in chapter II. In chapter III a choice of the literature which is relevant to this thesis is reviewed. The development of the study of heart wall motion, of angiocardiography and of computer systems which can detect endocardial wall motion is described. The various methods to study regional left ventricular wall motion and the techniques to assess global left ventricular function from pressure signals are discussed as well.

New information which came forth from the study of endocardial contours in humans and in pigs, and the inadequacy of current methods to assess regional wall motion, stimulated us to develop a method to study left ventricular wall motion which relies on the pattern of endocardial wall motion in normal individuals. In chapter IV the development of this method, which is implemented in the regional function analysis system, is dealt with. A description of this system and of the normal range of the computed parameters (displacement, velocity, regional ejection fraction) can be found in chapter V. Furthermore in this chapter the regional contribution to global ejection fraction or CREF, a new regional pump function parameter, is introduced. Also the normal sequence of contraction and relaxation is described.

The applicability of the method to assess regional wall motion in patients with abnormal contracting and malformed ventricles is evaluated in chapter VI. The stress of tachycardia is used to provoke additional asynergy in 12 patients with coronary artery disease. Although the majority of the ventricles are severely asynergic, the results suggest that even then regional wall motion data can be accurately computed with this method. The variability of the analysis system is tested in chapters VII and VIII. In chapter VII manual and automated assessment of global ejection fraction are compared and the relation between global ejection fraction and the sum of CREF values is studied. Both show a good correlation. The variability in appraisal of regional wall motion by simple visual inspection and the inter- and intra-observer variability of the assessment of regional function with the computer assisted analysis system,

have been further investigated in chapter VIII. The relation between quantitative determination of regional function and the results of visual reading of regional wall motion is studied as well. It is concluded that visual inspection of left ventricular performance is variable and thus liable to introduce error, while automated assessment of regional function is reproducible and from this point of view preferable.

The application of the analysis system to clinical research is demonstrated in chapters IX and X. Intracoronary injection of nifedipine – a powerful calcium antagonist – has profound effects on regional left ventricular function: it delays, prolongs, slows and depresses segmental contraction. It is shown that such a complex phenomenon can be studied with this system as it provides facilities for quantitative frame by frame analysis of regional wall motion and ventricular function. In chapter X the effect of recanalization of an occluded coronary artery on regional left ventricular function is studied in patients with acute myocardial infarction. It appears that quantitative analysis of regional left ventricular function is essential to study the possible therapeutic value of streptokinase intervention. Taken together, this thesis gives an impression of the development, evaluation and application of a regional left ventricular function analysis system which is currently employed at the Thoraxcenter. It is felt that such a system provides accurate and detailed information which is not available to the cardiologist who relies on visual inspection of the angiogram.

HOOFDSTUK IIb

SAMENVATTING EN OVERZICHT VAN DIT PROEFSCHRIFT.

In dit proefschrift wordt een systeem beschreven, dat met behulp van een computer films van de linker hartkamer, zoals die tijdens hartcatheterisatie worden gemaakt, op kwantitatieve wijze analyseert. Dit systeem, dat bestaat uit een elektronische schakeling die de endocardiale grens in het linker kamer angiogram zelfstandig herkent, en die verbonden is met een computer voor verdere verwerking van de gegevens, wordt in hoofdstuk I geïntroduceerd. In hoofdstuk II wordt een overzicht van dit proefschrift gegeven. In hoofdstuk III wordt een deel van de literatuur die op dit proefschrift betrekking heeft behandeld. Ondermeer komen de ontwikkeling van de angiocardiografie en van systemen die zelfstandig de beweging van de binnenste hartkamer grens op het angiogram kunnen waarnemen, aan de orde. Ook worden verschillende methoden waarmee men de regionale beweging van de linker kamerwand kan bestuderen, alsmede technieken waarmee de werking van de linker kamer uit drukmetingen bepaald kan worden, besproken.

Nieuwe gegevens die voortkwamen uit de bestudering van de beweging van endocardiale structuren bij mensen en biggen en de twijfelachtige waarde van de beschikbare methoden om de wandbeweging van de linker hartkamer te bestuderen, deden ons een methode voor het meten van de wandbeweging ontwikkelen, die gebaseerd is op het feitelijke bewegingspatroon van de wand bij normale personen. De ontwikkeling van deze methode, die toegepast wordt in het systeem dat de regionale hartwerking analyseert, wordt in hoofdstuk IV behandeld.

Een beschrijving van dit systeem, alsmede de normale waarden zoals die bepaald zijn voor regionale wandverplaatsing, wandsnelheid en regionale ejectie fractie, kan men in hoofdstuk V vinden. Tevens wordt in dit hoofdstuk de regionale bijdrage aan de ejectie fractie (CREF) — een nieuwe maat voor regionale pompfunctie — geïntroduceerd. Voorts wordt hier de normale volgorde van samentrekken en ontspannen van verschillende delen van de linker kamer beschreven.

In hoofdstuk VI wordt onderzocht of de methode die gebruikt wordt om de regionale wandbeweging vast te stellen — en die uitgaat van waarnemingen bij normale personen — ook toepasbaar is bij patienten met abnormaal samentrekkende en misvormde hartkamers. Bij 12 patienten met kransslagader vernauwing worden door de belasting die versnellen van de hartslag teweeg brengt nog meer wandbewegingsstoornissen opgewekt dan bij een rustig hartrithme reeds aanwe-

zig zijn. Ook dan kan de regionale wandbeweging met voornoemde methode nauwkeurig bepaald worden.

De variabiliteit en herhaalbaarheid van het analyse systeem worden in de hoofdstukken VII en VIII onderzocht. De resultaten van berekening van de ejectie fractie met de hand en met de computer komen goed overeen. Ook de ejectie fractie en de som van de CREF-waarden tonen een goede correlatie. In hoofdstuk VIII wordt getoond hoe verschillend twee beoordelaars van een angiogram de regionale wandbeweging met het blote oog inschatten. Tevens wordt hier beschreven welke verschillen de bepaling van de regionale hartwerking met de computer vertoont, indien de waarneming tweemaal door dezelfde onderzoeker, dan wel door twee verschillende onderzoekers wordt gedaan. Daarnaast wordt hier ook het verband tussen kwantitatieve bepaling van de regionale hartwerking en de resultaten van beoordeling van de regionale wandbeweging met het blote oog bestudeerd. De conclusie van dit hoofdstuk luidt dat beoordeling van de hartwerking met het blote oog wisselende resultaten kan opleveren, hetgeen fouten veroorzaakt, terwijl het verrichten van deze bepaling met de computer herhaalbaar is en daarom te prefereren valt.

De toepassing van het analyse systeem in de klinische research wordt in de hoofdstukken IX en X aan de hand van enkele voorbeelden getoond. Inspuiting van nifedipine — een krachtige calciumantagonist — in de linker kransslagader heeft een diep ingrijpend effect op de regionale werking van de linker hartkamer: het doet de samentrekking van de hartspier later beginnen, vertraagt en verlengt deze en maakt ze minder krachtig. Het blijkt dat men zo een ingewikkeld verschijnsel met dit systeem, dankzij de beeld voor beeld analyse van de regionale wandbeweging en hartwerking, goed kan bestuderen. In hoofdstuk X wordt de verandering in de regionale werking van de linker hartkamer, na het weer openen van de afgesloten kransslagader bij patienten met een vers hartinfarct, beschreven. Het blijkt dat voor het bestuderen van de therapeutische waarde van deze behandeling, kwantitatieve analyse van de regionale wandbeweging van wezenlijk belang is.

Samenvattend verschaft deze wijze van analyse van angiogrammen van de linker hartkamer nauwkeurige en gedetailleerde informatie, die de cardioloog die op het blote oog moet vertrouwen moet ontberen.

CHAPTER III

A REVIEW OF THE RELEVANT LITERATURE.

As early as 1698 Chirac (1) described significant changes in myocardial contraction after coronary occlusion. A number of investigators in the 19th century did comparable observations (2, 3), but a detailed description was only given as late as 1935 in the classical work of Tennant and Wiggers (4). With an optical myograph, which translates changes in length of the heart muscle in a curve, they showed clearly that ligation of a coronary artery produces distinct wall motion abnormalities. Initially the curves reflecting the activity of the ischemic myocardium were characterized by a smaller amplitude and a decreased duration of contraction compared to the control state, while after about a minute frankly inverted myograms were observed indicating systolic outward bulging. Prinzmetal (5) documented the motion pattern of ischemic heart muscle in dogs with high speed cinematography. He as well observed that soon after occlusion of the left anterior descending coronary artery the affected myocardium ceased to contract and showed "ballooning" within 10 to 12 beats. At first this phenomenon was confined to a small region near the apex of the left ventricle, but gradually the area became more extensive, after a while involving a considerable portion of the anterior wall. In some cases an early systolic contraction was followed by late systolic bulging.

The early radiologists (6, 7) tried to study heart wall motion in man affected by coronary disease, but were only able to detect severe wall motion disturbances as occur in clear-cut left ventricular aneurysm. Master (8) and his associates further refined the fluoroscopic methods and found reversal of pulsation and impaired pulsation in 73% of 80 patients with an 1 - 72 month old myocardial infarction.

Tools in the study of epicardial wall motion.

To preclude the subjectivity inherent with these observations a number of techniques and tools were developed to analyze the motion of the cardiac silhouette. Roentgenkymography (9), which was one of the first exponents of this development, uses a moveable mask of lead strips alternating with open spaces placed between the X-ray source and the patient. Movement of the lead grid during exposure of the roentgenfilm produces a display of heart wall motion

versus time. This technique was received with great hope but lacked precision and could only display the position of the cardiac border at random points throughout the cardiac cycle, without the possibility to relate the results to ECG or pulse curves. Nevertheless wall motion abnormalities in myocardial infarction were extensively studied with this method (10, 11). Only recently ECG-gated movement of the lead grid was realized (12), which takes one of the major drawbacks away.

In the mid-forties the electrokymograph (13, 14) was developed to analyze the cyclic events of cardiac motion continuously. A photomultiplier tube placed over the heart-border as it was projected on a fluoroscopy screen detected changes in light intensity caused by cardiac motion. The electrical signal so generated was transformed into a graphic recording. Dack (15), Dack and Paley (16) and Luisada (17) described normal and abnormal curves in detail and related the curves to the electrocardiogram, carotid pulse curve and phonocardiogram. In patients with myocardial infarction lack of systolic inward motion and paradoxical motion were shown. Bartley (18) found left ventricular wall motion abnormalities in 72% of patients who had sustained a myocardial infarction. A number of problems are responsible for the failure of this method, though initially promising, to become popular: because the heart border was not recorded directly a lack in linearity and reproducibility occurred as a certain amount of light reaching the centre of the photomultiplier tube emits a different current than the same amount of light striking its periphery (19). Other problems were the inability of the system to give quantitative data and the inadequate frequency response caused by the electronic filter necessary to eliminate the high frequency interference of the roentgenbeam. Recently epicardial photokymography (20), a technique very reminiscent of electrokymography was introduced. A silicon photocell is placed over the epicardial heart-lung border, which is displayed on the videomonitor of a fluoroscopy unit. Motion of the heart border causes a change in electrical current, which is translated into a graph. The same objections that made the electrokymograph impractical may be raised to this apparatus.

The radarkymograph (21), introduced in the late sixties, set the pace for a new development: the use of video-technique in the study of cardiac motion. A videocamera linked to the image intensifier converted the image of the beating heart into videoformat. The image as it is seen on a television screen is composed of a series of horizontal lines with varying light intensity; along each line the changing light intensity is carried by the video-signal as a voltage change. After electrical differentiation a rapid transition from dark to light, which is typical for the heart-lung border, is characterized by a voltage peak. Detection of the changing position of this peak translates cardiac motion into a linear graphic tracing. Studies of the left anterior and lateral heart border showed an abnormal motion pattern in 79% of 56 patients with acute myocardial infarction (22). The system suffered from substantial drawbacks such as the absence of a clearly

visible interface between the left ventricular wall and the diaphragm, which precluded analysis of inferior wall motion. But it was undoubtedly the cost and complexity of the necessary equipment that has limited its use to research laboratories. The same applies to "Vidian" (23), a system which automatically detects the motion of a part of the cardiac border contained in a window on a videoscreen. An electronic device finds the heart-lung border through detection of any signal that exceeds a pre-set intensity threshold.

Lastly, the cardiokymograph, previously termed displacement cardiograph, deserves mention. This device, invented in 1967 (24), but only recently applied to clinical cardiology (25, 26), uses an electromagnetic coil which is part of a high frequency oscillator as its transducer. Motion of any object within the electromagnetic field of this coil changes its inductance and consequently the frequency of the oscillator. When the coil is positioned on the chest wall over the heart, motion of the heart causes a change in oscillator frequency which is converted into a voltage change proportional to the original motion. The method has several limitations (27). First of all the detected wall motion cannot be quantitated and shows a poor reproducibility. Moreover the results are strongly dependent on the position of the subject, the grade of inspiration and the position of the transducer. Lastly, confusion may occur about which part of the heart shows the detected motion pattern, as one is unable to visualize the cardiac structure which is recorded.

Determination of endocardial wall motion.

With the systems described thus far only epicardial wall motion was studied, whereas the motion pattern of the endocardial contour contains indispensable information for the analysis of left ventricular function. At this moment there are three ways to visualise endocardial wall motion: contrast angiography, echocardiography and radionuclide angiography. Echocardiography, based on the principle that pulses of ultrasound are reflected by cardiac structures, permits recording of the position, movement and dimensions of the heart (28-30). Although the method is valuable in the qualitative description of wall motion, technical limitations (31) make it less appropriate for quantitative studies in a significant proportion of patients.

Radionuclide angiography makes use of Technetium 99m-labelled macro-aggregated serum albumin to image the cardiac chambers with a gamma scintillation camera (32). The multiple gated acquisition technique (MUGA) records frames at fixed intervals following the R-wave, and repeats this process over many cardiac cycles. The information is stored in an image memory and can be replayed in a way similar to contrast ventriculography (33). Since tracer is present in all cardiac chambers, overlap may make the borders hard to define. From the data obtained with MUGA left ventricular volume change during the

cardiac cycle and ejection fraction are calculated, which correlate well with the same parameters derived from contrast angiography (34). However, inadequate resolution precludes the accurate quantitative analysis of local wall motion phenomena.

Roentgen contrast angiography.

Contrast angiography is, thanks to its high resolving power, particularly suited to the study of regional wall motion. As was mentioned in the introduction to this thesis, Forssman showed in 1929 that a catheter could be introduced in the human heart without any harm (35). Courmand (36) developed heart catheterization to a clinical useful technique, which was used to determine intracardiac pressures, shunts and valve gradients in congenital and acquired heart disease (37, 38). In 1937 Castellanos (39) visualised the cardiac chambers of children by rapid injection of a radiopaque substance in a peripheral vein. Robb and Steinberg (40) applied the method to adults, but dilution of the contrast medium during its long travel from the antecubital vein to the heart made the quality of these angiocardiograms in most cases very poor. In 1947 Chavez (41) solved this problem by putting "the opaque substance in the place where it is needed". He introduced a 12 - 14 F rubber catheter through the external jugular vein into the right atrium or ventricle and injected 50 - 90 c.c. of a 70 per cent solution of diodrast in 0.75 - 1.0 second. Injection of contrast in the cardiovascular system was shown to be relatively safe and to offer invaluable information about cardiac function. A detailed analysis of volume change and motion pattern of the cardiac chambers was made possible by the introduction of cinefluorography by Rushmer (42-44). After injection of 25 ml of diodrast into the superior caval or right jugular vein of dogs, the circulation of the opacified blood was documented on 16 or 35 mm cinefilm. Examination of the motion picture films led to some interesting conclusions:

- the ventricles fill more rapidly than they empty,
- ventricular emptying is not complete; at end systole about 1/3 of the diastolic volume remains in the ventricle,
- the left ventricular volume is reduced during systole by reduction in diameter rather than by long axis shortening,
- wall thickness of both ventricles increases during systole.

Initially angiocardiography was applied on a small scale to patients with congenital and acquired valvular heart disease. However, after the introduction of selective coronary arteriography via the retrograde brachial (45) and percutaneous femoral (46) approach, and after the introduction of coronary bypass surgery (47), an explosive growth of the number of performed studies took place. As there appeared to be a narrow relation between left ventricular function and the results of medical and surgical therapy in patients with heart

disease (48-50), the need for quantification of left ventricular volume and wall motion was evident. Quantitative angiocardiology has offered significant contributions to the assessment of ventricular size and function in patients with both coronary and valvular heart disease (51-57).

The determination of cardiac volume.

The in vivo determination of cardiac volume is based on assumptions and empirical formulas and can therefore only be approximate. Fortunately stroke volume calculated from the measurement of end diastolic and end systolic volumes was shown to correlate well with stroke volume determined with the classic cardiac output techniques (58, 59). Many methods have been proposed for the measurement of left ventricular volume (60-64), but only few acquired general acceptance. Dodge's area-length method (60), based on the assumption that the left ventricular cavity can be represented by an ellipsoid, is used widely. Though initially developed for biplane angiocardiology, the method appeared to be also applicable to single plane films (61), in the antero-posterior and with higher accuracy in the right anterior oblique projection (65). Chapman's method (63), based on the assumption that the cross-sectional outline of the left ventricle is approximately circular or elliptical, divides the ventricle into thin slices. The volume of each slice is computed following the formula: $V = \pi h (A \times B) / 4$, where V is the volume of the slice in cm^3 , h is the height of the slice, A is the axis in one view and B the axis in the perpendicular view at the same level (in cm). Left ventricular volume is found by summing up the volume of all segments. This method gives a relatively accurate approximation of actual volume, but comprises a formidable amount of measurements and calculations, which restricts its use to centers provided with computer facilities (66).

The mechanical alterations of left ventricular function in heart disease are clearly visualised by a loop describing the relation between instantaneous left ventricular volume and pressure (67). Total mechanical work performed by the ventricle during a cardiac cycle, which is equal to the product of stroke volume and mean systolic pressure, is determined by planimetry of the area within and below this pressure-volume loop. To construct such a loop, frame by frame analysis of one or more cardiac cycles is essential, a time consuming and tedious activity, which initiated the search for automated left ventricular endocardial contour detection techniques.

Automated contour detection.

Many systems for the analysis of left ventriculograms with the use of a digital computer system have been reported (68-78). Most of them use a light pen or a

sonic pen to feed the boundary information in the computer. In the automated systems border recognition is based on videometry. The image information is stored on a videodisc or tape or is converted from cinefilm into videoformat. The video-image is build up from videolines with changing light intensities, carried by the videosignal as voltage changes and boundaries are characterized by a sudden change in brightness (i.e. voltage). The initial automated detection systems, which worked according to the simple principle of fixed thresholding (79, 80), could only be used when the contrast between the ventricular silhouette and its background was great and when the picture did not show intervening structures such as ribs and catheters. To cope with this problem semi-automated systems were designed, which needed an operator to set threshold voltages and to correct for background structures (81, 82). The important role of the operator brought inconsistency and subjectivity back in the analysis of the ventriculogram. Fortunately new systems were developed, which could define the endocardial border accurately, even in the case of a wide variation in image contrast due to background structures or incomplete mixing of the contrast medium.

Clayton developed one such system based on a general purpose computer (83). He recorded the ventriculogram on a videodisk, digitized the analog video-signal of each frame and processed these data with a digital computer. The border recognition algorithm combines four independent border recognition criteria by forming a product which is used to compute the probability that a given point should be designated as the border. Two terms of this point product are based on the assumption that the endocardial border is a continuous structure, which moves smoothly: the predicted border location in a given videoline is based on the location of border points in previous lines as well as on the direction of movement of the particular border point in the two previous TV-fields. With this system a reliable tracing of the left ventricular endocardial border is obtained even in less well opacified areas. Real-time analysis of a video angiogram requires data rates and a storage capacity which are not compatible with a general purpose computer: with the system described above quantization of each frame takes at least 12 seconds. The only way to realise real-time analysis — i.e. analysis of 50 TV-fields per second — is with a dedicated hard-wired system such as constructed meanwhile by our group (84-87). Here again the concept that the cardiac border is a continuous, smoothly moving structure, may be observed in the design of the system. The coordinates of the detected contour in the previous cineframe and the contour points in the previous videoline are stored in a memory and help to determine the probability that a particular point should be considered as part of the endocardial contour. These sophisticated systems were not only useful for the assessment of left ventricular volume but opened also new perspectives in the study of regional wall motion.

Regional wall motion.

The interest in regional wall motion and its hemodynamic significance was greatly stimulated by the work of Herman et al. (88, 89), who defined four types of local wall motion disturbance or "asynergy":

- akinesis, or total lack of motion of a part of the left ventricular wall,
- asyneresis, or diminished motion of a part of the wall,
- dyskinesis, or systolic paradoxical motion,
- asynchrony, or a disturbed temporal pattern of contraction.

A rather close relationship between electrocardiographic findings, the angiographic site of coronary stenosis and regional wall motion abnormalities was shown (90), although adequate collateral circulation may preserve a normal or nearly normal contraction pattern in areas perfused by a severely narrowed coronary artery (91), which explains why ventricular asynergy is not invariably present at rest in patients with coronary artery disease. In some cases a stress such as rapid atrial pacing (92, 93) may disrupt the balance between oxygen delivery and metabolic demand, and consequently induce asynergy. Akinesis and dyskinesis are generally recognized by gross inspection of the ventriculogram, but asyneresis and especially temporal disturbances of contraction require a detailed and quantitative analysis.

Wall motion models.

To perform an accurate description of wall motion, ideally specific points on the endocardial surface should be tracked. The only way to reach this goal is implantation of endocardial metal markers, as was performed in dogs (94), but is impractical in humans. Epicardial clips (95, 96, 97) and midwall markers (98, 99) have contributed considerably to the understanding of myocardial dynamics, but provide only remote information on actual endocardial motion. Many wall motion models have been proposed to approximate actual endocardial motion (88, 100-103), which reflects the problems investigators had to establish a geometric framework upon which to judge whether the motion of the endocardial contour is normal or abnormal. All these methods assess wall motion in terms of extent of shortening at specific points of an axis reference system, although it is highly unlikely that a particular endocardial site coincides with one of these axes during the entire cardiac cycle. The various geometric models developed in an attempt to track regional endocardial motion accurately, may be discussed on the basis of two items: the coordinate system and the reference system. Two coordinate systems are commonly employed to determine the excursion of the ventricular wall.

- Rectangular coordinates: points on the wall are assumed to move in a direction perpendicular to the ventricular long axis along lines termed hemiaxes.

The methods described by Herman et al (88) and Leighton et al (100) are examples of such a method.

— Polar coordinates: The position of points on the ventricular wall is specified by their distance from the origin — defined as the midpoint of the left ventricular long axis (101) or the center of area of the end systolic frame (102) — and by angles relative to a polar axis from the origin. In these polar coordinate systems the left ventricular long axis is considered as the polar axis.

To separate regional wall motion from motion of the heart as a whole caused by twist, translation and rotation, most methods require correction measures, such as coordinate system movement or rotation, in order to realign or superimpose the left ventricular contour. To execute these measures an internal reference system is applied, which couples the coordinate system to specific points within the heart such as valvular edges and the apex (88, 100-102). With an external reference system the coordinate system is not coupled to the motion of the heart, but to external landmarks such as ribs or lead markers on the chest wall serving as reference points (103). Brower (104) compared six methods to determine regional shortening from cine ventriculograms and concluded that no method proves to be ideal as the majority of the methods shows a poor correlation with visual observation of regional wall motion. Although Brower considered Chaitman's method (103), using an external reference system — i.e. without "correction"-procedures — impractical because of overestimation of wall motion in the basal and apical segments, it must be emphasized that this method yields a 100% score for detection of asynergy.

Determination of left ventricular function from pressure signals.

Invasive evaluation of left ventricular function may be accomplished by the study of the left ventriculogram or by the analysis of left ventricular pressure signals and their derivatives. Left ventricular end diastolic pressure can be measured directly from the left ventricular pressure tracing, which makes it an easy parameter to obtain. There exists only a loose relation between left ventricular end diastolic pressure and volume (57, 105), which is influenced significantly by left ventricular compliance. Large volume changes with a significant influence on left ventricular performance may result in only small changes of end diastolic pressure (106), whereas patients with increased muscle mass may have an elevated end diastolic pressure but show a normal filling volume (107). In daily clinical practice, elevation of the end diastolic pressure is most often related to impairment of left ventricular function and is to be considered as an index of abnormality, the extent of which has to be analyzed by other means.

In the last decade various methods have been developed to determine the functional state of the myocardial muscle from the change of pressure taking place in the isovolumic contraction period. The aim is to consider the heart in

terms of wall stress, elasticity and contractility, rather than as a pump developing pressure to generate blood flow. The basis for this view was laid by A.V. Hill's study of the properties of skeletal muscle (108). He explained the phenomena observed during muscular contraction by assuming a contractile element (CE) in series with an elastic element (SE). When activated the CE shortens, thus pulling on the springlike SE. If the muscle contracts unloaded the SE remains unstretched and contractile force is used fully for development of velocity. Under submaximal loading conditions contraction of the CE will stretch the SE until enough force is generated to move the load, leading to isotonic contraction. When a maximal load is attached a fully isometric contraction occurs, consisting of contraction of the CE with equal extension of the SE. Here contractile energy is fully converted into force. Determination of muscular velocity at different loads gives an inverse hyperbolic force-velocity relation, the fundamental law of Hill for skeletal muscle. As all points on the force-velocity curve are derived from isotonic muscular contractions – with constant length of the SE – the velocity of the CE (V_{CE}) can be equated with whole muscle velocity. It appeared that these principles can be applied to isolated heart muscle (109, 110) and to the whole heart (111).

However, in the intact heart cardiac muscle never contracts fully unloaded, as the end-diastolic pressure gives a resting load or preload which stretches the CE to a certain extent. This stretch causes more active tension generating sites of the actin and myosin filaments to face each other, thus enhancing maximal force development (P_0). The maximal extrapolated CE velocity at zero load (V_{max}) is – at least theoretically – not influenced by preload (111-113) because it is determined by the rate of force development of the active sites, rather than being dependent of the number of active sites facing each other. Positive inotropic interventions cause however an increase of both V_{max} and P_0 . Hugenholtz et al (112) determined V_{CE} (and by extrapolation V_{max}) from instantaneous wall stress during a full cardiac cycle. Wall stress was derived from intracavitary pressure, LV major and minor semiaxes and wall thickness as determined through frame by frame analysis, according to a formula developed by Mirsky (114). This way of calculating V_{max} is very time consuming because frame by frame analysis is needed (see appendix 1).

Assuming a completely synergistic left ventricular contraction, and excluding valvular insufficiency, in the pre-ejection phase a fully isometric contraction takes place and $V_{CE} = V_{SE}$ (velocity of SE). V_{SE} can be derived from intraventricular pressure (see appendix 2). The intracavitary pressure is recorded using a high fidelity tipmanometer catheter (115). A fluid-filled catheter system, though initially been used (116), introduces an important error caused by its limited dynamic response (117). Although from a theoretical point of view, V_{max} is a useful index of the contractile characteristics of the left ventricle, a considerable overlap was observed between values found in patients whose resting catheterization showed normal left ventricular function and those with ab-

normal function as shown by a reduced ejection fraction and raised end-diastolic volume and/or pressure (112, 118-120). Peterson et al. (120) compared the sensitivity of isovolumic- and of ejection phase indices and found a far better separation between normal and abnormal hearts with the latter indices. Kreulen et al. (121) compared the sensitivity of ejection fraction, regional wall motion and end diastolic pressure, with the sensitivity of the contractile indices to reveal left ventricular dysfunction. They concluded that calculation of the first three parameters identified almost all patients with cardiac disease, whereas the contractile indices were only sensitive to advanced stages of left ventricular failure.

The accuracy of V_{\max} is affected by a number of factors. First of all V_{\max} cannot be directly measured, but has to be determined by extrapolation from an often short and non-linear force velocity curve. Small errors in end-diastolic

Appendix 1.

V_{CE} can be considered during systole as the sum of the velocity of circumferential fiber-shortening (V_{cf}) and the velocity of elongation of the series elastic element (V_{SE}).

$$V_{CE} = V_{cf} + V_{SE}$$

Instantaneous V_{cf} can be determined from the instantaneous change in left ventricular radius (r):

$$2 \pi \cdot dr_i/dt$$

V_{SE} can be calculated from instantaneous wall stress (S, in gm/cm²). The stress-strain relation of the SE (109) is:

$$\frac{dS}{dl} = k \cdot S + c$$

where k is a constant defining the elastic properties of the SE and the intercept c is small and can be disregarded.

$$\frac{dS}{dl} = k \cdot S \quad \frac{dS}{dt} \cdot \frac{dt}{dl} = k \cdot S \quad \frac{dl}{dt} = V_{SE} = \frac{dS/dt}{k \cdot S}$$

Appendix 2.

In isometric systole: $V_{CE} = V_{SE} = \frac{dS/dt}{k \cdot S}$ and $S = \frac{P \cdot r}{2 \cdot h}$ (Laplace's law)

$$V_{CE} = \frac{d(P \cdot r / 2 \cdot h) / dt}{k(P \cdot r / 2 \cdot h)} = \frac{dP/dt}{k \cdot P}$$

where P is intracavitary pressure (gm/cm²)
 r is inner ventricular radius (cm)
 h is wall thickness (cm).

pressure assessment give major errors in V_{\max} (120), while linear and exponential extrapolation of the force-velocity curve give very different results. The k -constant is probably altered by pathologic states such as chronic myocardial infarction as has been shown in the intact canine left ventricle (122). It is not likely that the value of this constant, that is derived from animal papillary muscle studies (109), will be the same in the intact human heart and remains unchanged in health and disease. Most important is the fact that a pure isometric contraction is a requirement which the left ventricle cannot meet. A slight asynchrony of contraction and minor changes in shape as occur in the pre-ejection phase (123) may not influence the determination of V_{\max} . But in the case of serious asynchrony of the left ventricular contraction or when valvular insufficiency occurs, the assumption of an isometric contraction is violated and the isovolumic indices of contractility can no longer be determined with any degree of accuracy.

Ejection phase parameters.

Two important parameters of left ventricular performance may be derived from the ejection phase: the ejection fraction and the velocity of circumferential fiber shortening. The ejection fraction — the quotient of stroke volume and end diastolic volume — provides a better discrimination between mechanical and myocardial factors responsible for cardiac dysfunction than end diastolic volume alone. In chronic left ventricular pressure or volume overload, the ejection fraction remains practically normal, unless there is associated myocardial failure or disease (124, 125). Still, it is a valuable marker of heart disease. In one study of patients with valvular, myocardial and coronary heart disease, the ejection fraction identified 15 of 24 patients with left ventricular dysfunction (as determined by six parameters of left ventricular function). Combination of the results of ejection fraction and regional wall motion analysis identified 20 of 24 abnormal, whereas pressure derived contractile indices revealed left ventricular dysfunction in only seven patients (121). Like the isovolumic pressure derived indices, ejection fraction is a global parameter and is thus not able to describe regional function (126). The ejection fraction is a sensitive determinant of the prognosis of patients with coronary artery disease (127), after myocardial infarction (128), and of survival after valve replacement (129). Study of the ejection fraction during the first third part of the ejection phase further enhances its prognostic significance (130). Analysis of ejection phase parameters in three equal parts of the ejection phase provides an improved discrimination between normal and abnormal left ventricular pump function (131, 132). Because normal myocardium can develop force at a faster rate than diseased myocardium, normal ventricles displace their maximal volume in the first third, and abnormal ventricles in the second third of the ejection

phase. In the second and third part of systole the abnormal myocardium benefits from the decrease of wall stress. In agreement with these data, Leighton found abnormal regional wall motion at mid-systole in 27 of 42 patients with obstructive coronary artery disease and normal end systolic wall motion (133).

The concept of the velocity of circumferential fiber shortening (V_{cf}), introduced in 1968 by Gault et al. (134) is largely the offshoot of muscle mechanics. The time course of V_{cf} and of left ventricular wall stress throughout ejection may be described with the combined use of angiography and intracardiac pressure recording. As V_{cf} equals the sum of contractile element velocity (V_{CE}) and series elastic element lengthening or shortening velocity (V_{SE}), and V_{SE} at peak stress is equal to zero, V_{cf} at peak stress equals V_{CE} (135, 136). V_{cf} at peak stress appeared to be a sensitive but laborious index of left ventricular performance which reflects the inotropic state of the left ventricular myocardium. The subsequently introduced mean endocardial velocity of circumferential fiber shortening (137) may be derived from the angiogram with great ease, and provides a good discrimination between normal and abnormal left ventricular function as well (138), but lacks the fundamental base to be an actual determinant of the inotropic state. Although relatively preload independent (139-141), V_{cf} varies inversely with afterload: increase of afterload with angiotensine (139) or phenylephrine (141) decreases V_{cf} , whereas a decrease of afterload with amyl nitrite (139) causes a rise in V_{cf} . This implies — at least theoretically — that defined conditions of afterload are needed to interpret the ejection phase indices of contractility. When V_{cf} at peak stress is determined during two afterload states, part of a force velocity curve may be constructed (139) and extrapolated to zero load. In comparison with normal curves, the curves of patients with heart disease show a less steep slope and a lower V_{CE} intercept at zero load, which suggests depressed contractility. This offers an interesting opportunity to determine contractility in patients with asynchrony of the left ventricular contraction or valvular insufficiency, when the virtual absence of an isovolumic, synchronous contraction makes contractility determination from pressure signals inaccurate. The sensitivity of V_{cf} for acute changes in contractility is comparable to the sensitivity of pressure derived indices of contractility. Intervention with isoproterenol and propranolol showed a comparable or equal per cent change of both pk dP/dt and V_{cf} (141).

Intervention techniques.

Intervention techniques may be used to improve the discrimination between normal and abnormal subjects as assessed by the isovolumic indices of contractility. A considerable overlap exists between the contractile indices of normal individuals and patients with coronary artery disease (113, 138, 142). Some improvement in discrimination can be obtained with the application of iso-

metric exercise (113) or atrial pacing (142). Isometric exercise can be performed by sustained isometric contraction of the forearm flexor muscles, and produces a cardiovascular reflex consisting of an increase in heart rate, arterial blood pressure (afterload) and cardiac output (143-145). In normal subjects at low levels of forearm muscle contraction the increase in systemic arterial pressure is caused by augmentation of the cardiac output, while systemic vascular resistance remains unchanged. Hemodynamic data show no significant change in stroke volume, which implies that the increase in cardiac output is caused by a rise in heart rate. In patients with coronary artery disease an increase in peripheral resistance is at least partially responsible for the elevation of arterial pressure (146). The exact mechanism by which these changes are effected is not fully understood. Probably it is based on afferent neural impulses evoked by the accumulation of metabolites in the exercising extremity which result in general sympathetic activation (147). In normal individuals the isovolumic indices of contractility show a steep increase during isometric exercise, while only a small rise in filling pressure is observed. However in patients with heart disease stroke work increases only at the cost of a significant rise in end diastolic pressure, while the contractile indices rise only slightly, which reflects the limited contractility reserve (113).

Atrial pacing is another technique which improves the discrimination between normal and abnormal left ventricular function. In 1871 Bowditch (148) described the inverse relationship between the amplitude of contraction and the interval between contractions in the isolated frog heart. Although the working mechanism remains uncertain, the relation between heart rate and contractility seems to be an inherent property of heart muscle (149, 150). Sowton et al. (151) introduced the technique of rapid atrial pacing as a stress test of the left ventricle. Through an increase in oxygen consumption (152) — due to augmentation of the contractile state — and a reduction of the diastolic perfusion period of the coronary system, this procedure may evoke transient myocardial ischemia in patients with coronary artery disease. Thus the limited contractile reserve of patients with coronary artery disease is revealed, which improves the separation between normal and abnormal subjects (142). Application of intervention techniques to ventriculography provides invaluable information about the structural and functional qualities of the muscular wall.

Dynamic ventriculography.

Dynamic or intervention ventriculography evaluates cardiac function at rest and in a second state after a certain change of load or contractility (153). The purpose is twofold:

— first, to unmask compromised areas of myocardium, which show normal wall motion under basal conditions, but develop asynergy when stressed. The appro-

priate intervention techniques are rapid atrial pacing (92, 93, 154-157), isometric exercise (158) and beta adrenergic blockade (159). Reversible asynergy during rapid atrial pacing is suggestive of a critical coronary artery stenosis which provokes a discrepancy between increased oxygen consumption and restricted oxygen delivery. Thus the hemodynamic significance of a stenosis may be assessed. Isometric exercise which increases afterload, and beta adrenergic blockade, which decreases contractility, provide comparable information.

— second, to reveal ischemic but viable myocardium, which is asynergic under basal conditions, but may show improvement of wall motion after unloading or inotropic interventions. The appropriate measures are the application of nitroglycerin (160-163), postextrasystolic potentiation (164-166) and epinephrine (167).

Since revascularization of viable but depressed myocardium might correct segmental and ventricular dysfunction (161, 166), it is important to distinguish between viable but ischemic areas and scar tissue. Bodenheimer et al. (168) showed with needle biopsies that even in akinetic segments the majority of tissue may consist of viable muscle cells. Nitroglycerin decreases myocardial oxygen consumption by reduction of pre- and afterload (169, 170) and may thus improve wall motion of these heavily compromised areas, unless they consist of mere scar tissue. Epinephrine and postextrasystolic potentiation may both improve regional wall motion by an increase in contractility. The discovery of postextrasystolic potentiation is attributed to Langendorf, who announced it in 1885 (171). If a series of regular contractions is interrupted by a single extrasystole, systolic pressure and contractility are increased for one or more of the following beats (164, 172). This appears to be an inherent property of heart muscle but its causative mechanism remains unclear (173). In patients with coronary artery disease a significant association was shown between the effect of postextrasystolic potentiation on regional wall motion, and improvement of wall motion after successful bypass surgery (166).

To conclude a large number of publications is devoted to the study of left ventricular function. Although this review deals only with a minority of these articles it outlines the conceptual framework on which the rest of this study is built.

REFERENCES

1. Chirac P., *De motu cordis, adversaria analytica*, 1698 p. 121, cited by See, Bochefontaine and Roussy. *Compt. Rend. Acad. d. Sciences* 92: 86, 1881.
2. Erichsen J.E., On the influence of the coronary circulation on the action of the heart. *London Med. Gaz.* 2: 561, 1842.
3. Samuelson B., Ueber den Einfluss der Koronar-arterien-Verschliessung auf die Herzaktion. *Zeitschr. f. Klin. Med.* 2: 12, 1881.
4. Tennant R., Wiggers C.J., The effect of coronary occlusion on myocardial contraction. *Am. J. Physiol.* 112: 351, 1935.
5. Prinzmetal M., Schwartz L.L., Corday E., Spritzler R., Bergman H.C., Kruger H.E., Studies on the coronary circulation. 6. Loss of myocardial contractility after coronary artery occlusion. *Ann. Int. Med.* 31: 429, 1949.
6. Lenk R., Roentgendiagnose der Koronarsclerose in vivo. *Fortschr. a. d. Geb. d. Roentgenstrahlen* 35: 1265, 1926.
7. Kalish Z., Ueber ein radioskopisch diagnostizierten und autoptisch bestaetigten Fall von partiellen Herzaneurysma. *Wien. Klin. Wochenschrift.* 40: 1078, 1927.
8. Master A.M., Gubner R., Dack S., Jaffe H.L., The diagnosis of coronary occlusion and myocardial infarction by fluoroscopic examination. *Am. Heart Journal* 20: 475, 1940.
9. Goert Th., Rosenthal J., Ueber ein Verfahren zur Darstellung der Herzbewegung mittels Roentgenstrahlen (Roentgenkymographie). *München. Med. Wchnschr.* 59: 2033, 1912.
10. Sussman M.L., Dack S., Master A.M., The roentgenkymogram in myocardial infarction. 1. The abnormalities in left ventricular contraction. *Am. Heart Journal* 19: 453, 1940.
11. Dack S., Sussman M.L., Master A.M., The roentgenkymogram in myocardial infarction. 2. Clinical and electrocardiographic correlation. *Am. Heart Journal* 19: 464, 1940.
12. Dinsmore R.E., Wernikoff R.E., Miller S.W., Potsaid M.S., Information enhancement and dose reduction in chest radiography: the Intergrated Radiography System. Proceedings of the symposium on optimization of chest radiography. April 30 - May 2, 1979. University of Wisconsin and U.S. Bureau of Radiological Health, Madison, Wisconsin, 1979.
13. Henny C.G., Boone B.R., Electrokyomograph for recording heart motion utilising the roentgenoscope. *Am. J. Roentgenol.* 54: 217, 1945.
14. Luisada A., Fleischner F.G., Rappaport M.B., Fluorocardiography (electrokyomography). 1. Technical aspects. *Am. Heart J.* 35: 336, 1948.
15. Dack S., The ventricular pulsations in myocardial infarction; a fluoroscopic and kymographic study. *Dis. Chest.* 27: 282, 1955.
16. Dack S., Paley D., Electrokyomography 1. The ventricular electrokyomogram. *Am. J. Med.* 12: 331, 1952.
17. Luisada A.A., Fleischner F.G., Rappaport M.B., Fluorocardiography (electrokyomography). 2. Observations on normal subjects. *Am. Heart J.* 35: 348, 1948.
18. Bartley O., Electrokyomographic changes in myocardial infarction. *Acta radiol. (Stockholm)* 54: 81, 1960.
19. Zinsen H.F. Jr., Kay C.F., Benjamin J.M. Jr., The electrokyomograph: studies in recording fidelity. *Circulation* 2: 197, 1950.
20. Pichler M., Vas R., Tzivoni D., Hisch M., Diamond G., Forrester J., Detection of regional ischemic left ventricular dysfunction by epicardial photokymography. *Clin. Res.* 26: 259A, 1978.
21. Cohen L.S., Simon A.L., Whitehouse W.C., Schuette W.H., Braunwald E., Heartmotion videotracking (radarkymography) in diagnosis of congenital and acquired heart disease. *Am. J. Cardiol.* 22: 678, 1968.

22. Kazamias Th.A., Gander M.P., Ross J. Jr., Braunwald E., Detection of left ventricular wall motion disorders in coronary-artery disease by radarkymography. *New Eng. J. Med.* 285: 63, 1971.
23. Ludbrook P.A., Yin F.C.P., Peterson K.L., Characterization of left ventricular external wall motion in man by video dimension analyzer (Vidian). *Catheterization and cardiovascular diagnosis* 3: 21, 1977.
24. Vas R., Electronic device for physiological kinetic measurement and detection of extraneous bodies. *IEEE Trans. Biomed. Eng. BME* 14: 2, 1967.
25. Diamond G.A., Chag M., Vas R., Forrester J.S., Cardiokymography: Quantitative analysis of regional ischemic left ventricular dysfunction. *Am. J. Cardiol.* 41: 1249, 1978.
26. Vas R., Diamond G.A., Silverberg R.A., Grodan P.J., Marcus H.S., Buchbinder N.A., Forrester J.S., Assessment of the functional significance of coronary artery disease with atrial pacing and cardiokymography. *Am. J. Cardiol.* 44: 1283, 1979.
27. Crawford M.H., Moody J.M., O'Rourke R.A., Detwiler J., Limitations of the cardiokymograph for assessing left ventricular wall motion. *Am. Heart Journal* 97: 719, 1979.
28. Hertz C.H., Edler I., Die Registrierung von Herzwand-Bewegungen mit Hilfe der Ultraschall-Impuls Verfahrens. *Acustica* 6: 361, 1956.
29. Feigenbaum H., *Echocardiography*. Lea and Febiger, Philadelphia, 1981.
30. Roelandt J., *Practical echocardiology*. Research studies press, 1977.
31. Roelandt J., Dorp W.G. van, Bom N., Laird J.D., Hugenholtz P.G., Resolution problems in echocardiology: a source of interpretation errors. *Am. J. Cardiol.* 37: 256, 1976.
32. Mullins C.B., Mason D.T., Ashburn W.L., Ross J., Determination of ventricular volume by radioisotope angiography. *Am. J. Cardiol.* 24: 72, 1969.
33. Bacharach S.L., Green M.V., Borer J.S., Douglas M.A., Ostrow H.G., Johnston G.S., A real time system for multi-image gated cardiac studies. *J. Nucl. Med.* 18: 79, 1977.
34. Burow R.D., Strauss H.W., Singleto R., Pond M., Rehn R., Bailey I.K., Griffith L.C., Nickoloff E., Analysis of left ventricular function from multiple gated acquisition (MUGA) cardiac blood pool imaging: Comparison to contrast angiography. *Circulation* 56: 1024, 1977.
35. Forssman W., Die Sondierung des rechten Herzens. *Klin. Wochenschr.* 8: 2085, 1929.
36. Cournand A., Ranges H.A., Catheterization of the right auricle in man. *Proc. Soc. Exper. Biol. and Med.* 46: 462, 1941.
37. Bing R.J., Van Dam L.P., Gray F.D. Jr., Physiological studies in congenital heart disease. I. Procedures. *Bull. Johns Hopkins Hosp.* 80: 107, 1947.
38. Gorlin, R., Gorlin S.G., Hydraulic formula for calculation of the area of the stenotic mitral valve, other cardiac valves and central circulatory shunts. *Am. Heart J.* 41: 1, 1951.
39. Castellanos A., Pereiras R., Garcia A., La angiocardiografia, un método nueva para diagnóstico de las cardiopatías congénitas. *Archivos de la sociedad de estudios clínicos de la Habana*, 1937.
40. Robb G., Steinberg M.F., Visualisation of the chambers of the heart, the pulmonary circulation and great blood vessels in man. A practical method. *Am. J. Roentgenol.* 41: 1, 1939.
41. Chavez I., Dorbecker N., Celis A., Direct intracardiac angiocardiography. Its diagnostic value. *Am. Heart J.* 33: 560, 1947.
42. Rushmer R.F., Bark R.S., Hendron J.A., Clinical cinefluorography. *Radiology* 55: 588, 1950.
43. Rushmer R.F., Crystal D.K., Changes in configuration of the ventricular chambers during the cardiac cycle. *Circulation* 4: 211, 1951.

44. Rushmer R.F., Thal N., The mechanics of ventricular contraction. A cinefluorographic study. *Circulation* 4: 219, 1951.
45. Sones F.M., Shirey E.K., Cine coronary arteriography. *Mod. Concepts Cardiovasc. Dis.* 31: 735, 1962.
46. Judkins M.P., Percutaneous transfemoral selective coronary arteriography. *Rad. Clin. N. Amer.* 6: 467, 1968.
47. Favaloro R.G., Saphenous vein autograft replacement of severe segmental coronary occlusion - operative technique. *Ann. Thorac. Surg.* 5: 334, 1968.
48. Brusckhe A.V.G., Proudfit W.L., Sones F.M., Progress study of 590 consecutive non-surgical cases of coronary disease followed 5 - 9 years. II. Ventriculographic and other correlations. *Circulation* 47: 1154, 1973.
49. Hammermeister K.E., DeRouen T.A., Dodge H.T., Variables predictive of survival in patients with coronary disease. *Circulation* 59: 421, 1979.
50. Tyras D.H., Barner H.B., Kaiser G.C., Codd J.E., Laks H., Pennington D.G., Willman V.L., Long-term results of myocardial revascularization. *Am. J. Cardiol.* 44: 1290, 1979.
51. Rackley C.E., Dear H.D., Baxley W.A., Jones W.B., Dodge H.T., Left ventricular chamber volume, mass and function in severe coronary artery disease. *Circulation* 41: 605, 1970.
52. Hamilton G.W., Murray J.A., Kennedy J.W., Quantitative angiocardiology in ischemic heart disease. *Circulation* 45: 1065, 1972.
53. Moraski R.E., Russell R.O. Jr., Smith M., Rackley C.E., Left ventricular function in patients with and without myocardial infarction and one, two or three vessel coronary artery disease. *Am. J. Cardiol.* 35: 1, 1975.
54. Jones J.W., Rackley C.E., Bruce R.A., Dodge H.T., Cobb L.A., Sandler H., Left ventricular volumes in valvular heart disease. *Circulation* 29: 887, 1964.
55. Miller G.A.H., Kirklin J.W., Swan H.J.C., Myocardial function and left ventricular volumes in acquired valvular insufficiency. *Circulation* 31: 374, 1965.
56. Dodge H.T., Baxley W.A., Hemodynamic aspects of heart failure. *Am. J. Card.* 22: 24, 1968.
57. Kennedy J.W., Twiss R.D., Blackmon J.R., Dodge H.T., Quantitative angiocardiology. III: Relationship of left ventricular pressure, volume and mass in aortic valve disease. *Circulation* 38: 838, 1968.
58. Gribbe P., Comparison of the angiographic and direct Fick methods in determining cardiac output. *Cardiologia* 36: 20, 1960.
59. Wagner H.R., Gamble W.J., Albers W.H., Hugenholtz P.G., Fiberoptic-dye dilution method for measurement of cardiac output. Comparison with the direct Fick and the angiographic methods. *Circulation* 37: 694, 1968.
60. Dodge H.T., Sandler H., Ballew D.W., Lord J.D. Jr., The use of biplane angiocardiology for measurement of left ventricular volume in man. *Am. Heart J.* 60: 762, 1960.
61. Sandler H., Dodge H.T., The use of single plane angiocardiology for the calculation of left ventricular volume in man. *Am. Heart J.* 75: 325, 1968.
62. Arvidsson H., Angiocardigraphic determination of left ventricular volume. *Acta. Radiol.* 56: 321, 1961.
63. Chapman C.B., Baker O., Reynolds J., Bonte F.J., Use of biplane cinefluorography for measurement of ventricular volume. *Circulation* 18: 1105, 1958.
64. Greene D.G., Carlisle R., Grant C., Bunnell I.L., Estimation of left ventricular volume by one plane cineangiography. *Circulation* 35: 61, 1967.
65. Kennedy J.W., Trenholme S.E., Kasser I.S., Left ventricular volume and mass from single-plane cineangiocardiology. A comparison of anteroposterior and right anterior oblique methods. *Am. Heart J.* 80: 343, 1970.

66. Reiber J.H.C., Special-purpose computer for real-time calculation of left ventricular volumes. Thesis, Electronics laboratory, Technological University, Delft, 1971.
67. Rackley C.E., Behar V.S., Whalen R.E., McIntosh H.D., Biplane cineangiographic determination of left ventricular function: Pressure - volume relationships. *Am. Heart J.* 74: 766, 1967.
68. Heintzen P.H., Malerczyk V., Pilarczyk J., Scheel K.W., On-line processing of the video-image for left ventricular volume determination. *Comput. Biomed. Res.* 4: 474, 1971.
69. Wiscomb W.K., A hardware system for man-machine interaction in the study of left ventricular dynamics. *Roentgen-, Cine-, and Videodensitometry.* ed. by Heintzen P.H., G. Thieme Publishers pg. 156, 1971.
70. Robb R.A., Computer-aided contour determination and dynamic display of individual cardiac chambers from digitized serial angiocardiographic films. ed. by Heintzen P.H., G. Thieme Publishers pg. 170, 1971.
71. Marcus M.L., Schuette W.H., Whitehouse W.C., Bailey J.J., Glancy D.L., An automated method for measurement of ventricular volume. *Circulation* 45: 65, 1972.
72. Cole J.S., Brown D.D., Glaeser D.H., A semiautomated technique for the rapid determination of left ventricular volume from left ventricular cineangiograms. *Comput. Biomed. Res.* 7: 575, 1974.
73. Bove A.A., Kreulen T.H., Spann J.F., Computer analysis of left ventricular dynamic geometry in man. *Am. J. Cardiol.* 41: 1239, 1978.
74. Brower R.W., Meester G.T., Zeelenberg C., Hugenholtz P.G., Automatic data processing in the cardiac catheterization laboratory. *Comp. Prog. Biomed.* 7: 99, 1977.
75. Brower R.W., Meester G.T., Hugenholtz P.G., Quantification of ventricular performance: A computer-based system for the analysis of angiographic data. *Catheter. Cardiovasc. Diagn.* 1: 133, 1975.
76. Chow C.K., Kaneko T., Automatic boundary detection of the left ventricle from cineangiograms. *Comput. Biomed. Res.* 5: 388, 1972.
77. Smalling R.W., Skolnick M.H., Myers D., Shabetai R., Cole J.C., Johnston D., Digital boundary detection, volumetric and wall motion analysis of left ventricular cineangiograms. *Comput. Biol. Med.* 6: 73, 1976.
78. Eiho S., Kuwahara M., Fujita M., Sasayama S., Kawai C., Boundary detection of left ventricle from cineangiograms and analysis of regional left ventricular wall motion. *Sixth Computer Radiology* pg. 221, 1979.
79. Covvey H.D., The measurement of left ventricular volumes from T.V. with a PDP 8/1 D.E.C. Users Soc., papers and presentations pg. 255, 1970.
80. Sturm R.E., Wood E.H., The video quantizer: an electronic photometer to measure contrast in roentgen fluoroscopic images. *Mayo Clin. Proc.* 43: 803, 1968.
81. Ritman E.L., Sturm R.E., Wood E.H., Biplane roentgen videometric system for dynamic (60/sec) studies of the shape and size of circulatory structures, particularly the left ventricle. *Am. J. Cardiol.* 32: 180, 1973.
82. Slager C.J., Verbeek B.E., Meester G.T., Davidse J., Hugenholtz P.G., Automated recognition of left ventricular contours from video images. *Circulation* 43 & 44 (Suppl. II): 227, 1971.
83. Clayton P.D., Harris L.D., Rumel S.R., Warner H.R., Left ventricular videometry. *Comp. Biomed. Res.* 7: 369, 1974.
84. De Jong L.P., Slager C.J., Automatic detection of the left ventricular outline in angiographs using television signal processing techniques. *IEEE Transactions on biomedical engineering.* Vol. BME 22 pg. 230, 1975.
85. Slager C.J., Reiber J.H.C., Schuurbiens J.C.H., Meester G.T., Contouromat - A hardware left ventricular angio-processing system. I. Design and application. *Comput. Biomed. Res.* 11: 491, 1978.

86. Reiber J.H.C., Slager C.J., Schuurbijs J.C.H., Meester G.T., Contouromat – A hard-wired left ventricular angio-processing system. II. Performance evaluation. *Comput. Biomed. Res.* 11: 503, 1978.
87. Slager C.J., Reiber J.H.C., Meester G.T., Automated detection of left ventricular contour. Concept and application. In "Roentgen-Video-Technique for dynamic studies of structure and function of the heart and circulation". 2nd International workshop conference. (P.M. Heintzen and J.H. Buersch Eds.). Georg Thieme Publishers, Stuttgart, p. 158, 1978.
88. Herman M.V., Heinle R.A., Klein M.D., Gorlin R., Localized disorders in myocardial contraction. Asynergy and its role in congestive heart failure. *New Engl. J. Med.* 277: 222, 1967.
89. Herman M.V., Gorlin R., Implications of left ventricular asynergy. *Am. J. Cardiol.* 23: 538, 1969.
90. Herman M.V., Elliott W.C., Gorlin R., An electrocardiographic, anatomic, and metabolic study of zonal myocardial ischemia in coronary heart disease. *Circulation* 35: 834, 1967.
91. Sesto M., Schwarz F., Regional myocardial function at rest and after rapid ventricular pacing in patients after myocardial revascularization by coronary bypass graft or by collateral vessels. *Am. J. Cardiol.* 43: 920, 1979.
92. Pasternac A., Gorlin R., Sonnenblick E.H., Haft J.I., Kemp H.G., Abnormalities of ventricular motion induced by atrial pacing in coronary artery disease. *Circulation* 45: 1195, 1972.
93. Dwyer E.M. Jr., Left ventricular pressure – volume alterations and regional disorders of contraction during myocardial ischemia induced by atrial pacing. *Circulation* 42: 1111, 1970.
94. Rushmer R.F., Crystal D.K., Wagner C., The functional anatomy of ventricular contraction. *Circ. Res.* 1: 162, 1953.
95. Harrison D.C., Goldblatt A., Braunwald E., Mason D., Studies on cardiac dimensions in intact unanesthetized man. *Circ. Res.* 13: 448, 1963.
96. McDonald I.G., The shape and movements of the human left ventricle during systole. *Am. J. Cardiol.* 26: 221, 1970.
97. Brower R.W., Katen H.J. ten, Meester G.T., Direct method for determining regional myocardial shortening after bypass surgery from radiopaque markers in man. *Am. J. Cardiol.* 41: 1222, 1978.
98. Ingels N.B. Jr., Daughters G.T., Stinson E.B., Alderman E.L., Measurement of midwall myocardial dynamics in intact man by radiography of surgically implanted markers. *Circulation* 52: 859, 1975.
99. Ingels N.B. Jr., Daughters G.T., Stinson E.B., Alderman E.L., Evaluation of methods for quantitating left ventricular segmental wall motion in man using myocardial markers as a standard. *Circulation* 61: 966, 1980.
100. Leighton R.F., Wilt S.M., Lewis R.P., Detection of hypokinesis by quantitative analysis of left ventricular cineangiograms. *Circulation* 50: 121, 1974.
101. Harris L.D., Clayton P.D., Marshall H.W., Warner H.R., A technique for the detection of asynergistic motion of the left ventricle. *Comput. Biomed. Res.* 7: 380, 1974.
102. Rickards A., Seabra-Gomes R., Thurston P., The assessment of regional abnormalities of the left ventricle by angiography. *Eur. J. Cardiol.* 5: 167, 1977.
103. Chaitman B.R., Bristow J.D., Rahimtoola S.H., Left ventricular wall motion assessed by using fixed external reference systems. *Circulation* 48: 1043, 1973.
104. Brower R.W., Meester G.T., Computer based methods for quantifying regional left ventricular wall motion from cine ventriculograms. *Computers in Cardiology*, pg. 55, IEEE Computer Society 1976.

105. Rackley C.E., Hood W.P., Rolett E.L., Young D.T., Left ventricular end-diastolic pressure in chronic heart disease. *Am. J. Med.* 48: 310, 1970.
106. Sarnoff S.J., Berglund E., Ventricular function. I. Starling's law of the heart studied by means of simultaneous right and left ventricular function curves in the dog. *Circulation* 9: 706, 1954.
107. Kennedy J.W., Twiss R.D., Blackmon J.R., Dodge H.T., Quantitative angiocardio-graphy III. Relationships of left ventricular pressure, volume, and mass in aortic valve disease. *Circulation* 38: 838, 1968.
108. Hill A.V., Heat of shortening and dynamic constants of muscle. *Proc. Roy. Soc. (Biol.)*. 126: 136, 1938.
109. Sonnenblick E.H., Series elastic and contractile elements in heart muscle: changes in muscle length. *Am. J. Physiol.* 207: 1330, 1964.
110. Sonnenblick E.H., Force-velocity relations in mammalian heart muscle. *Am. J. Physiol.* 202: 931, 1962.
111. Levine H.J., Britman N.A., Force-velocity relations in the intact dog heart. *J. Clin. Invest.* 43: 1383, 1964.
112. Hugenholz P.G., Ellison R.C., Urschel C.W., Mirsky I., Sonnenblick E.H., Myocardial force-velocity relationships in clinical heart disease. *Circulation* 41: 191, 1970.
113. Krayenbuehl H.P., Rutishauser W., Schoenbeck M., Amende I., Evaluation of left ventricular function from isovolumic pressure measurements during isometric exercise. *Am. J. Cardiol.* 29: 323, 1972.
114. Mirsky I., Left ventricular stresses in intact human heart. *Biophys. J.* 9: 189, 1969.
115. Krayenbuehl H.P., Rutishauser W., Wirz P., Amende I., Mehmel H., High-fidelity left ventricular pressure measurements for the assessment of cardiac contractility in man. *Am. J. Cardiol.* 31: 415, 1973.
116. Falsetti H.L., Mates R.E., Carroll R.J., Gupta R.L., Bell A.C., Analysis and correction of pressure wave distortion in fluid-filled catheter systems. *Circulation* 49: 165, 1974.
117. Yanof H.M., Rosen A.L., McDonald N.M., McDonald D.A., A critical study of the response of manometers to forced oscillations. *Phys. Med. Biol.* 8: 407, 1963.
118. Mason D.T., Spann J.F. Jr., Zelis R., Amsterdam E.A., Comparison of the contractile state of the normal, hypertrofied, and failing heart in man. In: *Cardiac Hypertrophy*, edited by Alpert H., New York, Academic press 1971.
119. Graber J.D., Conti C.R., Lappe D.L., Ross R.S., Effect of pacing induced tachycardia and myocardial ischemia on ventricular pressure-velocity relationships in man. *Circulation* 46: 74, 1972.
120. Peterson K.L., Skloven D., Ludbrook P., Uther J.B., Ross J. Jr., Comparison of isovolumic and ejection phase indexes of myocardial performance in man. *Circulation* 49: 1088, 1974.
121. Kreulen Th.H., Bove A.A., McDonough M.T., Sands M.J., Spann J.F., The evaluation of left ventricular function in man. A comparison of methods. *Circulation* 51: 677, 1975.
122. Forwand S.A., McIntyre K.M., Lipana J.G., Levine H.J., Active stiffness of the intact canine left ventricle. With observation on the effect of acute and chronic myocardial infarction. *Circ. Res.* 19: 970, 1966.
123. Karliner J.S., Bouchard R.J., Gault J.H., Dimensional changes of left ventricle prior to aortic valve opening. A cineangiographic study in patients with and without left heart disease. *Circulation* 44: 312, 1971.
124. Bunnell I.L., Grant C., Greene D.G., Left ventricular function derived from the pressure-volume diagram. *Am. J. Med.* 39: 881, 1965.
125. Miller G.A.H., Kirklin J.W., Swan H.J.C., Myocardial function and left ventricular volumes in acquired valvular insufficiency. *Circulation* 31: 374, 1965.

126. Rogers W.J., Russell R.O. Jr., Moraski R.E., Coghlan H.C., Zisserman D., Rackley C.E., Comparison of indices of muscle and pump performance in patients with coronary disease. *Catheter. Cardiovasc. Diagn.* 1: 17, 1975.
127. Nelson G.R., Cohn P.F., Gorlin R., Prognosis in medically-treated coronary artery disease. Influence of ejection fraction compared to other parameters. *Circulation* 52: 408, 1975.
128. Schulze R.A., Strauss H.W., Pitt B., Sudden death in the year following myocardial infarction: relation to ventricular premature contractions in the late hospital phase and left ventricular ejection fraction. *Am. J. Med.* 62: 192, 1977.
129. Forman R., Firth B.G., Barnard M.S., Prognostic significance of preoperative left ventricular ejection fraction and valve lesion in patients with aortic valve replacement. *Am. J. Cardiol.* 45: 1120, 1980.
130. Battler A., Slutsky R., Karliner J., Froelicher V., Ashburn W., Ross J. Jr., Left ventricular ejection fraction and first third ejection fraction early after acute myocardial infarction: value for predicting mortality and morbidity. *Am. J. Cardiol.* 45: 197, 1980.
131. Johnson L.L., Ellis K., Schmidt D., Weiss M.B., Cannon P.J., Volume ejected in early systole. A sensitive index of left ventricular performance in coronary artery disease. *Circulation* 52: 378, 1975.
132. Slutsky R., Karliner J.S., Battler A., Peterson K., Ross J. Jr., Comparison of early systolic and holosystolic ejection phase indexes by contrast ventriculography in patients with coronary artery disease. *Circulation* 61: 1083, 1980.
133. Leighton R.F., Pollack M.E.M., Welch T.G., Abnormal left ventricular wall motion at mid-ejection in patients with coronary heart disease. *Circulation* 52: 238, 1975.
134. Gault J.H., Ross J. Jr., Braunwald E., Contractile state of the left ventricle in man. Instantaneous tension-velocity-length relations in patients with and without disease of the left ventricular myocardium. *Circ. Res.* 22: 451, 1968.
135. Levine H.J., Forwand S.A., McIntyre K.M., Schechter E., Effect of afterload on force-velocity relations and contractile element work in intact dog heart. *Circ. Res.* 18: 729, 1966.
136. Sonnenblick E.H., Parmley W.W., Urschel C.W., The contractile state of the heart as expressed by force-velocity relations. *Am. J. Cardiol.* 23: 488, 1969.
137. Karliner J.S., Gault J.H., Eckberg D., Mullins C.B., Ross J. Jr., Mean velocity of fiber shortening. A simplified measure of left ventricular myocardial contractility. *Circulation* 44: 323, 1971.
138. Peterson K.L., Skloven D., Ludbrook P., Uther J.B., Ross J. Jr., Comparison of isovolumic and ejection phase indexes of myocardial performance in man. *Circulation* 49: 1088, 1974.
139. Quinones M.A., Gaasch W.H., Cole J.S., Alexander J.K., Echocardiographic determination of left ventricular stress-velocity relations in man. With reference to the effects of loading and contractility. *Circulation* 51: 689, 1975.
140. Rankin L.S., Moos S., Grossman W., Alterations in preload and ejection phase indices of left ventricular performance. *Circulation* 51: 910, 1975.
141. Mahler F., Ross J. Jr., O'Rourke R.A., Covell J.W., Effects of changes in preload, afterload and inotropic state on ejection and isovolumic phase measures of contractility in the conscious dog. *Am. J. Cardiol.* 35: 626, 1975.
142. Brower R.W., Remme W.J., Katen H.J. ten, Brand M. van den, Quantification of the atrial pacing stress test: normal values and limits between normal and abnormal for coronary artery disease in man. *Comput. in Cardiol. IEEE Comp. Soc., Long Beach, California* pg. 591, 1977.
143. Lind A.R., Taylor S.H., Humphreys P.W., Kennelly B.M., Donald K.W., Circulatory effects of sustained voluntary muscle contraction. *Clin. Sci.* 27: 229, 1964.

144. Grossman W., McLaurin L.P., Saltz S.B., Paraskos J.A., Dalen J.E., Dexter L., Changes in the inotropic state of the left ventricle during isometric exercise. *Brit. Heart J.* 35: 697, 1973.
145. Helfant R.H., De Villa M.A., Meister S.G., Effect of sustained isometric handgrip exercise on left ventricular performance. *Circulation* 44: 982, 1971.
146. Kovowitz C., Parmley W., Donoso D., Marcus H., Ganz W., Swan H.J.C., Effects of isometric exercise on cardiac performance. The grip test. *Circulation* 44: 994, 1971.
147. Longhurst J.C., Mitchell J.H., Reflex control of the circulation by afferents from skeletal muscle. In: *International review of physiology: Cardiovascular physiology III*, edited by Guyton A.C., Young D.B., Baltimore, University Park Press, 1979, pp. 125-148.
148. Bowditch H.P., Ueber die Eigenthuemlichkeiten der Reizbarkeit welche die Muskelfasern der Herzens zeigen. *Ber. Saechs. Ges. (Akad.) Wiss.* 23: 652, 1871.
149. Covell J.W., Ross J. Jr., Taylor R., Sonnenblick E.H., Braunwald E., Effects of increasing frequency of contraction on force-velocity relation of left ventricle. *Cardiovasc. Res.* 1: 2, 1967.
150. Mahler F., Yorán C., Ross J. Jr., Inotropic effect of tachycardia and post-stimulation potentiation in the conscious dog. *Am. J. Physiol.* 227: 569, 1974.
151. Sowton G.E., Balcon R., Cross D., Frick M.H., Measurement of the angina threshold using atrial pacing. *Cardiovasc. Res.* 1: 301, 1967.
152. Boerth R.C., Covell J.W., Pool P.E., Ross J. Jr., Increased myocardial oxygen consumption and contractile state associated with increased heart rate in dogs. *Circ. Res.* 24: 725, 1969.
153. Cohn P.F., Gorlin R., Dynamic ventriculography and the role of the ejection fraction. *Am. J. Cardiol.* 36: 529, 1975.
154. Krayenbuehl H.P., Schoenbeck M., Rutishauser W., Wirz P., Abnormal segmental contraction velocity in coronary artery disease produced by isometric exercise and atrial pacing. *Am. J. Cardiol.* 35: 785, 1975.
155. Schwarz F., Ensslen R., Thormann J., Sesto M., Effects of nitroglycerin, postextrasystolic potentiation and pacing induced ischaemia on wall motion in patients with ischaemic heart disease. *Brit. Heart J.* 39: 44, 1977.
156. Tomoike H., Franklin D., Ross J. Jr., Detection of myocardial ischemia by regional dysfunction during and after rapid pacing in conscious dogs. *Circulation* 58: 48, 1978.
157. Sesto M., Schwarz F., Regional myocardial function at rest and after rapid ventricular pacing in patients after myocardial revascularization by coronary bypass graft or by collateral vessels. *Am. J. Cardiol.* 43: 920, 1979.
158. Flessas A.P., Conolly G.P., Handa S. et al., Effects of isometric exercise on the end diastolic pressure, volumes, and function of the left ventricle in man. *Circulation* 53: 839, 1976.
159. Helfant R.H., Herman M.V., Gorlin R., Abnormalities of left ventricular contraction induced by beta adrenergic blockade. *Circulation* 43: 641, 1971.
160. Dove J.T., Shah P.M., Schreiner B.F., Effects of nitroglycerin on left ventricular wall motion in coronary artery disease. *Circulation* 49: 682, 1974.
161. Helfant R.H., Pine R., Meister S.G., Feldman M.S., Trout R.G., Banka V.S., Nitroglycerin to unmask reversible asynergy. Correlation with post coronary bypass ventriculography. *Circulation* 50: 108, 1974.
162. McAnulty J.H., Hattenhauer M.T., Rösch J., Kloster F.E., Rahimtoola S.H., Improvement in left ventricular wall motion following nitroglycerin. *Circulation* 51: 140, 1975.
163. Henning H., Crawford M.H., Karlner J.S., O'Rourke R.A., Beneficial effects of nitroglycerin on abnormal ventricular wall motion at rest and during exercise in patients with previous myocardial infarction. *Am. J. Cardiol.* 37: 623, 1976.

164. Hoffman B.F., Bartelstone H.J., Scherlag B.J., Cranefield P.F., Effects of postextrasystolic potentiation on normal and failing hearts. *Bull. N.Y. Acad. Med.* 41: 498, 1965.
165. Cohn P.F., Gorlin R., Herman M.V., Sonnenblick E.H., Horn H.R., Cohn L.H., Collins J.J. Jr., Relation between contractile reserve and prognosis with coronary artery disease and a depressed ejection fraction. *Circulation* 51: 414, 1975.
166. Popio K.A., Gorlin R., Bechtel D., Levine J.A., Postextrasystolic potentiation as a predictor of potential myocardial viability: preoperative analyses compared with studies after bypass surgery. *Am. J. Cardiol.* 39: 944, 1977.
167. Horn H.R., Teichholz L.E., Cohn P.F., Herman M.V., Gorlin R., Augmentation of left ventricular contraction pattern in coronary artery disease by an inotropic catecholamine. The epinephrine ventriculogram. *Circulation* 49: 1063, 1974.
168. Bodenheimer M.M., Banka V.S., Trout R.G., Hermann G.A., Pasdar H., Helfant R.H., Local characteristics of the normal and asynergic left ventricle in man. *Am. J. Med.* 61: 650, 1976.
169. Williams J.F. Jr., Glick G., Braunwald E. Studies on cardiac dimensions in intact unanesthetized man: 5. Effects of nitroglycerin. *Circulation* 32: 767, 1965.
170. Mason D.T., Braunwald E., Effects of nitroglycerin and amyl nitrite on arteriolar and venous tone in the human forearm. *Circulation* 32: 755, 1965.
171. Langendorff O., Ueber elektrische Reizung des Herzens. *Arch. Physiol. (Arch. Anat. Physiol., Phys. Abt.)* 284, 1885.
172. Hoffman B.F., Bindler E., Suckling E.E., Postextrasystolic potentiation of contraction in cardiac muscle. *Am. J. Physiol.* 185: 95, 1956.
173. Cohn P.F., Editorial: Evaluation of inotropic contractile reserve in ischemic heart disease using postextrasystolic potentiation. *Circulation* 61: 1071, 1980.

CHAPTER IVa

ENDOCARDIAL LANDMARK MOTION; A NEW APPROACH TO THE ASSESSMENT OF REGIONAL LEFT VENTRICULAR PERFORMANCE

C.J. Slager, T.E.H. Hooghoudt, J.H.C. Reiber, J.C.H. Schuurbiens, P.D. Verdouw, P.G. Hugenholtz (submitted for publication in *Circulation Research*).

Abstract

In this study the hypothesis is tested that the motion pattern of small irregularities at the left ventricular endocardial border (endocardial landmarks), which can be detected in the contrast cineangiogram with an automated endocardial outlining system, indeed reflects the motion pattern of the endocardial wall. In 8 pigs metal markers were inserted with a new percutaneous retrograde transvascular approach. Marker motion was recorded with roentgen cinematography. Linear regression analysis of the directions of the systolic metal marker- and endocardial landmark-pathways shows a correlation coefficient of $r = 0.86$ and a SEE of 10.3° . This implies that the motion pattern of the landmarks may be used to describe the direction of endocardial wall motion. The endocardial landmark pathways in 23 normal human left ventricles form the base for the description of left ventricular wall motion in the normal individual.

Keywords: Left ventricular wall motion, endocardium, metal marker, automated outlining system.

INTRODUCTION

In this study a method to assess left ventricular wall motion, which relies on the pathways of anatomical structures at the endocardial border, is described and evaluated. Almost all previously described methods (1-5) to assess left ventricular wall motion are based on preconceived notions about the motion pattern of the left ventricular wall and lack a sound anatomical base.

Although contrast angiography provides detailed information on left ventricular wall motion, quantitative manual analysis of ventriculograms has not been able to reveal the actual pathways of specific sites on the endocardium. In animals these pathways could easily be followed with endocardially implanted metal clips (6-8) and roentgen-cinematography. For obvious reasons this approach was never performed in humans. In contrast, midwall motion (9) and epi-

cardial motion (10-13) have been studied in humans with surgically implanted markers. However, due to wall thickening major differences in extent and direction exist between the motion of neighbouring endocardial, midwall and epicardial sites (6, 14).

In an attempt to track specific sites of the endocardium in humans a new high resolution automated outlining system (15) was used. This revealed small irregularities at the left ventricular contrast border, which can be followed throughout the cardiac cycle by analysis of consecutive frames of the cine-angiogram. The hypothesis that these irregularities – which will further be referred to as “landmarks” – represent specific anatomical sites, has been tested and will be discussed in this article. The mean systolic pathways of these “anatomical landmarks” in normal individuals have been used to define a method for the assessment of left ventricular wall motion.

MATERIAL AND METHODS

a. Acquisition of left ventricular angiograms.

The first study group consisted of 23 individuals, submitted to a diagnostic heart catheterization because of suspected heart disease, who appeared to have no hemodynamic or angiographic abnormality. Patients were studied after an overnight fast without premedication; all drugs which might influence left ventricular contractile function were stopped at least 24 hours prior to the study. Left ventricular cineangiograms were made at resting heart rate, during injection of 0.75 ml/kg Urographin 76* at a rate of 16 - 18 ml/s with a 7 or 8 French angiographic catheter. The 30° RAO projection of the opacified ventricle was filmed at a rate of 40 - 80 (typical 50) frames per second with a 35 mm Arriflex cine-camera. During angiography care was taken to keep the patients' position with regard to the X-ray equipment unchanged, while respiratory motion was prevented by sustained respiration. For calibration purposes a centimeter grid was filmed at midthoracic level.

The second study group consisted of 8 pigs with a mean weight of 24 kg \pm 3 kg (mean \pm SD). The animals were sedated with 120 mg of azaperone i.m. (Stresnil**), subsequently they received 150 mg of metomidate (Hypnodil**), via a dorsal vein on the ear. After intubation the animals were ventilated with a Bennett respirator (BA-4***), with a mixture of 33% O₂ and 67% N₂O. Respiratory rate and tidal volume were adjusted according to arterial blood gases, which were frequently measured. A double lumen 8 F Courmand catheter was

* Schering AG., Berlin, Bergkammen, G.B.R.

** Janssen Pharmaceutica, Beerse, Belgium.

*** Bennett Respiration Inc., Los Angeles, California, U.S.A.

positioned in the superior vena cava via the left jugular vein for the continuous administration of the anesthetic (Pentothal 12-15 ml/kg/hr). Left ventricular pressures were obtained from catheters with a micromanometer at the tip (7 F Millar*). A 7 F Gorlin pacing catheter was introduced into the coronary sinus. A fixed heart rate of 10 bpm above resting heart rate was chosen and maintained during the study.

A left ventriculogram was made during injection of 0.75 ml/kg Urographin 76 through an 8 F angio catheter at a rate of 12 ml/s. The opacified ventricles were filmed from the left lateral projection at a rate of 50 frames per second. During angiography artificial respiration was stopped to exclude extracardiac motion.

b. Insertion of metal markers in pigs

After the acquisition of a technical satisfactory cineangiogram, specific sites of the endocardial wall were marked with small metal darts. For this purpose a spring-loaded insertion device (figure 1) attached to the tip of a flexible catheter** with tip steering facilities was used. The combination of a sharp barbed

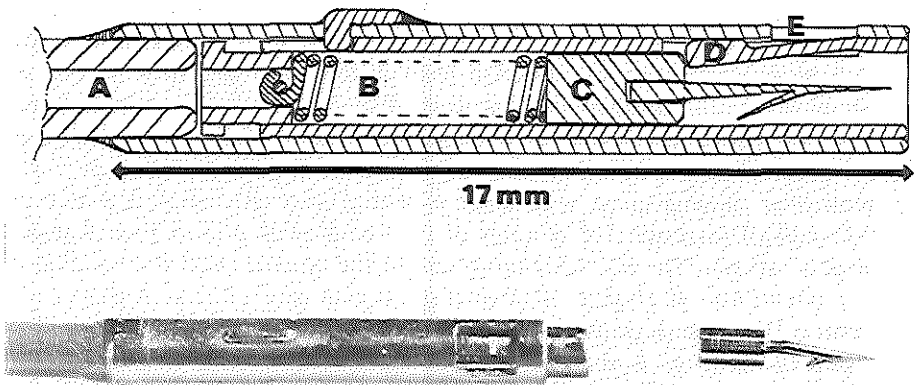


Figure 1. Schematic drawing and photograph of spring loaded metal marker insertion device attached to the tip of a 7 F catheter. The inner tube - including trigger lever D - is advanced by manual injection of saline into the catheter A, thus releasing metal marker C.

hook and a blunt body guarantees both an excellent fixation of the marker with minimal damage of the myocardium and an accurate delineation of the endocardium.

In each pig five markers were inserted along the anterior and inferoposterior margin of the left ventricle in a pattern outlining the ventricular cavity as seen

* Millar Instruments Inc., Houston, Texas.

** USCI Muller Guide System and Variflex 7 F catheter.

in the left lateral projection (figure 2). Care was taken to insert the marker in the outermost position. In order to detect possible myocardial injury due to the insertion procedure, the ECG and left ventricular pressure were monitored continuously. Once marker insertion was completed a second left ventricular angiogram was made with identical X-ray geometry and with the respirator turned off. Here again for calibration purposes a centimeter grid was filmed. An interval of at least 30 minutes was observed between the consecutive angiograms.

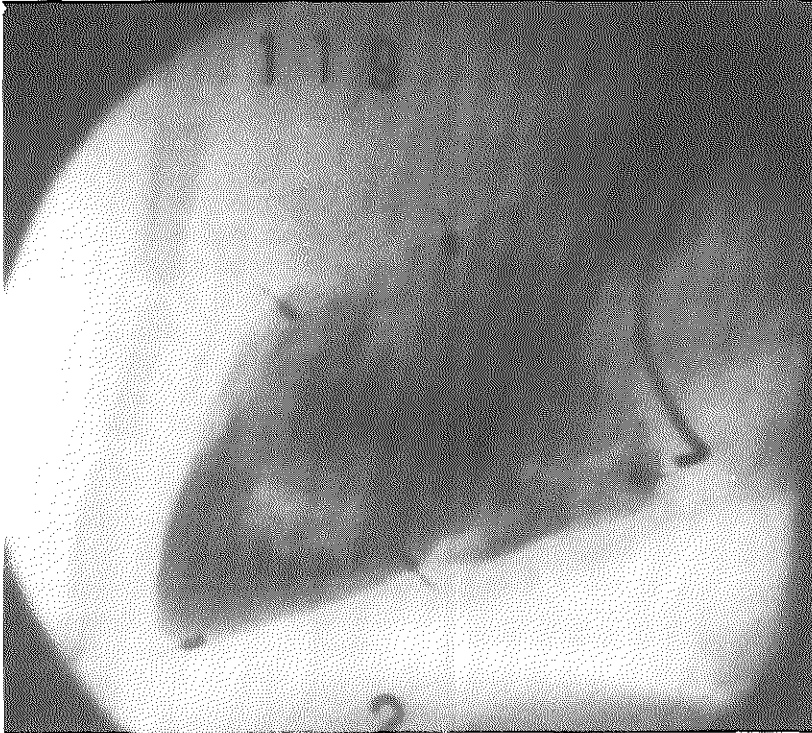


Figure 2. End diastolic frame from pig left ventricular angiogram with metal markers outlining the left ventricular cavity as seen in the left lateral projection.

c. Analysis of left ventricular angiograms

The endocardial outlines of all ventriculograms in this study were determined frame by frame with an automated contour detection system, the 'Contour-omat' (15). In each frame left ventricular volume was determined according to Simpson's rule (16). End diastole and end systole were defined as the moment of maximal and minimal left ventricular volume respectively. The detected contours of all frames of the systolic period were displayed on a videomonitor and were recorded on a single 8.3 x 10.8 cm Polaroid photograph. As the con-

tours were displayed according to a fixed external reference system (1) no procedures such as translation and rotation were applied. Figure 3a shows such a set of superimposed contours. Small irregularities at the left ventricular contrast border can be followed through the systolic period, however the information is partially obscured by the overlap of the successive contours. Therefore a shift procedure (17) was applied, to obtain more detailed information on the motion pattern of these "landmarks". After enlargement of the photographs the systolic pathways of these landmarks were drawn manually. Subsequent correction for the previously added shift yielded the actual systolic trajectories with respect to the original frame of reference (figure 3b).

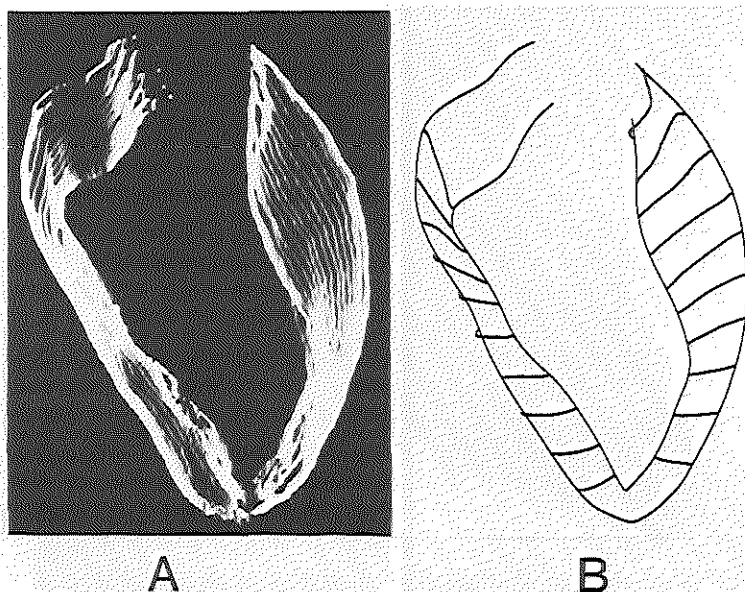


Figure 3a. Result of automated frame by frame analysis of the endocardial contours in the systolic period from a left ventricular cine angiogram.

Figure 3b. The pathways of small irregularities at the left ventricular contrast border (endocardial landmarks) were analyzed, resulting in a pattern of systolic trajectories (for details see text).

For each ventricle a non-indexed rectangular coordinate system was defined, with its origin coinciding with the end-diastolic apex, defined as the point at maximal distance from the superior aspect of the aortic valve (18). A basal transverse axis, which extends from the mitral valve fornx to a point on the opposite anterior wall, was constructed, so that an isosceles triangle with its vertex at the ventricular apex was the result of this procedure (figure 4). The ventricular long axis was defined as the median of this triangle through the

vertex; the y-axis of the coordinate system coincides with this line.

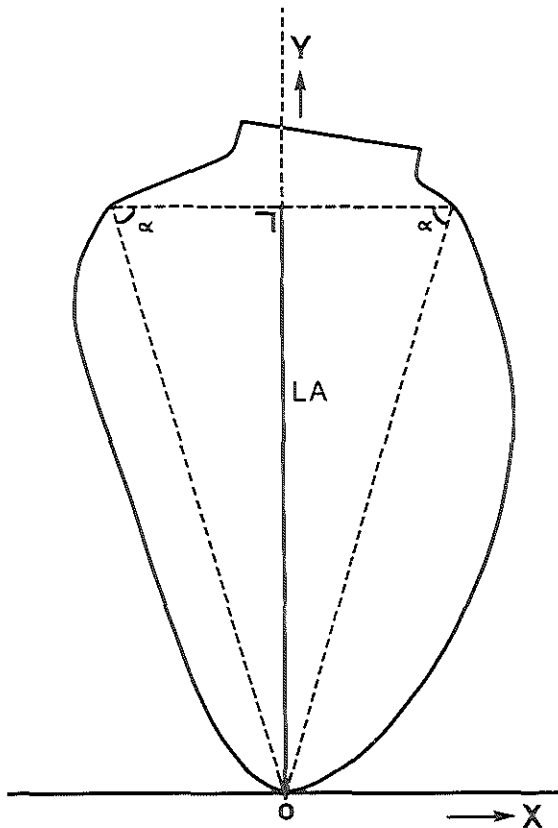


Figure 4. The median of an isosceles triangle with its vertex at the ventricular apex and its base extending from the mitral valve fornix, coincides with the y-axis of the applied rectangular coordinate system. Left ventricular long axis length (LA) is defined as the distance from base to apex.

To be able to compare the pathways of the landmarks of ventricles with different shapes and sizes, a normalization procedure was performed. From base to apex twenty points were defined by the intersections of the end diastolic contour and ten equidistant lines perpendicular to the y-axis (figure 5). These points were used as the end diastolic starting points for the assessment of the pathways of the endocardial landmarks. For both human and pig ventricles left ventricular dimensions were normalized such that for each study group, the end diastolic long axis lengths became equal to the mean value. After this procedure, corresponding starting points had equal y-coordinates.

Next, the (normalized) systolic trajectories with corresponding starting

points were shifted along the x-axis, such that the starting points coincided

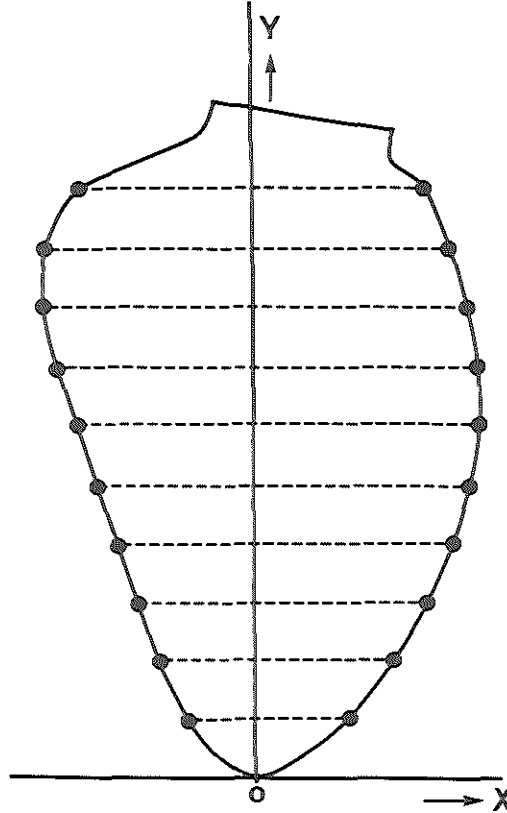


Figure 5. From base to apex at equidistant y-levels 20 end diastolic starting points are defined for the assessment of pathways of the endocardial landmarks.

and had an x-coordinate equal to the mean x-value (figure 6). The mean values and the standard deviations of the x- and y-components of the trajectory-vectors, originating from a corresponding starting point, were calculated.

d. Analysis of the motion pattern of implanted metal markers

From the projected contrast angiogram the end diastolic and end systolic contours and the respective positions of the implanted metal markers were drawn on a sheet of paper. Again a non-indexed rectangular coordinate system was defined as described above. With reference to this coordinate system the calibrated x- and y-coordinates of the end diastolic and end systolic marker positions were computed, thus defining the systolic marker pathways.

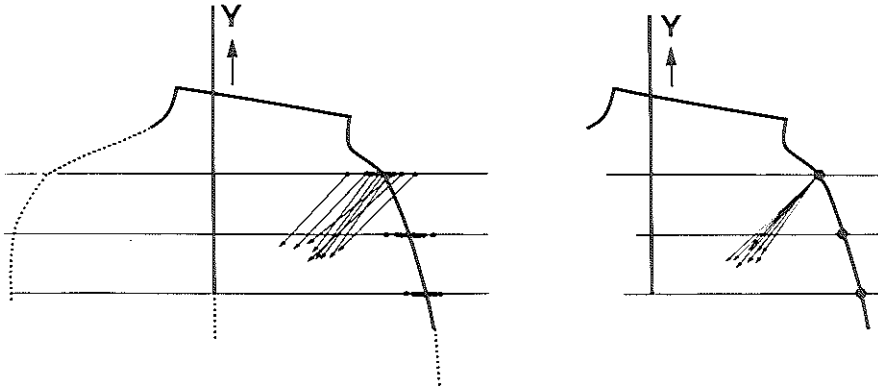


Figure 6. After normalization of the left ventriculograms for long axis length, corresponding starting points were shifted along the x-axis such that they coincide and have an x-coordinate equal to the mean x-value.

e. Comparison of endocardial landmark and metal marker pathways

With respect to the coordinate system, the individual pathways were divided into their x- and y-components, expressed as Δx and Δy . The direction of each pathway was defined as the acute angle between the pathway and the x-axis, in

formula: $\alpha = \text{arc tangent } \frac{|\Delta x|}{\Delta y}$ (figure 7). By means of linear regression analysis

the extent and direction of the metal marker pathways denoted as Δx_{metal} , Δy_{metal} and α_{metal} , were compared with the nearest corresponding endocardial landmark pathway denoted as Δx_{endo} , Δy_{endo} and α_{endo} .

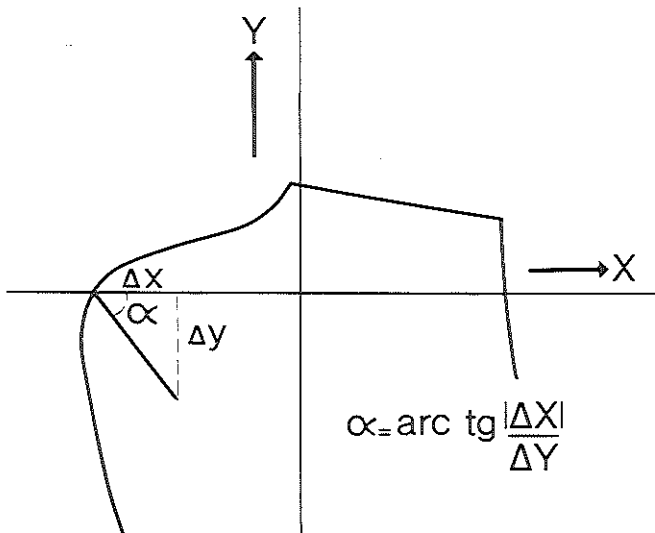


Figure 7. The direction of the pathways is defined as the acute angle between the pathway and the x-axis.

RESULTS

a. *Left ventriculograms in humans*

Figure 8 shows the normalized starting point positions which define the normalized shape of the end diastolic left ventricular contour in this study group of 23 normal human subjects. Mean left ventricular long axis length was 8.3 ± 1.3 cm (mean \pm SD). The mean x-coordinates and the standard deviations of the starting points after normalization are displayed as well.

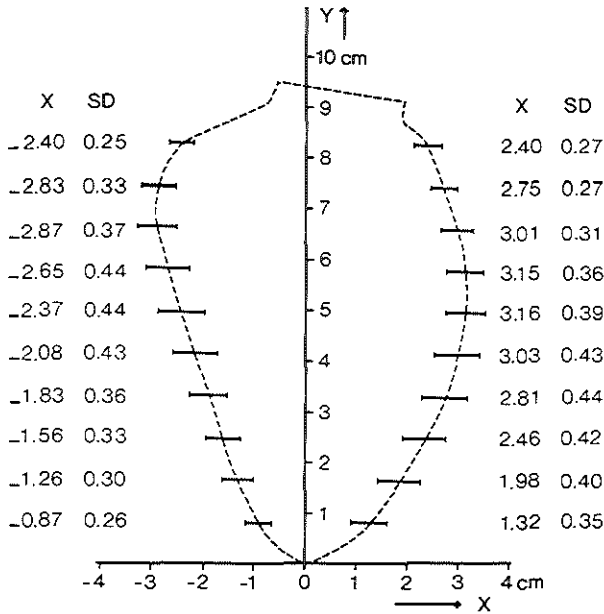


Figure 8. Normalized shape of the end diastolic left ventricular contour of 23 normal human subjects. Dimensions are expressed in cm. Mean left ventricular long axis length is 8.3 ± 1.3 cm (mean \pm SD).

In figure 9 the mean systolic pathways of the endocardial landmarks in the study group of normal individuals are shown. The x- and y-components of each particular pathway are expressed as Δx and Δy . The standard deviations are given as well and are expressed in the figure by rectangles. In figure 10 the points of intersection of the pathways extending from the ten pairs of opposing starting points are depicted. The x- and y-coordinates of the intersection points are given as well. In one case no point of intersection could be found within the ventricular cavity, because of an almost parallel course of the facing trajectories.

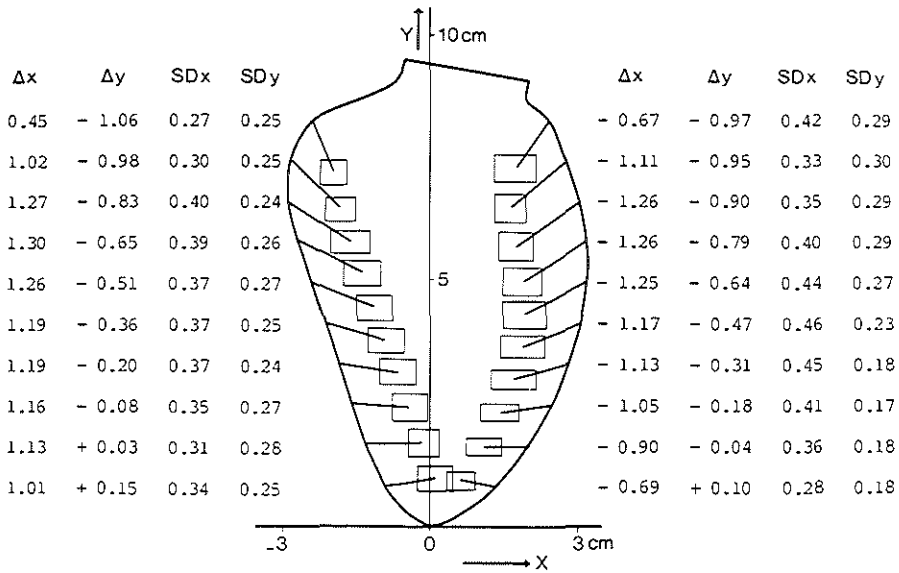


Figure 9. Mean systolic left ventricular endocardial landmark pathways in normal human individuals. The x- and y-components of each pathway are expressed as Δx and Δy . The rectangles represent the standard deviation of Δx and Δy .

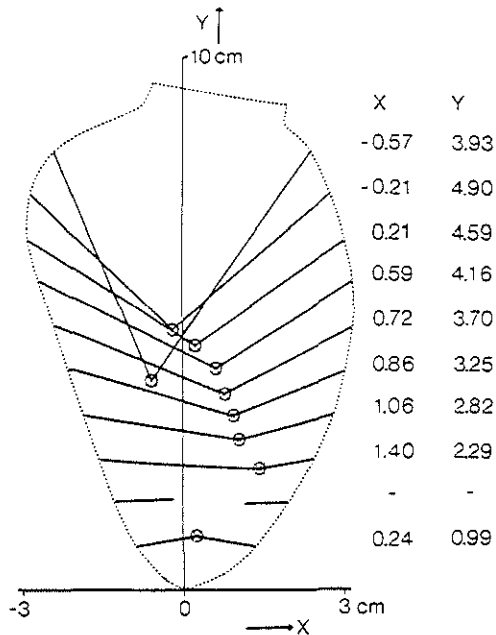


Figure 10. Points of intersection of the pathways extending from the 10 pairs of opposing starting points. The x- and y-coordinates of the intersection points are given.

b. *Hemodynamics before and after metal marker insertion in pigs*

In table I the mean and standard deviations of the hemodynamic variables left ventricular end diastolic volume (LVEDV), ejection fraction (EF), end diastolic pressure (LVEDP) and peak dP/dt (peak rate of change of pressure) as well as the heart rate (HR), before and after metal marker insertion are shown. To evaluate the statistical significance of the hemodynamic changes during the study, the paired t-test was applied (border of significance: $p = 0.05$).

Table I. *Hemodynamic data before and after implantation of metal markers in 8 pigs.*

		control	markers implanted	statistical significance
LVEDV	(ml)	28.5 ± 5.2	29.4 ± 6.7	NS
EF	(%)	61.4 ± 14.2	56.3 ± 12.0	NS
LVEDP	(kPa)	1.4 ± 0.3	1.1 ± 0.5	NS
pk dP/dt	(kPa/s)	230 ± 37	191 ± 52	NS
HR	(bpm)	88 ± 5	87 ± 3	NS

Abbreviations: LVEDV: left ventricular end diastolic volume, EF: ejection fraction, LVEDP: left ventricular end diastolic pressure, HR: heart rate, bpm: beats per minute, NS: not significant.

c. *Endocardial wall motion in pigs*

In figure 11 the normalized systolic pathways of the endocardial landmarks of each individual pig (1a - 8a) are shown. For each individual pig ventricle the systolic pathway of the implanted metal markers is shown as well (1b - 8b). Linear regression analysis of the x- and y-components of corresponding pathways of endocardial landmarks (Δx_{endo} and Δy_{endo}) and of metal markers (Δx_{metal} and Δy_{metal}) gives a correlation coefficient of $r = 0.74$ and $r = 0.86$ respectively ($|\Delta x_{\text{endo}}| = 0.16 \text{ cm} + 1.2 |\Delta x_{\text{metal}}|$, $\Delta y_{\text{endo}} = -0.13 \text{ cm} + \Delta y_{\text{metal}}$, $n = 41$).

The relation between the directions of the endocardial pathways and of the metal marker pathways was also evaluated with linear regression analysis (figure 12) ($\alpha_{\text{endo}} = 0.86 \alpha_{\text{metal}} - 2.9^\circ$, $n = 33$). In this comparison the apical segments were excluded, as the displacement of these segments is characterized by very short trajectories, which makes accurate assessment of the motional direction almost impossible.

In figure 13 the normalized shape of the end diastolic left ventricular contours of the eight pigs of this study is shown. Mean left ventricular long axis length was $7.3 \pm 0.4 \text{ cm}$ (mean \pm SD). The mean systolic pathways of the endocardial landmarks are shown as well. The x- and y-components are expressed as Δx and Δy . The standard deviations are displayed in the figure by rectangles.

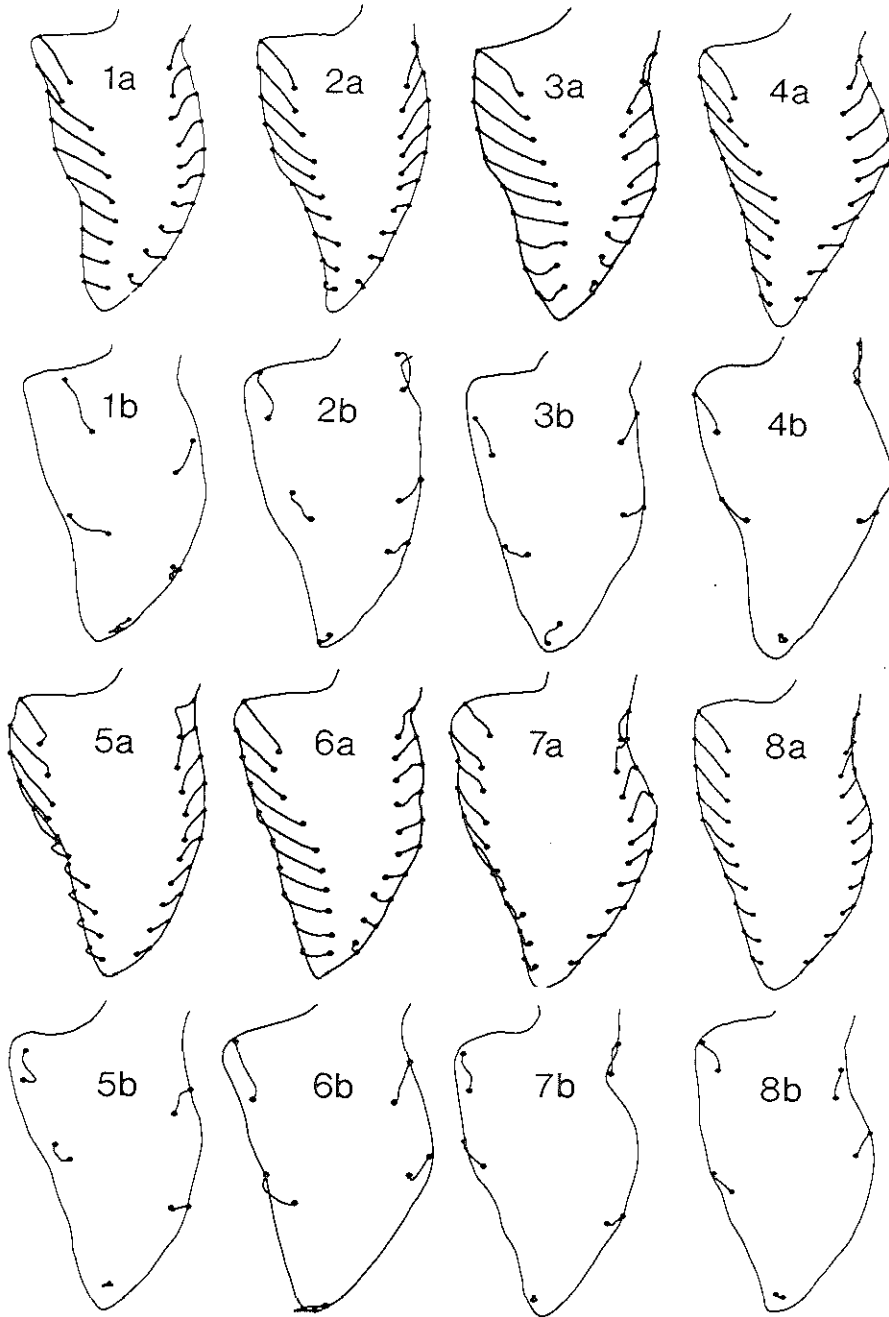


Figure 11. Normalized left ventricular systolic pathways of the endocardial landmarks of each individual pig are shown (1a - 8a). In 1b - 8b the systolic pathways of the implanted metal markers in the same pig ventricles are shown.

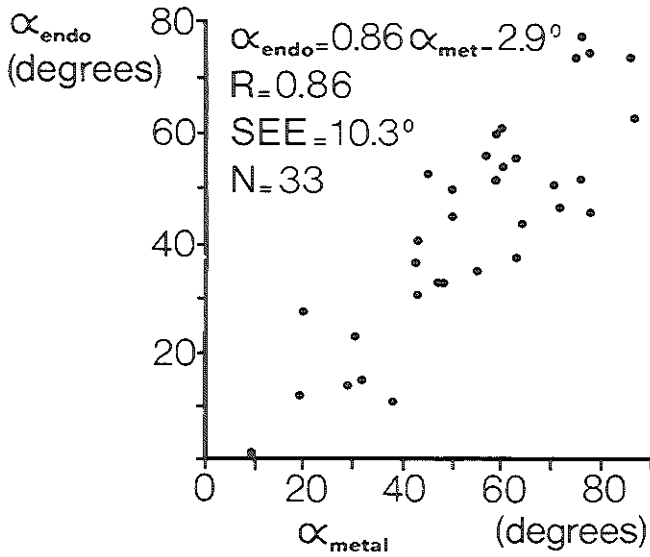


Figure 12. Relation between the directions of endocardial pathways (α_{endo}) and of metal marker pathways (α_{metal}).

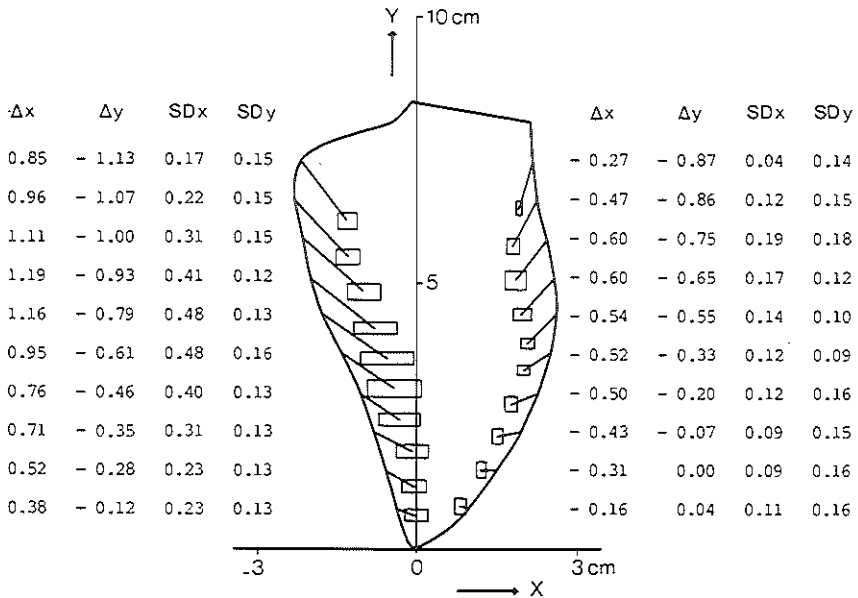


Figure 13. Normalized shape of left ventricular end diastolic contours in 8 pigs. Mean left ventricular long axis length is 7.3 ± 0.4 cm (mean \pm SD). The mean systolic pathways of the endocardial landmarks are shown as well. The rectangles represent the standard deviations of the respective x- and y-components (Δx and Δy) of the pathways.

DISCUSSION

Quantitative analysis of left ventricular wall motion in humans from angiograms, has been hampered by the lack of an accurate and generally accepted procedure to track specific sites at the endocardial border. Early experience with an automated endocardial outlining system (19) suggested the existence of endocardial landmarks which reappeared in consecutive frames of the cineangiogram, and could thus be followed over the cardiac cycle. The aim of this study is to test the hypothesis that the motion pattern of these landmarks reflects the motion pattern of actual anatomical structures at the endocardial border.

It is obvious that in humans no direct proof of this hypothesis could be reached, as this would need endocardial marker implantation, which is presently the most accurate method to assess local endocardial wall motion. The animal experiment was thus chosen to compare the motion pattern of endocardial landmarks and of metal markers. To insert the metal markers the percutaneous retrograde transvascular approach was chosen, in order to minimize the damage afflicted to the myocardium. Analysis of hemodynamic variables (table I) and ECG, before and after marker insertion indeed showed no signs of significant cardiac damage resulting from the procedure. In one pig a minor change of the T-wave was observed. In no case, visual inspection of the myocardium revealed any detectable damage at the place of marker insertion (figure 14).

Linear regression analysis of the endocardial landmark and metal marker pathways in pigs, shows an acceptable correlation coefficient of the y-components ($r = 0.86$), but a much lower correlation coefficient of the x-components ($r = 0.74$). This discrepancy can be explained by the exaggerated endocardial inward motion, which is observed on the contrast angiogram. This overestimation of systolic wall motion is caused by expression of contrast media from the intertrabecular spaces (2, 7, 11, 20-22), and is in agreement with the discrepancy in observed per cent wall thickening between the contrast media method (23-25) and the bead and clip (7) and ultrasonic crystal (26, 27) methods. Comparison of the direction of the endocardial landmark and metal marker pathways, shows a fairly good correlation ($r = 0.86$) and a rather small standard error of the estimate of 10.3° . Taken together, these data imply that the endocardial trajectories indeed represent the motion of actual anatomical landmarks.

In humans, in the various segments from base to apex, the y-components of the endocardial landmark trajectories show a gradually decreasing descent towards the apex. This agrees with the systolic descent of the base which is observed by many authors in the animal experiment (6, 28-30) and in humans (11, 12, 31). The apical landmark motion in the y-direction is very small, although in many cases visual inspection of the contrast angiogram would suggest a considerable apical ascent towards the base. This seeming contradiction is caused by complete extrusion of contrast media from the apex in late systole.

Through analysis of contrast angiograms, many authors came to the erroneous conclusion that the apex moves considerably towards the base during systole (32, 33), and consequently overestimated long axis shortening (31-33). In

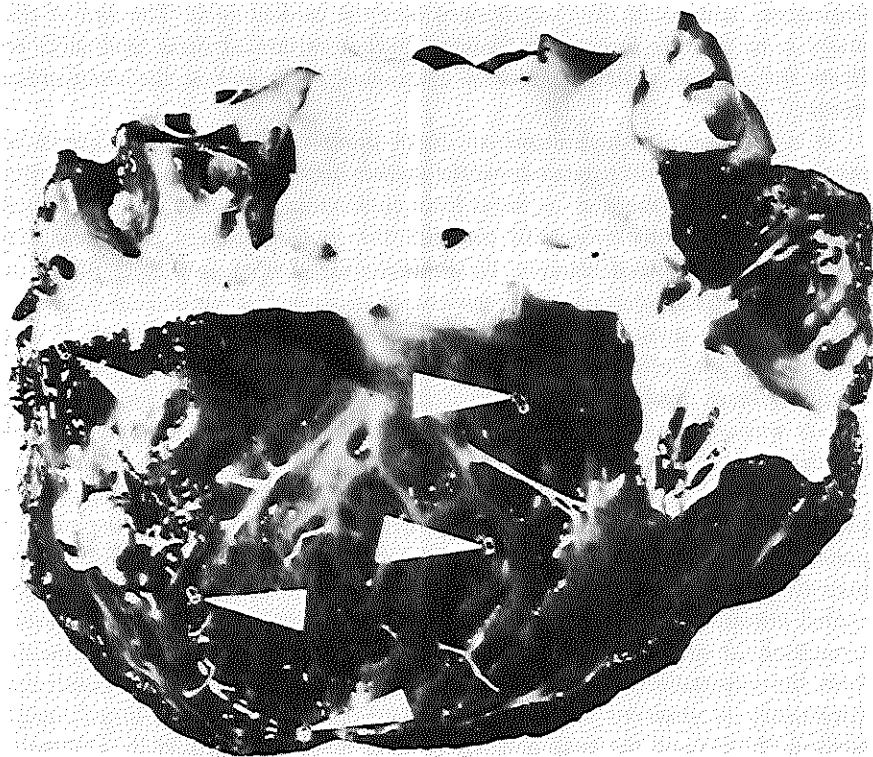


Figure 14. Pig left ventricle dissected after the experiment. Arrows indicate the inserted metal markers.

addition, contrast angiograms suggest a substantial rotation of the apex along the left ventricular long axis, a phenomenon which is partially due to exclusion of dye by the posterior papillary muscle. However, earlier studies with epicardial and endocardial markers had unmistakably shown that the apex is remarkably stationary during systole (6, 11, 12, 28). Accordingly, the systolic motion of the apical metal markers as displayed in figure 11, 6b, is only minute, although the contrast angiogram in many instances would suggest considerable apical ascent and rotation (figure 15). The observed pattern of endocardial landmark motion

in normal human subjects, is believed to provide a good approximation of actual endocardial wall motion. To make the observed motion pattern applicable to the analysis of regional wall motion in other subjects, it was formulated as a generalized mathematical expression. The points of intersection of landmark trajectories originating from starting points at equal y-levels clearly do not coincide into one central point, but rather can be connected by a curved central axis. (figure 10).

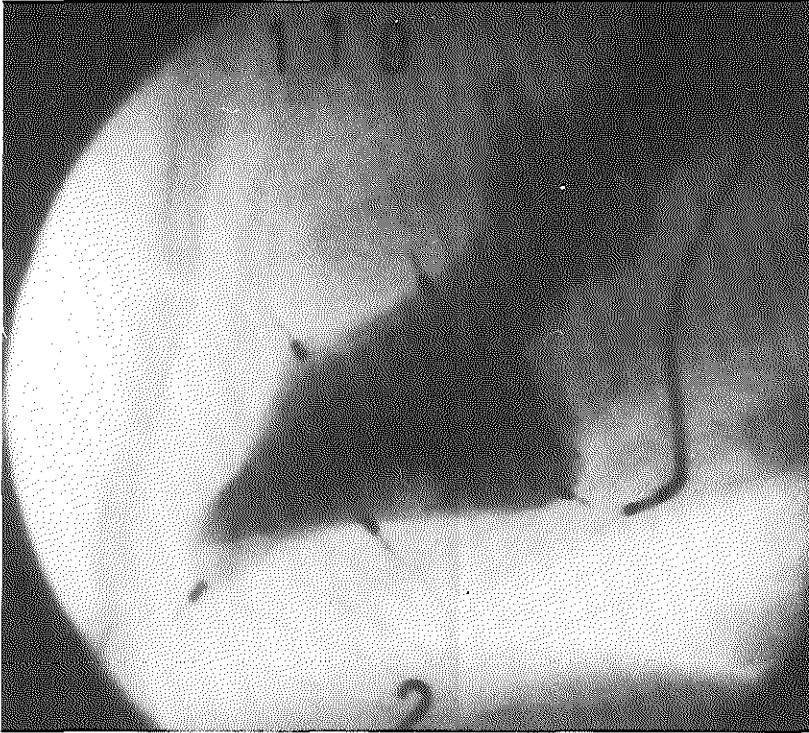


Figure 15. End systolic frame of left ventricular cineangiogram after marker insertion. The corresponding end diastolic frame is shown in figure 2. Squeezing of contrast from the apex may result in an apparent rotation and ascent of the apex as observed on the contrast angiogram, while the end diastolic and end systolic metal marker positions are almost identical (see figure 11, 6b).

The midpoints of corresponding opposite end diastolic starting points, which from base to apex show a similar curved course, were used to obtain a simple but still accurate approximation of the successive x-coordinates of the points of intersection, in formula:

$$X_{PI} = 0.5 (X_{SPa} + X_{SPi})$$

where: X_{PI} is the x-coordinate of the point of intersection and
 X_{SPa} is the x-coordinate of the starting point at the anterior wall and
 X_{SPi} is the x-coordinate of the starting point at the inferoposterior
 wall.

A good approximation of the y-coordinates of the points of intersection (Y_{PI}) is obtained from the y-coordinate of the corresponding starting points (Y_{SP}) and from left ventricular end diastolic long axis length (LA), according to the

$$\text{formula: } Y_{PI} = LA \left[0,57 - 0,53 \left| 1 - 1,1 \frac{Y_{SP}}{LA} \right| 1,4 \right]$$

where: Y_{PI} is the y-coordinate of the point of intersection and
 Y_{SP} is the y-coordinate of the starting points.
 LA is the end diastolic left ventricular long axis length.

In figure 16 the points of intersection and the direction of regional wall

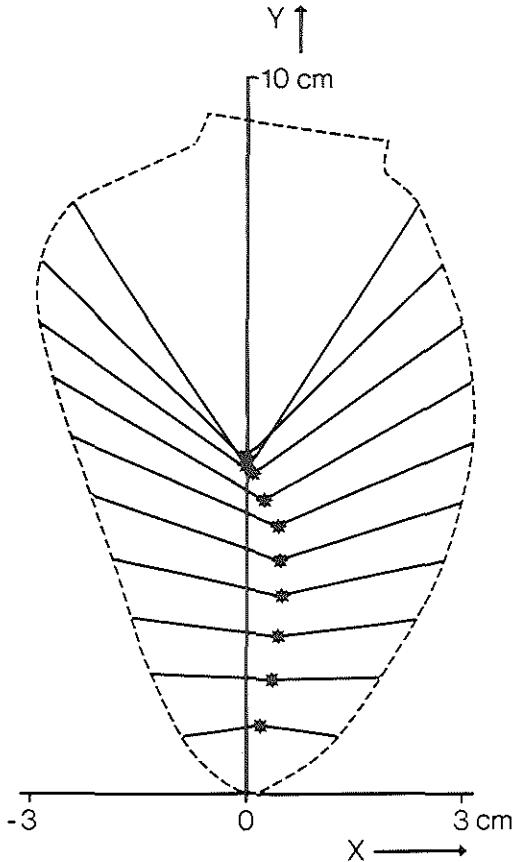


Figure 16. Points of intersection of the trajectories and direction of regional wall motion as derived from the normalized end diastolic contour using the mathematical expression described in the text.

motion as derived from the normalized end diastolic contour (figure 8), using the mathematical expressions described above, are shown. Comparison of figure 10 and figure 16 clearly show that this mathematical description provides a good approximation of the direction of the actually measured endocardial wall motion trajectories.

To conclude: the motion pattern of irregularities appearing at the endocardial border, as detected with an automated technique for the analysis of cineangiograms, reflects the motion pattern of actual anatomical structures. Using this technique, a detailed description of normal endocardial wall motion has been made, which provides the base for the further development of methods to quantify regional left ventricular function.

REFERENCES

1. Chaitman B.R., Bristow J.D., Rahimtoola S.H., Left ventricular wall motion assessed by using fixed external reference systems. *Circulation* 48: 1043, 1973.
2. Herman M.V., Heinle R.A., Klein M.D., Gorlin R., Localized disorders in myocardial contraction. *N. Eng. J. Med.* 227: 222, 1967.
3. Leighton R.F., Wilt S.M., Lewis R.P., Detection of hypokinesis by a quantitative analysis of left ventricular cineangiograms. *Circulation* 50: 121, 1974.
4. Harris L.D., Clayton P.D., Marshall H.W., Warnet H.R., A technique for the detection of asynergistic motion in the left ventricle. *Comp. Biomed. Res.* 7: 380, 1974.
5. Rickards A., Seabra-Gomes R., Thurston P., The assessment of regional abnormalities of the left ventricle by angiography. *Eur. J. Cardiol.* 5: 167, 1977.
6. Rushmer R.F., Crystal D.K., Wagner C., The functional anatomy of ventricular contraction. *Circ. Res.* 1: 162-170, 1953.
7. Mitchell J.H., Wildenthal K., Mullins C.B., Geometrical studies of the left ventricle utilizing biplane-cinefluorography. *Fed. Proc.* 28: 1334-1343, 1969.
8. Carlsson E., Milne E.N.C., Permanent implantation of endocardial tantalum screws. A new technique for functional studies of the heart in the experimental animal. *J. Assoc. Can. Radiol.* 19: 304-309, 1967.
9. Ingels N.B., Daughters G.T., Stinson E.B., Alderman E.L., Measurement of midwall myocardial dynamics in intact man by radiography of surgically implanted markers. *Circulation* 52: 859, 1975.
10. Harrison D.C., Goldblatt A., Braunwald E., Glick G., Mason D.T., Studies on cardiac dimensions in intact, unanesthetized man. I. Description of techniques and their validation. *Circ. Res.* 13: 448, 1963.
11. McDonald I.G., The shape and movements of the human left ventricle during systole. *Am. J. Cardiol.* 26: 221, 1970.
12. McDonald I.G., Contraction of the hypertrophied left ventricle in man studied by cineradiography of epicardial markers. *Am. J. Cardiol.* 30: 587-594, 1972.
13. Brower R.W., ten Katen H.J. and Meester G.T., Direct method for determining regional myocardial shortening after bypass surgery from radiopaque markers in man. *Am. J. Cardiol.* 41, 1222, 1978.
14. Wildenthal K., Mitchell J.H., Dimensional analysis of the left ventricle in unanesthetized dogs. *J. Appl. Physiol.* 27: 115, 1969.

15. Slager C.J., Reiber J.H.C., Schuurbiens J.C.H. and Meester G.T., Contouromat: A hard-wired left ventricular angioprocessing system. I. Design and application. *Comput. Biomed. Res.* 11: 491, 1978.
16. Chapman C.B., Baker O., Reynolds J. and Bonte F.J., Use of biplane cinefluorography for measurement of ventricular volume. *Circulation* 18: 1105, 1958.
17. Slager C.J., Hooghoudt T.E.H., Reiber J.H.C., Schuurbiens J.C.H., Booman F. and Meester G.T., Left ventricular contour segmentation from anatomical landmark trajectories and its application to wall motion analysis. *Computers in Cardiology*, pp. 347-350, IEEE Computer Society, Long Beach, Calif. 1979.
18. Brower R.W., Evaluation of pattern recognition rules for the apex of the heart. *Catheterization and Cardiovascular Diagnosis* 6: 145, 1980.
19. Slager C.J., Reiber J.H.C., Schuurbiens J.C.H. and Meester G.T., Automated detection of left ventricular contour. Concept and application. In: *Roentgen-Video-Techniques*. Ed. P.H. Heintzen and J.H. Buersch. pp. 158-167. Georg Thieme Stuttgart, 1978.
20. Chapman C.B., Baker O., Mitchell J.H., Experiences with a cinefluorographic method for measuring ventricular volume. *Am. J. Cardiol.* 18: 25, 1966.
21. Mitchell J.H. and Mullins C.B., In: *Factors influencing myocardial contractility*, edited by Tanz R.D., Kavalier F., Roberts J. New York: Academic, 1967, p. 177.
22. Hugenholz P.G., Kaplan E., Hull E., Determination of left ventricular wall thickness by angiocardigraphy. *Am. Heart J.* 78: 513, 1969.
23. Sandler H. and Dodge H.T., Left ventricular tension and stress in man. *Circulation Res.* 13: 91, 1963.
24. Eber L.M., Greenberg H.M., Cooke J.M. and Gorlin R., Dynamic changes in left ventricular free wall thickness in the human heart. *Circulation* 39: 454, 1969.
25. Dumesnil J.G., Ritman E.L., Frye R.L., Gau G.T., Rutherford B.D. and Davis G.D., Quantitative determination of regional left ventricular wall dynamics by Roentgen Videometry. *Circulation*, 50: 700, 1974.
26. Sasayama S., Franklin D., Ross J. Jr., Kemper W.S., Mc Kown D., Dynamic changes in left ventricular wall thickness and their use in analyzing cardiac function in the conscious dog. *Am. J. Cardiol.* 38: 870, 1976.
27. Osakada G., Sasayama S., Kawai C., Hirakawa A., Kemper W.S., Franklin D. and Ross, J. Jr., The analysis of left ventricular wall thickness and shear by an ultrasonic triangulation technique in the dog. *Circulation Res.* 47: 173, 1980.
28. Hamilton W.F., Rompf J.H., Movements of the base of the ventricle and the relative consistency of the cardiac volume. *Amer. J. Physiol.* 102: 559, 1932.
29. Tsakiris A.G., van Bernuth G., Rastelli G.C., Bourgolis M.J., Titus J.L. and Wood E.H., Size and motion of the mitral valve annulus in anesthetized intact dogs. *J. Appl. Physiol.* 30: 611, 1971.
30. Hinds J.E., Hawthorne E.H., Mullins C.B. and Mitchell J.H., Instantaneous changes in the left ventricular lengths occurring in dogs during the cardiac cycle. *Fed. Proc.* 28: 1351, 1969.
31. Brower R.W. and Meester G.T., Computer based methods for quantifying regional left ventricular wall motion from cine ventriculograms. *Computers in Cardiology*, pp. 55-62, IEEE Computer Society, Long Beach, California, 1976.
32. Leighton R.F., Wilt S.M. and Lewis R.P., Detection of hypokinesis by a quantitative analysis of left ventricular cineangiograms. *Circulation* 50: 121, 1974.
33. Rickards A., Seabra-Gomes R. and Thurston P., The assessment of regional abnormalities of the left ventricle by angiography. *Europ. J. Cardiol.* 5: 167, 1977.

ACKNOWLEDGEMENT

The authors wish to express their gratitude to Mr J. van Oosten, of the Technical University of Delft, who constructed with great craftsmanship the springloaded insertion device used in this study.

Although some aspects of the paper "Left ventricular contour segmentation from anatomical landmark trajectories and its application to wall motion analysis" (Chapter IVb) were already described in chapter IVa, this preliminary report is added to inform the reader about the progress made in 1979 with the development of a new method to analyze regional left ventricular wall motion.

(See following pages)

CHAPTER IVb

LEFT VENTRICULAR CONTOUR SEGMENTATION FROM ANATOMICAL LANDMARK TRAJECTORIES AND ITS APPLICATION TO WALL MOTION ANALYSIS

C.J. Slager, T.E.H. Hooghoudt, J.H.C. Reiber, J.C.H. Schuurbiens, F. Booman and G.T. Meester, Reprinted from *Computers in Cardiology*, IEEE Computer Society, 1979, pp. 347-350.

Summary

A new model is proposed for measuring left ventricular (LV) wall motion from cineangiograms. The model is based on data about the endocardial wall motion derived from anatomical landmark trajectories which could be defined from automatically detected LV contours. The systolic motion of 23 normal left ventricles is described and clinical applications are discussed.

INTRODUCTION

For the quantitative assessment of segmental wall motion from left ventricular (LV) angiograms a great number of methods have been proposed (1, 2). The ultimate goal of these measurements is to derive local contraction parameters from LV motion data. The reasons behind the existence of so many different methods are:

- 1) there is a lack of knowledge concerning the true local motion of the endocardial wall in the intact left ventricle. As a result of this it is not possible to define reliable vectors at different endocardial locations along which motion can be measured;
- 2) even if it was known how the endocardium moves locally, at this moment there is no reliable way to discriminate between motion and contraction. In this paper new data on the local endocardial motion are presented. Based on this information a method to determine local LV wall motion and its clinical applications will be discussed.

Anatomical landmarks

In previous publications (3) we have shown that it is possible to obtain true information on the local endocardial contraction by studying LV outlines that

that have been detected automatically with the hardwired contour detector, the Contouromat. These outlines show many small details that appear to correspond with local endocardial irregularities. In Fig. 1 an illustration is given of the method which is used to derive local LV motion from these details. Fig. 1A shows a superimposition of a systolic set of LV outlines. The successively detected anterior and inferior contour segments have been translated in opposite directions, in such a way that almost no overlap occurs between the outlines. The dots in the upper part of the picture represent successively added distances. In Fig. 1B small line segments have been traced that follow the observed local motion patterns which are caused by consistently appearing outline details. Guided by these many small traced lines the observer draws as a next step trajectories that cover the complete period to be analyzed (Fig. 1C). In this example these trajectories are drawn at random locations in order to show that they may be indicated anywhere. As a final step, the intersection points of the trajectories and the outlines are translated to the original positions by subtracting the added shift distances (Fig. 1D).

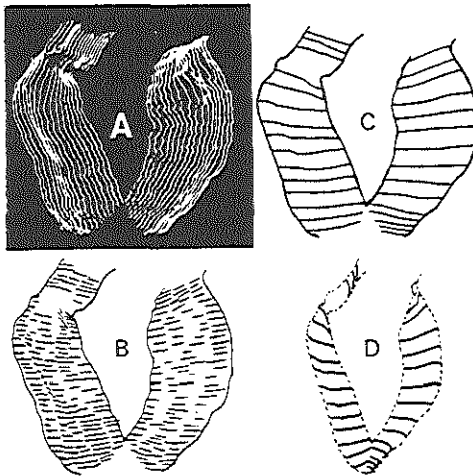


Fig. 1. Small details in the automatically detected left ventricular (LV) outlines (a) corresponding with small anatomical landmarks, can be used to reconstruct the local endocardial wall motion (d). For a more detailed explanation see text.

In this example with a rather narrow apex, the opposite walls completely fill up the apex portion of the ventricle near end systole (ES). This can be concluded from following the landmark trajectories near the apex. As a result the ES contrast silhouette shows an apical point of which the endocardial location does not correspond with the end diastolic (ED) apex location. Therefore, obtaining a good observer agreement for the determination of the apparent ES

apex, as will be the case with this example, is not a guarantee for the correct determination of the true ES apex location.

False patterns which may have been generated by intervening background structures during the outlining procedure can be clearly recognized because their appearance deviates strongly from the normal observed patterns. In a normally contracting part of the ventricle there is a continuous change in the observed number of details since some of them disappear as a result of the enfolding behavior of the endocardial wall. Inherently, others will be generated because newly enclosed spaces between the trabeculations reach the border of the LV contrast silhouette. Rotation probably plays a less important role; because its effect is proportional to the cosine of the angle of rotation. Nevertheless all the details which appear or disappear at a certain location of the outline belong to the same small endocardial area, so that all the different detail trajectories in that region will still point into the same direction.

Validation

As a first step to validate the developed trajectories-method, the intra-observer variability has been measured by tracing at four different occasions the trajectories of 13 different sets of contours, representing normal LV systolic silhouettes at 20 msec intervals. A fixed rectangular coordinate system with the y-axis passing through the apex and the mitral valve-aortic junction, was defined for the ED outline. For both the anterior and inferior outlines 10 trajectories were traced. The beginning points of the trajectories were chosen at evenly distributed positions between the base and the apex on the ED outline. The positions of the ES end points were determined for calculating the intra-observer variability. Measured over a total of 1040 trajectories the observer produced a mean standard deviation of 1.4 mm in the y-direction. Determination of the standard deviation in the x-direction which will be much smaller than the 1.4 mm was not meaningful as the x-components of the trajectories are mainly dependent on the actual detected contour position.

The method was also validated by simultaneously filming a LV contrast silhouette and small roentgenopaque rings sutured to the endocardium with Roentgencinematography. For the time being a total of 10 isolated post mortem left ventricles of pigs, periodically forced into a compressed state with the aid of a sucking pump, were used. It is emphasized that for the ultimate goal of the experiment simulation of normal LV motion is not required. The only intention was to investigate the accuracy of deriving local endocardial motion from the angiograms and to demonstrate that the anatomical landmarks are meaningful and that they are not artifacts generated by the Contouromat. Three rings were visible at each side of the contrast silhouette; for each side a fixed rectangular coordinate system was defined with the y-axis passing through the ring near the

base and the ring near the apex. During the experiment 3 rings got lost so that a total of 57 rings could be compared with the neighboring anatomical landmarks. Linear regression analysis resulted in a correlation coefficient of 0.93 between the y-components of the trajectories and the y-components of the ring motion. The standard error of the estimate (s.e.e.) equals 1.22 mm, which can be explained from the observer variability. A slight underestimation of the y-component by 8% can be concluded from the slope of the regression equation:

$$y_{\text{landmarks}} = 0.92 y_{\text{rings}}$$

The best linear fit through the x-components yielded a much lower correlation coefficient of 0.59. The regression equation is described by:

$$x_{\text{landmarks}} = 3.4 \text{ mm} + 0.89 x_{\text{rings}}$$

This result can be explained from the strong enfolding of the endocardium during this experiment which caused the outlines to be detected too far inside. For this reason this result should not be considered to be representative for normal contracting human left ventricles.

Landmark trajectories in 23 normals

For 23 patients, who appeared to have completely normal haemodynamic findings and no coronary artery stenosis as judged by experienced observers, the systolic landmark trajectories have been determined from their LV angiograms. In Fig. 2 the normalized, mean systolic contours are shown at 4 equal time intervals from the moment with the largest volume (ED) until the moment with the smallest volume (ES). For each ventricle a non-indexed rectangular coordinate system was defined with the origin located at the ED apex location and with the y-axis passing through the midpoint of the basal transverse axis. To define this base line denoted $y = y_b$, the mitral valve fovea is determined and the distance from the apex to this point encircled to define the intersection point of the base line with the anterior part of the contour. On the ED outline a total of 20 identification points were defined having y-coordinates equal to $ny_b/10$ with $n = 1, 2 \dots 10$ (Fig. 2). In the figure the dotted lines represent the mean traced systolic trajectories for the different segments. Mean standard deviations of the endsystolic trajectory points are 2.5 mm for the y-direction and 3.5 mm for the x-direction. Descent of the base line towards the apex during the systolic interval equals 12.6% of y_b . Motion of the transverse axis between segments 10 and 20 towards the base equals 1.5% of y_b . When constructing the best linear fit through the midpoints of the ED and of the ES transverse axes (connecting opposite segments like 2-12, 3-13 etc.) and com-

paring both lines, a systolic anticlockwise rotation of 2.5° was found. Both lines intersect at $x = 0,05$ cm and $y = 8.2$ cm.

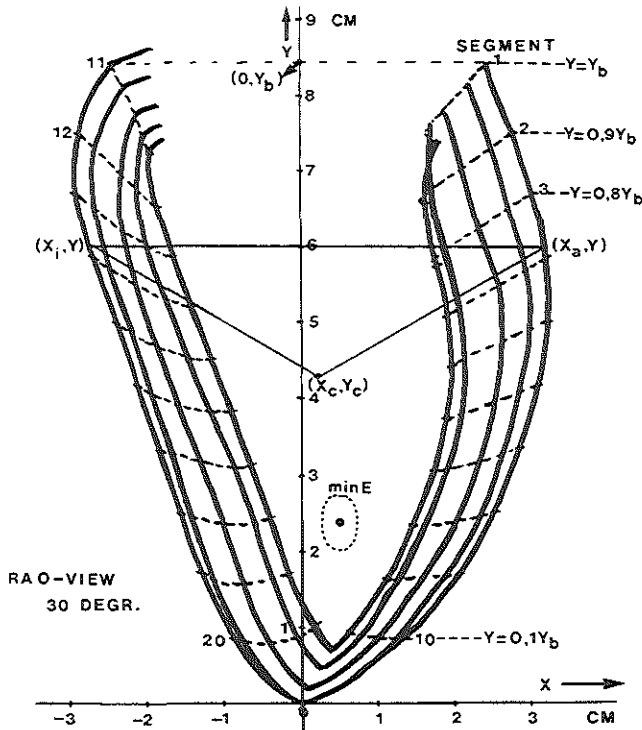


Fig. 2. Normalized systolic contours, averaged over a total number of 23 LV angiograms of normal patients at 4 equal time distances from ED to ES. The dotted lines represent the averaged landmark trajectories for 20 well-defined ED outline locations. For each pair of two opposite ED contour points (X, Y) and (X_a, Y) , a center of contraction (X_c, Y_c) is defined.

In the figure an area of minimum error has been indicated, useful as center of contraction, following the approach in Ref. 2. Although there is good agreement between the two approaches for the location of this area, an important difference remains between the motion derived from the landmark trajectories and the motion of the intra-myocardial markers. The landmarks move in a more transversal way which can be explained from the influence of the thickening muscle between the endocardium and the intra-myocardial markers. This means that using a single point as center of contraction will certainly not be optimal when determining endocardial LV motion from contrast angiograms. An average overestimation of 4.3 mm per segment resulted when the systolic wall motion of the 23 normals was determined by measuring the distance between the ED and ES outlines along radii pointing towards the center of the minimum error area. It has appeared that by defining a separate center of contraction for each two opposing ED contourpoints, having the same y-coordinate, an accurate mathematical description can be given for the averaged direction of the ana-

tomical landmark trajectories. Let (x_i, y) be the x, y coordinates of a point on the inferior wall and (x_a, y) the coordinates of a point on the anterior wall. Then the center of contraction having x, y coordinates (x_c, y_c) can be calculated from expressions (1) and (2):

$$x_c = (x_a + x_i) / 2 \quad (1)$$

$$y_c = y_b (0.57 - 0.53 | 1 - 1.1 Y/Y_b | \sqrt{2}) \quad (2)$$

This function allows the determination of local wall motion at any location chosen on the ED outline. For our studies the model will be used to determine local wall motion at those ED-outline locations which have y -coordinates equal to $n y_b/10$ with $n = 1, 2 - 10$. The accuracy of this approximation of the landmark trajectories can be estimated by comparing the measured distances between the average ED and ES contours of the 23 normals along the averaged landmark trajectories and the calculated trajectories. Averaged over all segments the difference between both methods is negligible. For the individual segments the absolute difference was less than 0.8 mm.

Clinical application

For the routine measurement of LV wall motion, all contours of the complete cardiac cycle are determined with the aid of the Contouromat and the contours are sent to a PDP 11-34 computer system via a special purpose interface. Following expressions (1) and (2) LV wall motion is measured starting from the 20 ED locations as defined before. For the time being a non-indexed coordinate system is preferred, which is based on the ED contour. Current realignment methods are based on non-proven assumptions about LV motion and contraction; quite often artificial motion at unexpected location is introduced as a result of the realignment. Furthermore most of these methods are heavily dependent on the ES apex location which cannot be derived accurately from the angiogram.

In Fig. 3 an example is given of a computer generated output showing the ED and ES contours which correspond with the largest and smallest ventricular volumes, respectively. The ED position of segment 11 was indicated by the user. The other 19 ED segment positions as well as the defined trajectories were determined with the computer program of the model described earlier. Inspection of these plots does not reveal any wall motion abnormalities. In the left of the picture the patient's name, film identification number, film frame numbers of the outlines, the corresponding volume data, indexed for body surface area (BSA), the heart rate (HR) and the total cardiac index (TCI) are displayed.

A.
LVC79A.501
ED FILM FRAME: 88
ES FILM FRAME: 108

EDV: 44.8 ML/M²
ESV: 12.3 ML/M²
SV: 32.4 ML/M²
EF: 80.9 %
HR: 51 B/MIN
TCI: 2.6 L/MIN/M²
BSA: 2.0 M²
WTM: CM

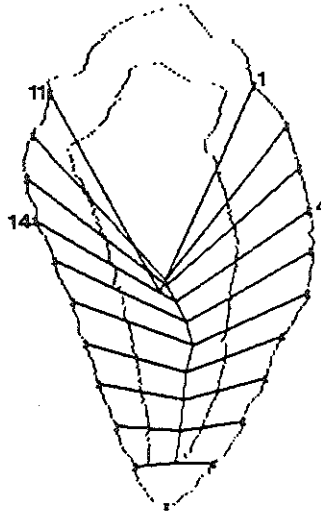


Fig. 3. Computer output of patient study showing the ED and the ES contour of an apparently normal left ventricle. Wall motion is computed along the 20 straight lines calculated following the mathematical description of the landmark trajectories in normals. Patient administrative data and computed haemodynamic parameters are listed.

In Fig. 4 the wall displacement and velocity have been plotted versus time for segment 14 of the same patient. The vertical bars at frame numbers 88, 108 and 146 represent the ED, ES and ED moments respectively, which correspond with the extremes of the volume curve. Filming speed is 50 frames per second so that the time interval between successive frames equals 20 ms. The plot shows that the onset of relaxation is delayed by more than 100 msec after the ES moment. This was a consistent observation for the total inferior wall, while part of the anterior wall showed an early relaxation over the same period. Other plots routinely generated by the computersystem are: ventricular volume (V) versus time, dV/dt versus time and composed views of all the distance-time or velocity-time curves of the anterior and the inferior part of the ventricle.

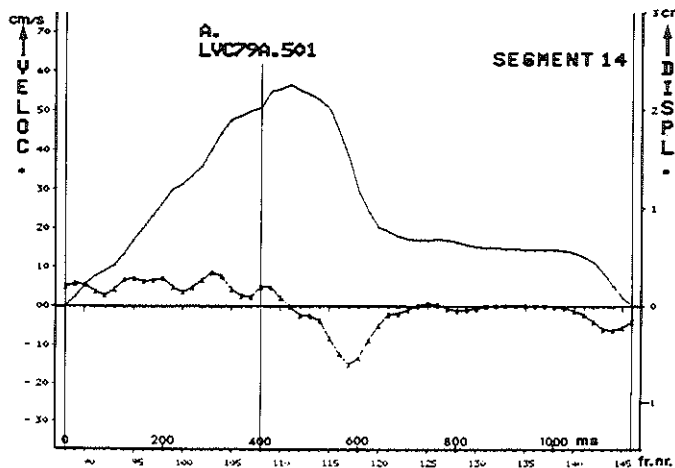


Fig. 4. Displacement and velocity curves as a function of time for inferior segment 14. An extended period of contraction past the ES moment (frame 108) can readily be observed.

Normal ranges

A subgroup of 16 normals has been analyzed using the computer generated model to define normal values for different wall motion parameters. For these measurements also the diastolic period was included. Requirements for inclusion in this subgroup were: (1) presence of a complete, well opacified cardiac cycle, (2) no diaphragmatic motion beyond 2 mm. In Fig. 5 the ranges of maximum systolic displacement are indicated for 19 segments; segment 11 was excluded because interference of the mitral valve makes these data unreliable in many cases. The numbers and the bars at the various segments represent the average total endocardial displacement in cm with the associated standard deviations. For all segments, except 1 and 11, an excellent correlation was found between the average maximal displacement D_{\max} and the corresponding y/y_b value, whereby y equals the y -coordinate of the particular segment (in cm) and y_b equals the y -coordinate of segments 1 and 11 at end-diastole:

$$D_{\max, \text{anterior}} = 0,59 \text{ cm} + 1,19 y/y_b \quad (3)$$

($r = 0.992$; s.e.e. = 0.04 cm)

$$D_{\max, \text{inferior}} = 0,79 \text{ cm} + 1,13 y/y_b \quad (4)$$

($r = 0.991$; s.e.e. = 0.04 cm)

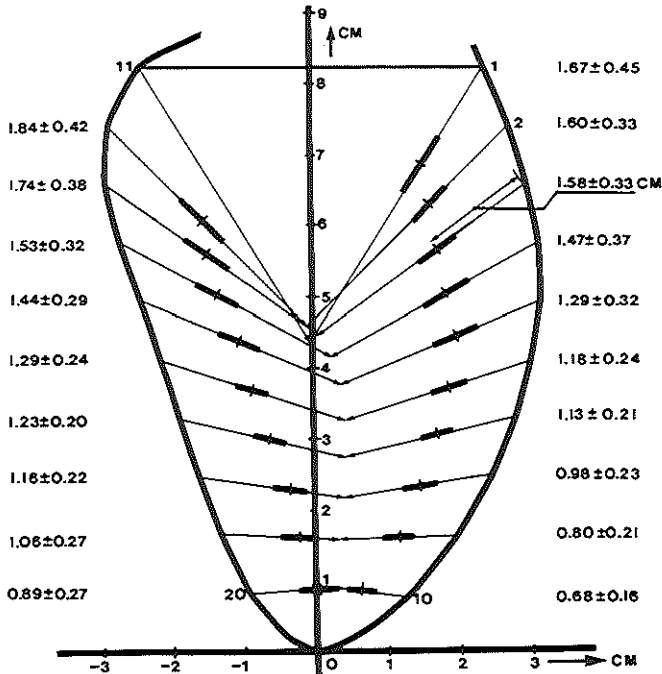


Fig. 5. In a subgroup of 16 normal LV angiograms wall motion has been measured using the described LV wall motion model. In this figure the maximum systolic displacement with the associated standard deviations are shown for the various segments.

The first derivative of the wall displacement with respect to time, being instantaneous wall velocity, has been averaged over the systolic period; results are shown in Fig. 6. As can be observed and as follows from equations (3) and (4), there is an almost linear decrease in mean velocity from base to apex.

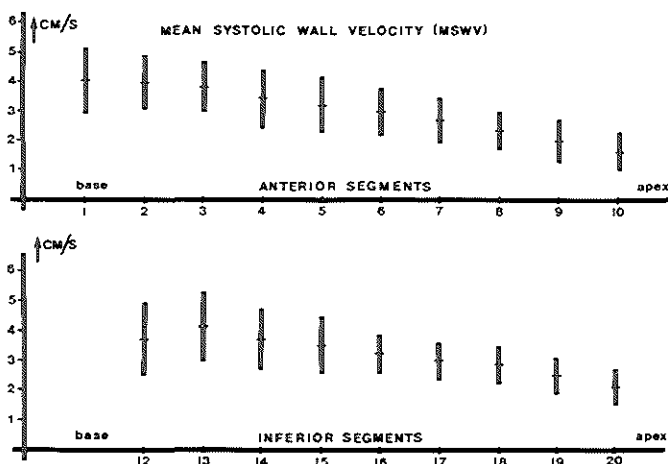


Fig. 6. For nineteen segments the mean systolic wall velocity has been calculated. An almost linear decrease in mean velocity exists from base to apex.

REFERENCES

1. Brower R., Meester G.T., Computer-based methods for quantifying regional left ventricular wall motion from cine ventriculograms. *Comput. Cardiol.* pp. 55-62, 1976.
2. Ingels N.B., Mead C.W., Daughters G.T., Stinson E.B. and Alderman E.L., A new method for assessment of left ventricular wall motion. *Comput. Cardiol.* pp. 57-61, 1978.
3. Slager C.J., Reiber J.H.C., Schuurbiens J.C.H. and Meester G.T., Automated detection of left ventricular contour. Concept and application. In: *Roentgen-Video-Techniques*, ed. P.H. Heintzen and J.H. Bürsch, pp. 158-167. Georg Thieme Stuttgart, 1978.

CHAPTER V

QUANTITATIVE ASSESSMENT OF REGIONAL PUMP- AND CONTRACTILE FUNCTION PART I: THE NORMAL HUMAN HEART

T.E.H. Hooghoudt, M.D., C.J. Slager, M.Sc., J.H.C. Reiber, Ph.D., J.C.H. Schuurbiers, G.T. Meester, M.D., P.G. Hugenholtz, M.D. (material contained in this chapter has been submitted in a modified form to *Am.J. Cardiol.*)

Abstract

Aim of this study was to define normal values for left ventricular endocardial wall motion and its derived parameters of regional contractile and pump function. Left ventriculograms (30° RAO) of 20 normal subjects were processed frame by frame by an automated dedicated hard-wired contour-detector, interfaced to a minicomputer. Wall motion was computed for 20 segments based on an anatomical model derived from endocardial landmark trajectories. From displacement data, segmental wall velocity and the regional contribution to global ejection fraction (CREF), a new determinant of regional pump function, were derived. In this group of normal subjects median segmental values for systolic left ventricular wall displacement range from 0.72 cm in the apex to 1.68 cm in the basal area, while values for mean systolic velocity vary from 1.40 - 4.00 cm/s for different areas of the heart. The regional contribution to global ejection fraction ranges from 0.9% in the apical region to 5.2% in the mid-ventricular segments. From base to apex a linear relation is found between displacement and velocity values at a given segment and its distance to the base ($r \leq -0.97$). Frame by frame analysis of the cineangiogram provides additional information on the time sequence of segmental wall motion. To conclude, these parameters, determined with this new wall motion model, form a base for the description of normal and abnormal left ventricular function.

Key words: left ventricular segmental wall motion, endocardial landmark trajectories, regional contribution to ejection fraction.

INTRODUCTION

Since coronary heart disease is often regional in character, the assessment of regional left ventricular function under resting conditions and during intervention studies may elicit both the functional significance of coronary artery

stenosis and the extent of jeopardized areas of myocardium (1). Such assessment may be of great importance in the selection of patients for bypass surgery. Although ejection fraction (2) and the isovolumic indices of contractility (3) are useful parameters of global cardiac function, in these measurements regional dysfunction may be masked by compensatory action of healthy wall segments. On the other hand regional pump- and contractile function may be derived from regional wall motion itself. For this purpose a number of methods has been proposed (4-8), which almost all introduce a considerable error, both in extent and direction of determined wall motion (9). Also the temporal aspects of left ventricular performance bear important information (10, 11), although their analysis is often omitted because manual frame by frame analysis is so tedious.

For all these reasons a system for the automated quantitative analysis of regional left ventricular wall motion, pump- and contractile function and their temporal aspects, was developed. For the accurate assessment of regional endocardial wall motion a new wall motion model was devised which relies on the actual trajectories of endocardial anatomical structures (12, 12b). The present study describes the findings in 20 normal human hearts.

Patient population and methods

Left ventricular angiograms from patients who after a complete right and left heart catheterization including coronary arteriography showed completely normal hemodynamic findings, normal coronary angiograms and normal left ventricular wall motion as judged by at least two experienced observers form the basic material for the study. Most patients had been submitted to cardiac catheterization to exclude coronary artery disease as a cause of chest pain, or because of murmurs which required investigation. After exclusion of technically unsatisfactory films, due to movement of the patient with regard to the X-ray equipment and/or respiratory movement during ventriculography, twenty such left ventriculograms were selected. The 30° RAO ventriculogram was obtained after injection of 0.75 ml/kg Urografin 76 (Schering AG)* as contrast agent in the left ventricular cavity, by filming the image intensifier output-screen with an Arriflex 35-mm camera at a rate of 40-80 (typical 50) frames per second. The cycle with the maximum contrast of the left ventricle – excluding extrasystolic and postextrasystolic beats – was chosen for analysis; usually this was the 3rd - 5th beat after the start of contrast injection. This excluded a significant volume load from the injected contrast agent (13).

Analysis of the left ventriculogram was performed with a dedicated hard-wired system, the video-contourdetector Contouromat (14). A simplified block diagram of this automated outlining system is shown in figure 1. Films are

* Schering AG, Berlin, Bergkammen G.B.R.

projected with a Vanguard** projector and converted into video format with a Philips*** videocamera. The cineangiogram is rotated such that the long axis of the left ventricle is about perpendicular to the direction of the video scanlines. With this optimized orientation there will never be more than two contour points on a videoline, one for the left and one for the right border.

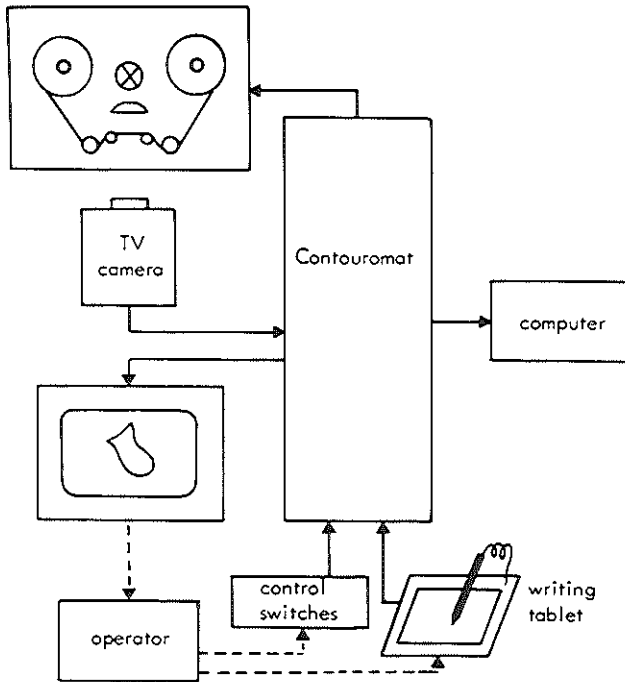


Fig. 1. Simplified block diagram of the automated endocardial outlining system.

Contour detection is based upon a refined thresholding technique which uses an analog comparator to compare the videosignal with the reference level. As soon as the videosignal crosses the reference level, the comparator changes state, indicating the presence of a border point. The reference level is determined by three factors:

- the local brightness of structures surrounding the detected border, assessed on a line to line basis.
- the “expectation window”, a narrow window which adapts dynamically to the ventricular shape. The center of this window is defined as having the

** Vanguard Instruments Corporation, Melville, L.I., New York.

*** Philips, Eindhoven, The Netherlands.

same x-coordinate as the last detected border point in the previous videoline. The comparator is enabled during the expectation window period only. During this period, the calculated reference level is assigned a probability function such that the center of the expectation window has the highest probability to be the next border point.

— the endocardial border in the last detected frame. Because the border position changes little from frame to frame, the margin in the current frame can be approximated with the margin of the previous frame. During contour detection the stored border positions of the previous contour are used to assign a probability function to the reference level.

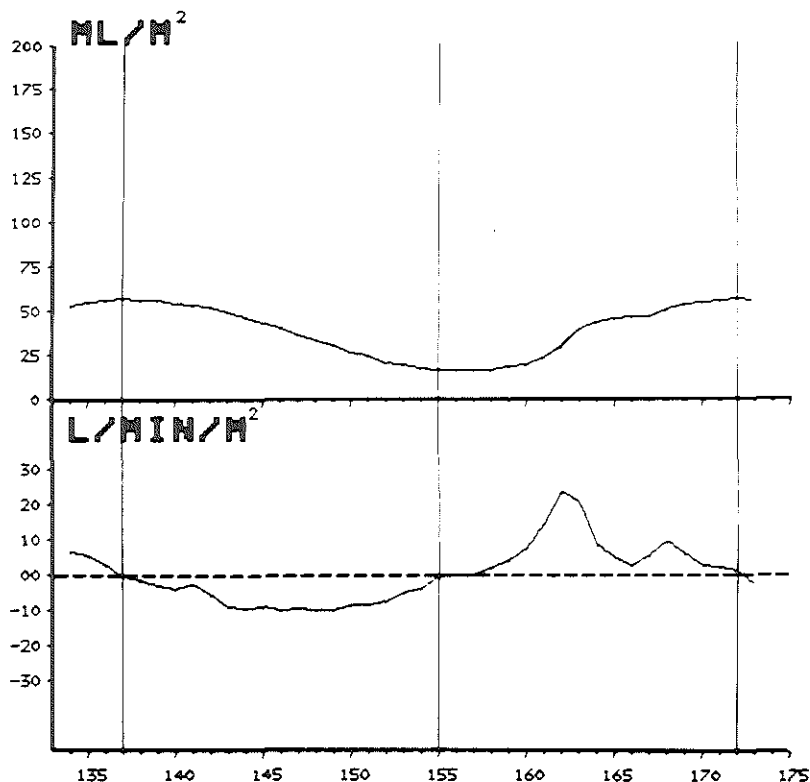


Fig. 2. Graphic display of the time course of left ventricular volume, corrected for body surface area, and its time derivative. Vertical bars indicate the end-diastolic and end-systolic frames.

The great advantage of this complex way of contour detection is that the detection process is rather insensitive to shading, nonhomogeneous mixing of the contrast agent in the left ventricle, and overlapping of roentgen-opaque

EDV:	57.6	ML/M ²
ESV:	16.4	ML/M ²
SV:	41.1	ML/M ²
EF:	71.4	%
HR:	88	B/MIN
TCI:	3.6	L/MIN/M ²
BSA:	1.6	M ²
WTH:		CM

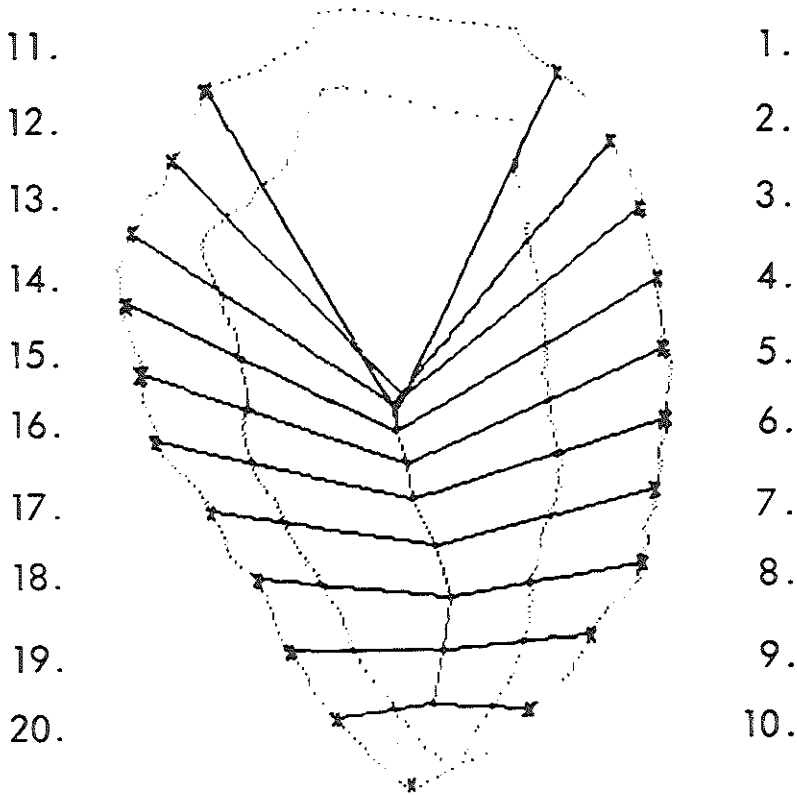


Fig. 3. Example of the computer output showing the end-diastolic and end-systolic contours of the 30° RAO angiogram in their relative proportions and place. The corresponding volume data, ejection fraction and other parameters are shown in the upper right corner. Left ventricular segmental wall motion is determined along a system of coordinates derived from the endocardial landmark trajectories in normals and is studied in twenty separate segments, ten in the anterior and ten in the inferoposterior wall.

structures such as diaphragm, ribs and catheters, because the reference level is adjusted accordingly. The left ventricular contour is detected at a rate of 50 TV fields/sec. Including operator interaction, mean processing time is 7 - 10 seconds per frame or 3 - 15 minutes per cardiac cycle (15).

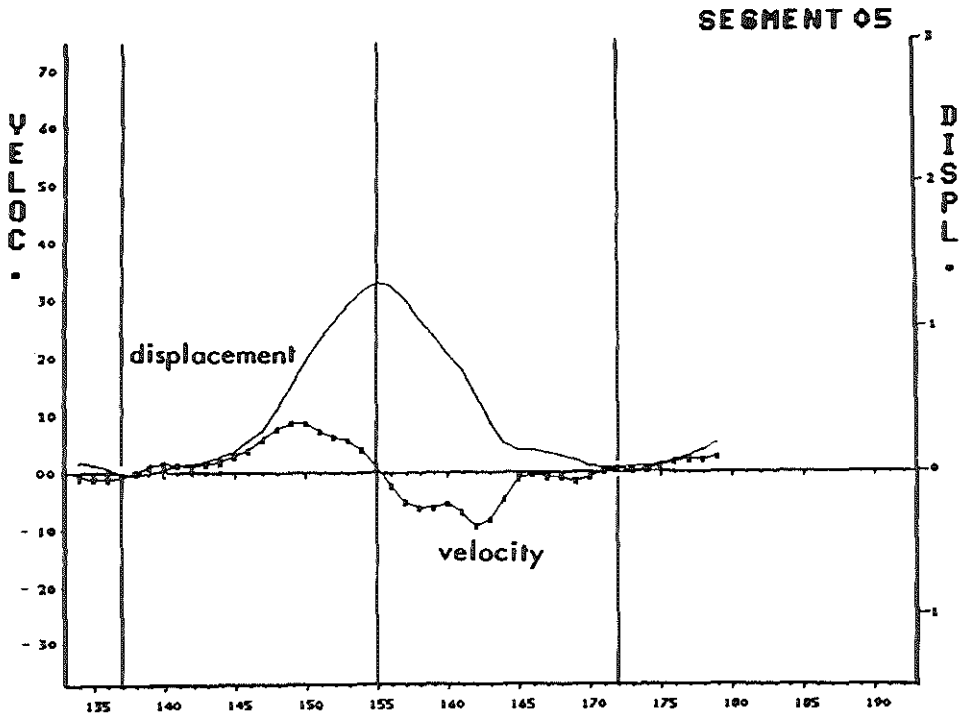


Fig. 4. For every segment a plot is generated showing left ventricular wall displacement and velocity as a function of time.

All data from the Contouromat are coded in a special purpose interface and stored with a PDP-11/34 minicomputer onto a RK-05 disk (Digital Equipment Corporation). The first step in processing of these data is the calculation of left ventricular volume from all analyzed cineframes according to Simpson's rule and the graphical display of instantaneous volume and its time derivative (fig. 2). The end-diastolic and end-systolic frames, defined as the frames with the maximal and minimal volume respectively, are so marked by the operator via the writing tablet. From the left ventricular volume data over the systolic period, ejection fraction, stroke volume and total cardiac output are computed. The end-diastolic and end-systolic contours are displayed on the computer video monitor with the computed values for ejection fraction, stroke volume and cardiac output. Next the computer generates a system of coordinates along which regional left ventricular wall motion is determined (fig.3). This method to analyze left ventricular wall motion is based on the endocardial landmark trajectories as previously established in a group of normal indivi-

duals (12). Over a full cardiac cycle, starting in end diastole, segmental wall displacement is determined in twenty segments, ten in the anterior and ten in the inferoposterior wall. Regional wall velocity is calculated as the first derivative of the instantaneous displacement function after a three point

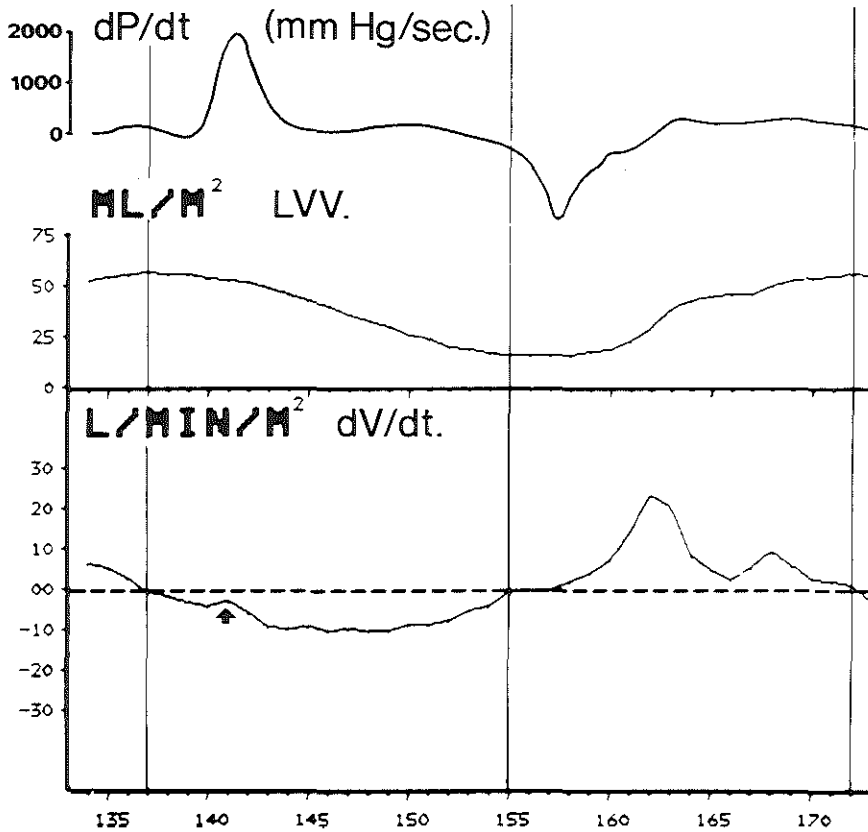


Fig. 5. A typical example of the relation between the dV/dt curve and the dP/dt curve as observed in normals: the temporal position of the distinct notch in the dV/dt curve agrees closely with peak dP/dt .

smoothing function has been applied to the data (fig. 4). From these data mean systolic velocity is calculated for each segment. To eliminate the influence of the pre-ejection period on mean systolic velocity, left ventricular segmental wall velocity is determined during the actual ejection period. Since the exact moment of aortic valve opening is hard to define from the ventriculogram and the interval between peak dP/dt and aortic valve opening under general conditions is less than 20 msec (16, 17), the ejection phase is considered to begin at peak dP/dt . As in some instances simultaneously recorded left ventricular pressure data were not available, the moment of aortic valve opening was de-

rived from the curve showing the first derivative of volume vs time (fig. 5). A distinct notch occurring less than 20 msec after peak dP/dt directly followed by a rapid decrease in left ventricular volume was taken to have a close temporal relationship to aortic valve opening.

For all 20 segments the regional contribution to global ejection fraction (CREF) is derived from systolic wall displacement data and left ventricular long axis shortening. To achieve this, the end diastolic lumen — from the level of the mitral valve edge to the apex — is divided into ten slices of equal height, each corresponding to two opposite segments of the model (fig. 6). Each slice is divided into two halves by the left ventricular axis of symmetry. The volume

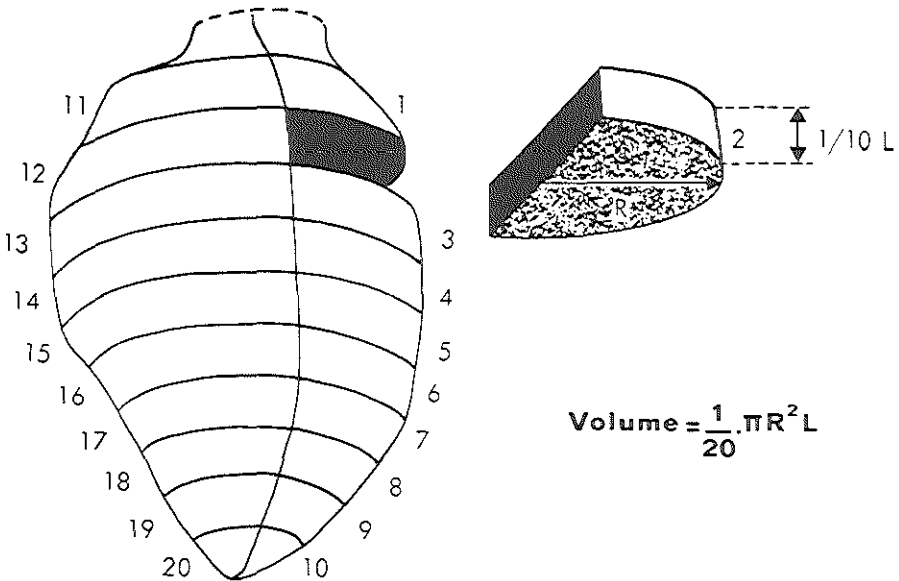


Fig. 6. The regional contribution to global ejection fraction (CREF) is determined in 20 half slices of equal height, each corresponding to a segment of the wall motion model shown in figure 3.

of each half slice is computed in end diastole (ED) and end systole (ES) according to the formula:

$$\frac{1}{2} \times \pi R^2 \times \frac{1}{10} L = \frac{1}{20} \cdot \pi R^2 L,$$

where R is the radius of a particular slice and L left ventricular long axis length extending from base to apex.

During systole the volume of a particular half slice decreases mainly as a consequence of the decrease of radius which is determined by the x-component (x) of the displacement vector (d) (fig. 7), and only slightly by left ventricular long axis shortening. In normals a percentage of 14% long axis shortening,

as previously assessed (12), was applied to the calculations. The CREF is defined as the change of volume during ejection of a particular segment normalized for left ventricular end diastolic volume:

$$\frac{\text{ED half slice volume (ml)} - \text{ES half slice volume (ml)}}{\text{global left ventricular end diastolic volume (ml)}} \times 100 = \text{CREF (\%)}$$

The sum of CREF data of all 20 segments (SUMCREF) will equal global ejection fraction. From the systolic volume change, the regional ejection fraction (REF) is determined according to the formula:

$$\frac{\text{ED half slice volume (ml)} - \text{ES half slice volume (ml)}}{\text{ED half slice volume (ml)}} \times 100 = \text{REF (\%)}$$

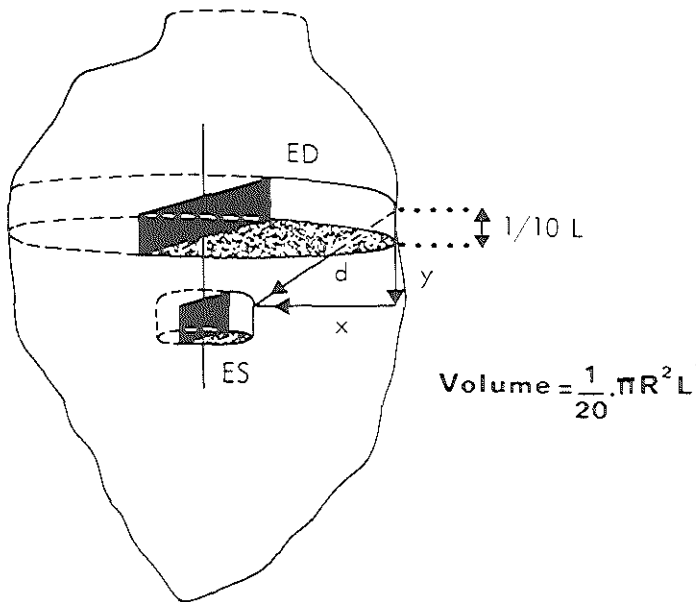


Fig. 7. The regional contribution to global ejection fraction is determined from the systolic decrease of volume of the half slice which corresponds to a particular wall segment. This volume is determined according to the displayed formula. The systolic volume change is mainly a consequence of the decrease of radius (R) of the half slice, which is expressed by the x -component (x) of the displacement vector (d). L = left ventricular long axis length, extending from base to apex.

RESULTS

In the twenty normal individuals, calibrated displacement (cm) and velocity (cm/s) values were determined in all twenty segments. The 10% and 90% limits of segmental wall displacement in cm as well as the median are shown in figure 8.

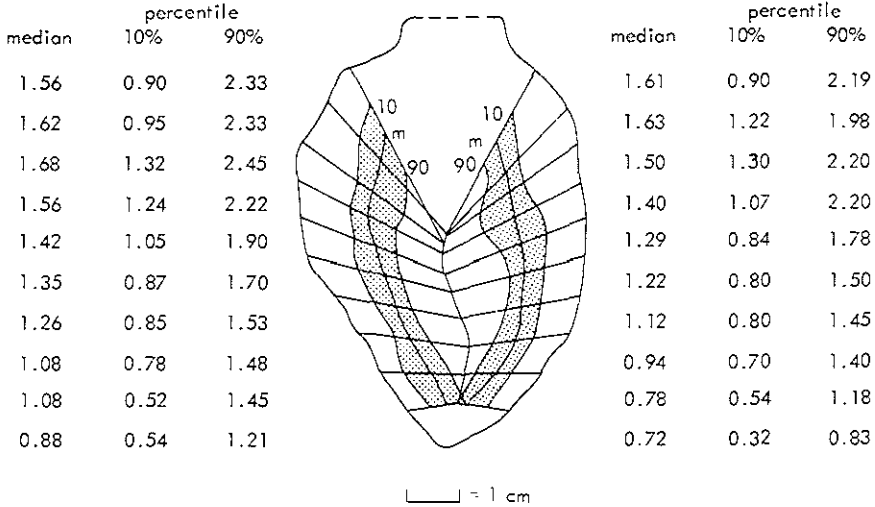


Fig. 8. Median, 10th and 90th percentile values of left ventricular wall displacement (cm) in normal subjects. The ventriculograms were made in the 30° RAO position.

When the segments 1 and 11, which in some cases are less reliable due to interference from aortic and mitral valve motion are excluded, correlation coefficients of -0.99 and -0.98 are found between median values of local displacement of specific segments in the anterior and inferoposterior wall, respectively, and their distance to the base (fig. 9). Mean systolic segmental wall velocity (MSV) and wall velocity during the actual ejection period (EPV) are displayed in figures 10 and 11 and in table I. Here again a linear decrease is observed in the median values viewed from base to apex (MSV vs distance to base: $r = -0.98$ and -0.97 ; EPV vs distance to base: $r = -0.99$ and -0.99 in the anterior and inferoposterior wall respectively). The normal range of values for the regional contribution to global ejection fraction is shown in figure 12 and table II, while figure 13 gives the normal values of regional ejection fraction.

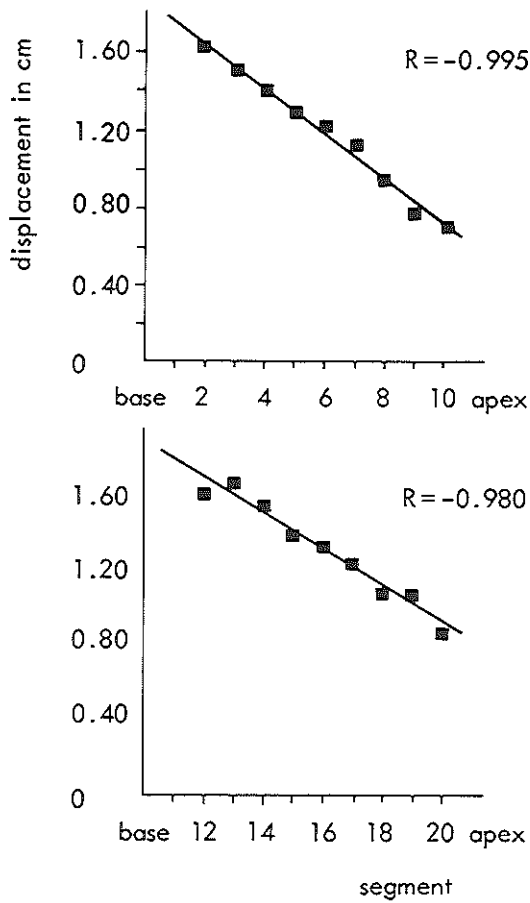


Fig. 9. In this group of normal subjects an approximate linear relationship has been found between the median value of displacement of a particular segment and its distance to the base.

DISCUSSION

In the present study a new method to determine regional wall motion is introduced and applied to the assessment of regional left ventricular pump and contractile function. The search for this new wall motion model was initiated by the inadequacy of the currently available methods (4-8). The very existence of these different methods to analyze left ventricular wall motion indicates that no exact and generally accepted procedure is available to track fixed points along the endocardial wall.

Nearly all methods show a considerable error of determined wall motion in comparison with midwall markers (9), and are liable to introduce artefacts (18), as most approaches include procedures to "correct" for translation and rotation. Daughters et al. (19) showed however that sustained respiration and a fixed geometric position of the patient with regard to the X-ray equipment reduces translation to a minimum, and that long axis rotation may be neglected.

Table I. *Mean systolic wall velocity (MSV) and ejection phase velocity (EPV) in normal individuals*

segment	MSV			EPV		
	10% cm/s	median cm/s	90% cm/s	10% cm/s	median cm/s	90% cm/s
1.	2.40	3.65	5.55	2.50	4.10	6.00
2.	2.75	3.83	5.75	3.00	4.20	6.18
3.	2.80	4.00	5.50	2.90	4.24	6.00
4.	2.50	3.60	5.60	2.80	3.90	6.20
5.	2.05	3.30	5.70	2.25	3.20	5.70
6.	1.85	2.80	5.00	2.05	2.96	5.00
7.	1.85	2.60	4.70	1.95	2.50	4.70
8.	1.74	2.30	3.60	1.30	2.30	4.02
9.	1.25	1.65	3.16	1.30	2.05	3.50
10.	0.60	1.40	2.40	0.60	1.50	2.30
11.	2.55	3.15	5.50	2.25	3.55	6.00
12.	2.10	3.65	5.00	2.50	4.15	5.04
13.	3.20	3.85	6.00	3.25	4.15	6.10
14.	2.65	3.70	5.78	3.10	3.82	5.80
15.	2.25	3.45	6.00	2.50	3.55	6.00
16.	2.25	3.13	5.00	2.40	3.30	5.25
17.	2.25	2.88	4.62	2.20	3.05	4.62
18.	1.90	2.75	4.25	2.00	2.90	4.47
19.	1.55	2.50	3.86	1.70	2.75	4.35
20.	1.20	2.20	3.00	1.35	2.58	3.35

A new approach was developed with the aid of an automated contour detector. This high resolution outlining system detects small irregularities at the endocardial border and thus preserves information which is lost with manual analysis of a ventriculogram. The hypothesis that these irregularities represent specific anatomical structures has been tested in cadaver hearts (12) and in pigs (12b). The mean systolic pathways of these "anatomical landmarks" were measured in normal individuals. This forms the base for the definition of the wall motion model applied to this study (fig. 3). As segmental wall motion is determined according to these mean pathways, the direction and extent of measured wall motion will be very accurate in normal subjects, although it is obvious that even this method will not track the actual motion of all endocardial points.

In fact the method will introduce some error when applied to abnormally contracting hearts. However, in general, a subnormal regional contraction will cause a decrease of both the x- and the y-component of the displacement vector d (fig. 14), which results in a decrease in the extent, but not in a major change in direction of wall motion. Thus, the normal pattern of wall motion may be the closest general approximation applicable to the abnormal ventricle.

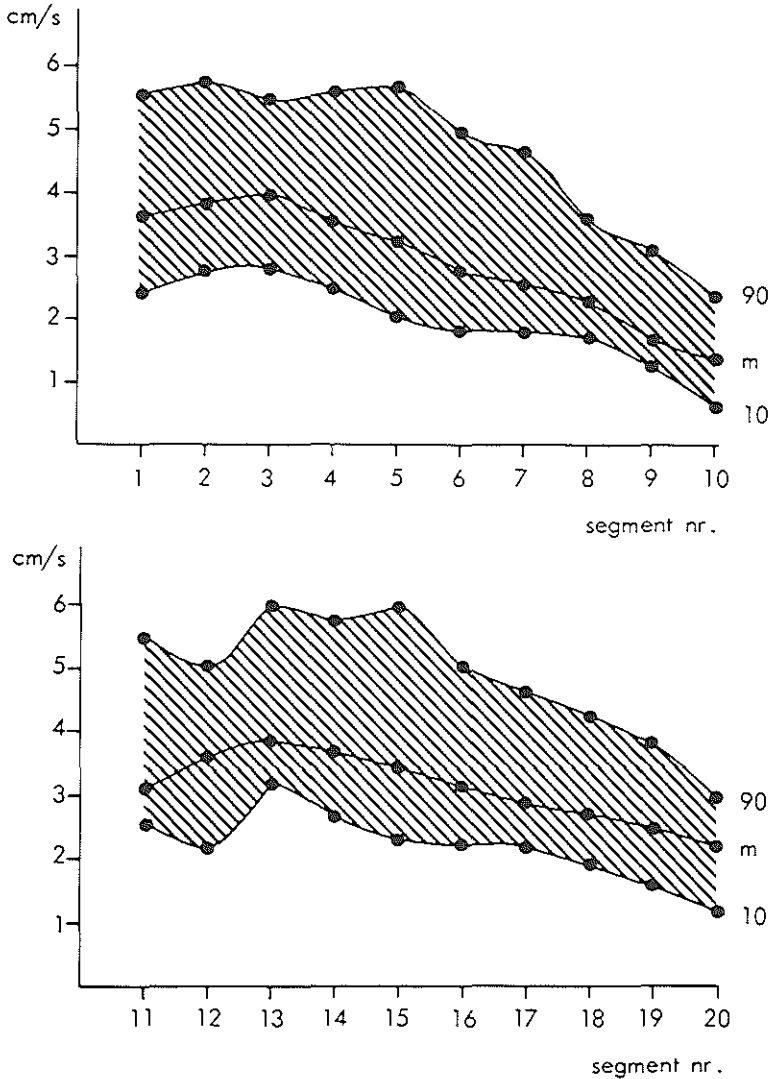


Figure 10. Mean systolic velocity for all twenty segments in twenty normal subjects. The median, 10th and 90th percentile are shown. The upper figure gives the data for the anterior segments, the lower figure for the inferoposterior segments.

The right anterior oblique projection was selected for analysis of the ventriculograms. This implies that the septal and posterolateral wall are not visualized. Coronary heart disease however is seldom confined to these wall segments (20). Analysis of the left anterior oblique angiogram is less rewarding because of technical limitations, such as the foreshortening effect of the septal and postero-

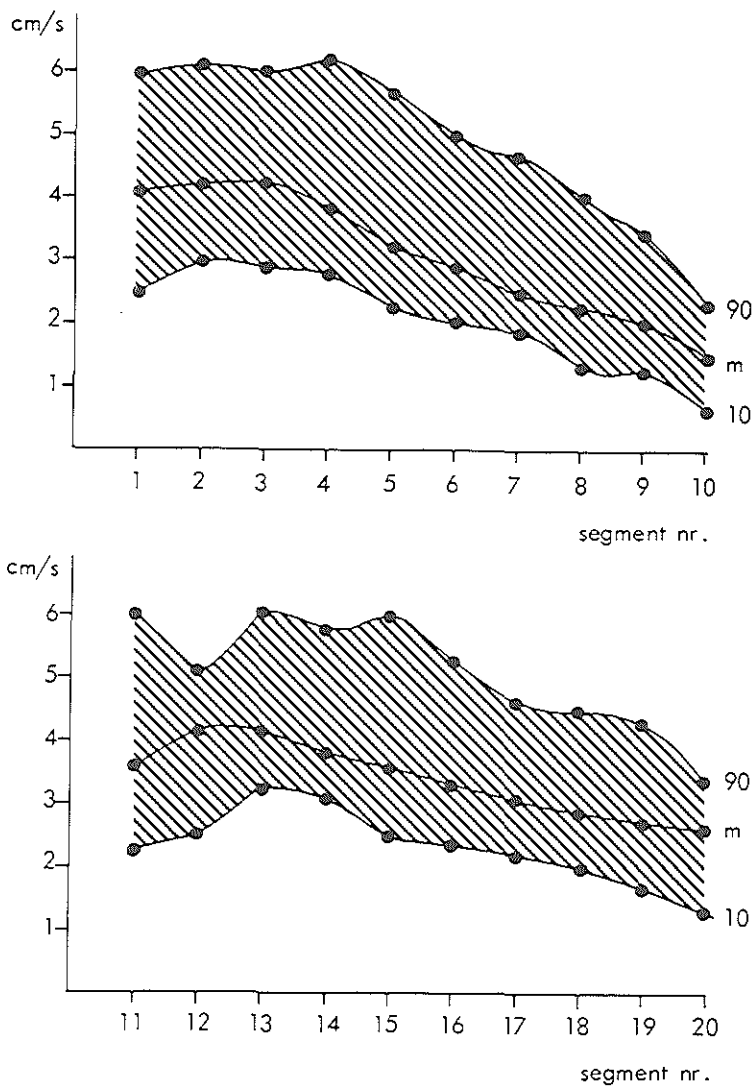


Figure 11. Ejection period velocity: median, 10th and 90th percentile in twenty segments in normal subjects.

lateral wall and the imperfect delineation of the ventricular silhouette at the level of the mitral valve.

Although most authors normalize regional wall motion for the end-diastolic diameter, we opted for absolute displacement values, which then remain applicable for further calculations. With this method, displacement is shown to have a narrow range (fig. 8), while a close relationship is observed between the data of neighbouring segments, as is reflected by a smooth decrease of displacement

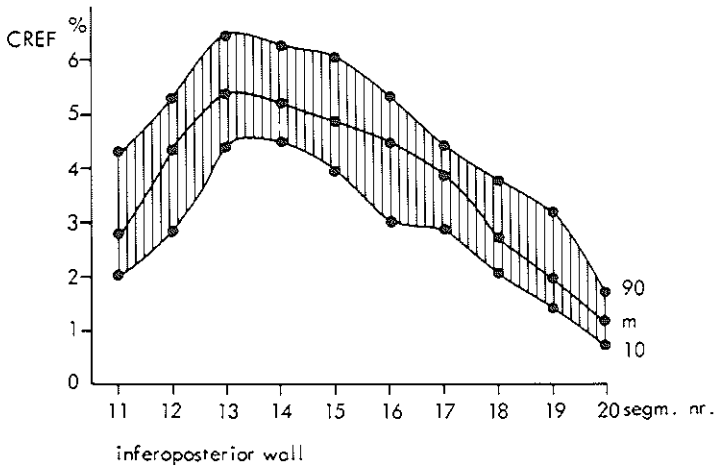
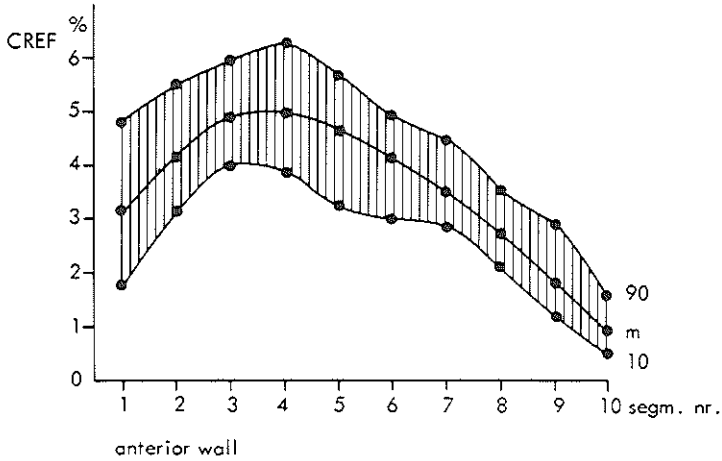


Figure 12. Regional contribution to the global ejection fraction (CREF), calculated for twenty segments in normal subjects. The median, 10th and 90th percentile are shown. Ventriculograms were made in the 30° RAO position.

Table II. *Regional contribution to global ejection fraction in normal individuals.*

segment	10%	median	90%
	%	%	%
1.	1.7	3.1	4.8
2.	3.2	4.2	5.5
3.	4.0	4.9	5.9
4.	3.9	5.0	6.3
5.	3.2	4.7	5.7
6.	3.0	4.1	4.9
7.	2.9	3.5	4.5
8.	2.0	2.7	3.5
9.	1.2	1.8	2.9
10.	0.5	0.9	1.5
11.	2.0	2.7	4.2
12.	2.8	4.4	5.3
13.	4.4	5.4	6.5
14.	4.5	5.2	6.3
15.	4.0	4.9	6.1
16.	3.0	4.5	5.3
17.	2.9	3.9	4.4
18.	2.0	2.7	3.8
19.	1.4	1.9	3.2
20.	0.7	1.0	1.7

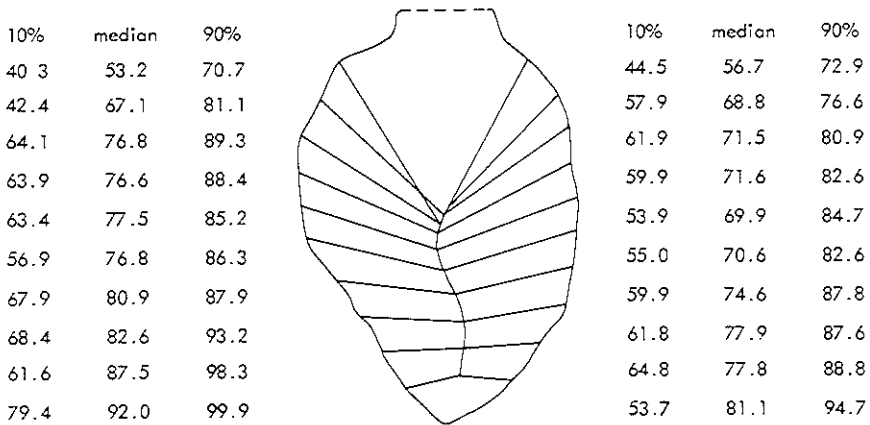


Figure 13. Percentage of blood ejected (regional ejection fraction) as calculated in twenty left ventricular segments in normal subjects. The ventriculograms are of the 30° RAO projection.

Notice that the apical segments in systole practically occlude their part of the ventricular lumen though their contribution to global ejection fraction is small (fig. 12).

data from base to apex (fig. 9). A comparative study of other wall motion models shows on the contrary a very irregular distribution of the extent of wall motion over the left ventricular silhouette (18). We consider this a strong argument in favor of this method, as it is hardly conceivable that wall motion in normal subjects would show major differences between adjoining segments.

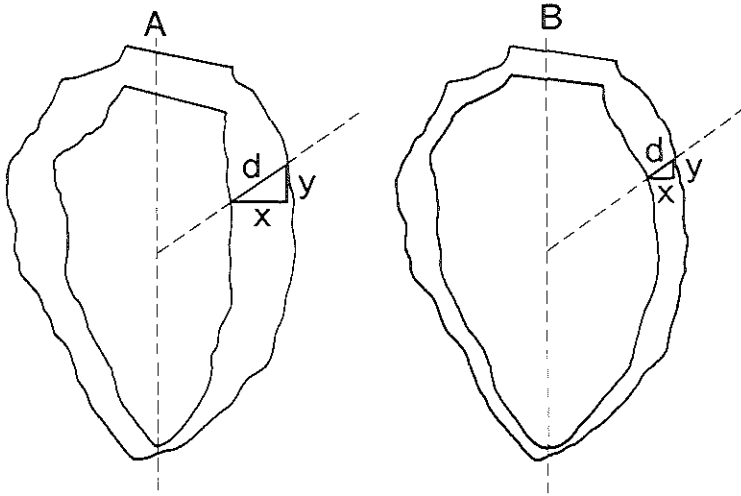


Figure 14. The end-diastolic and end-systolic endocardial contours of a normal contracting and a hypokinetic left ventricle are shown. Although the extent of displacement (d) is decreased in the latter case, the direction of wall motion is not essentially changed since both the x - and the y -component of the displacement vector d are diminished.

In this study, segmental wall velocity, the time derivative of segmental displacement, is introduced as an index of regional left ventricular performance reflecting the inotropic state. The myocardial inotropic state is commonly assessed by the isovolumic indices of contractility. However, these indices disregard the regional character of left ventricular (dys)function, while their capacity to discriminate between normal and abnormal function is inferior to that of the ejection phase indices (21). Since their theoretical basis is violated when contraction is asynchronous or when the mitral valve is insufficient, the isovolumic parameters are further disadvantaged. To what extent these conditions also affect the present method must be further investigated.

Gault et al. (22) showed that the myocardial contractility may be assessed during the ejection phase. At peak stress, the circumferential fiber-shortening velocity (V_{cf}) — computed as $2\pi dR/dt$ — equals the contractile element velocity (V_{CE}) and thus can be regarded as an index of the contractile state. Mean V_{cf} (23) was shown to reflect the inotropic state with almost the same accuracy,

although it lacks the fundamental base of instantaneous velocity at peak stress. As V_{cf} assessed in the RAO view is the mean of velocities of the anterior and inferoposterior wall, depressed contractile function in one wall segment may still be obscured by normal function of the other. Determination of segmental wall velocity – computed as dR/dt – solves this problem. The mean circumferential velocity data described by Gault et al. (22) show after correction for the computational method (i.e. division through 2π) an excellent agreement with the mean systolic velocity (MSV) data in the current study. The average radial wall velocity in their group of individuals without left ventricular disease was $23.3/6.28 = 3.7$ cm/sec., while we find median MSV values of 3.3 - 4.0 cm/sec. in the midventricular wall segments. As exclusion of the pre-ejection period was shown to have significant influence on mean velocity data and to improve the separation between normal subjects and patients with impaired left ventricular function (23), mean ejection phase velocity (EPV) is also determined. Accordingly, median values of EPV are somewhat higher than those of mean systolic velocity (MSV).

In patients with coronary heart disease a subnormal ejection fraction, or a decrease of ejection fraction during interventions such as rapid atrial pacing (24), is often caused by a regional disturbance of pump function. Although regional ejection fraction (25) may be used as a determinant of regional performance, the contribution of a given wall segment to global ejection is assessed with this method. Normalization of regional volume displacement for end diastolic volume yields a new parameter of regional pump function (CREF), which expresses quantitatively to what extent a particular segment contributes to global ejection fraction. CREF values in normal subjects (fig. 12, table II) show that the midventricular segments are of prime importance for the ejection of blood: segments 4, 5, 14 and 15 contribute 15.6 - 24.4% to global ejection fraction, whereas the apical segments 9, 10, 19 and 20 contribute only 3.8 - 9.3%. Though the apical segments contribute only little to global ejection fraction, blood is ejected from this area more completely than from the midventricular segments, as is expressed by the regional ejection fraction (fig. 13). The basal segments 1, 2, 11, and 12 which because of their relation to the noncontractile structures of aortic and mitral valve are restricted in their inward excursions, have the lowest values of regional ejection fraction, but contribute with 9.7 - 19.8% still importantly to global ejection fraction.

A number of studies has shown that analysis of the time course of left ventricular performance may reveal left ventricular dysfunction even when quantitative analysis of the end diastolic and end systolic contours show no abnormality (26, 27). Particularly the ejection fraction in the first third of systole appears to be a sensitive determinant of left ventricular function (28). To study the asynchrony of contraction, which is a typical consequence of coronary heart disease (10), frame by frame analysis of the left ventriculogram is indispensable. Our system tracks the regional endocardial motion throughout the entire cardiac

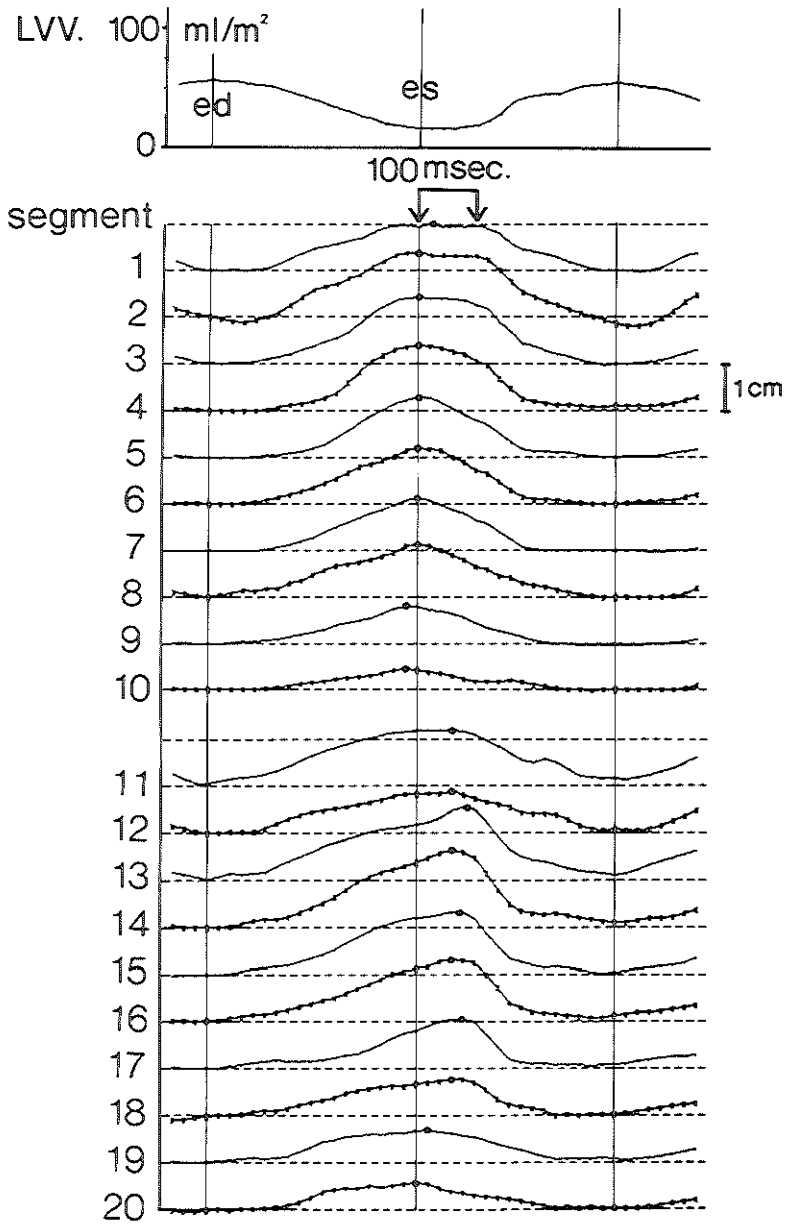


Figure 15. A typical example of left ventricular segmental wall displacement with respect to time in twenty segments in a normal subject: the apical segments show a lag in the onset of contraction, while a delay of relaxation is observed in the posterior wall segments. During early diastole left ventricular volume (LVV) remains constant, while the anterior wall segments move outward and the posterobasal segments move inward.

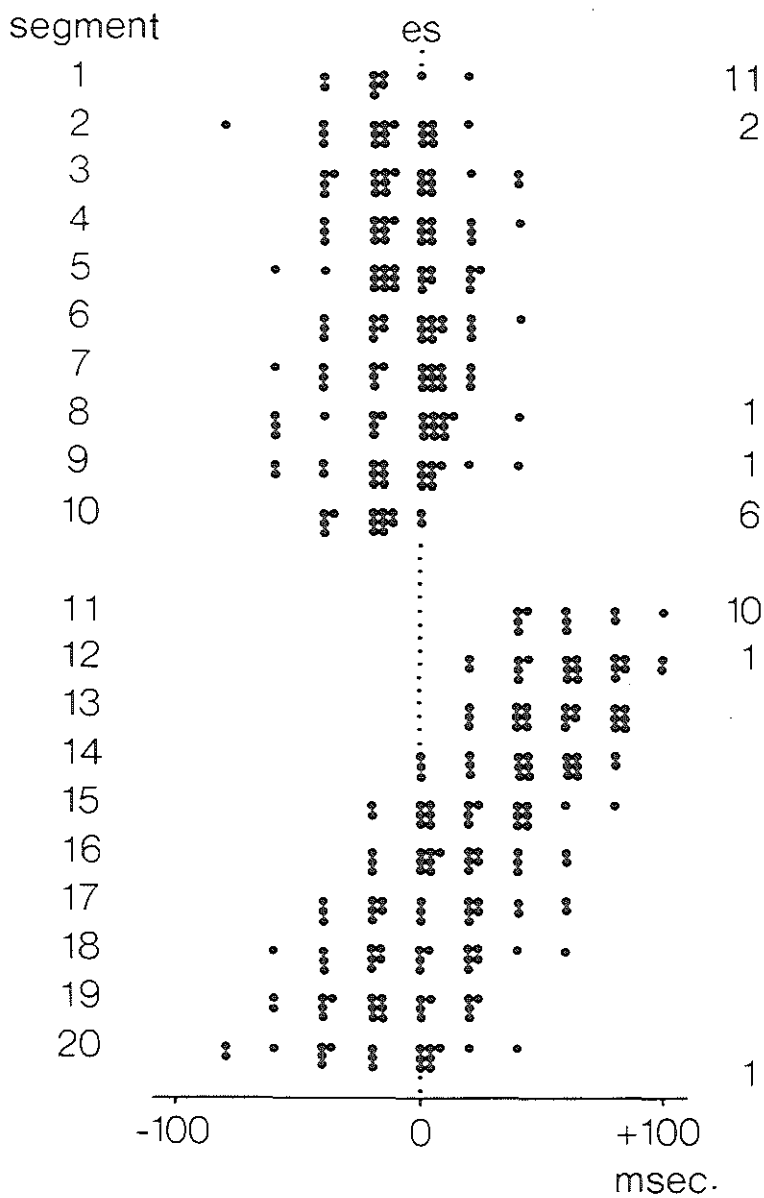


Figure 16. Time between end-systole (es) and the moment of maximal inward displacement in 20 segments of the 30° RAO left ventriculogram of 20 normal subjects. A consistent delay of relaxation is observed in the posterobasal segments. In 33 of 400 segments the moment of maximal displacement could not be determined accurately. The data of these segments are not displayed, but their occurrence is indicated by a number in the respective segment.

cycle at 20 msec intervals and may provide data on global ejection fraction and CREF at any moment during the cardiac cycle. Although left ventricular contraction in normal man is essentially synchronous, some variability in the time sequence of regional wall motion may be observed. In agreement with the study of Clayton et al. (29) the earliest onset of contraction occurs in the inferior wall segments, with some time-lag in the apical segments (fig. 15). Figure 16 shows the time measured between end systole (determined from volume measurements) and the moment of maximal inward wall displacement for the 20 segments in the 20 patients of the study group. As is suggested by the case shown in figure 15, inward wall motion proceeds in the posterobasal area beyond end-systole, defined as the frame with minimal volume.

In conclusion, a new wall motion model, based on the motion pattern of endocardial anatomical structures is described. Regional wall motion is automatically assessed with the aid of an automated contourdetector, and provides the basis for the assessment of indices of regional pump- and contractile function. This study provides a framework of normal values of these indices, which may be used as a reference for the quantitative analysis of left ventricular function in patients with heart disease.

REFERENCES

1. Popio K.A., Gorlin R., Bechtel D., Levine J.A., Postextrasystolic potentiation as a predictor of potential myocardial viability: preoperative analyses compared with studies after coronary bypass surgery. *American Journal of Cardiology* 39: 944-953, 1977.
2. Nelson G.R., Cohn P.F., Gorlin R., Prognosis in medically-treated coronary artery disease. Influence of ejection fraction compared to other parameters. *Circulation* 52: 408-412, 1975.
3. Hugenholtz P.G., Ellison R.C., Urschel C.W., Mirsky I., Sonnenblick E.H., Myocardial force-velocity relationships in clinical heart disease. *Circulation* 41: 191-202, 1970.
4. Herman M.V., Heinle R.A., Klein M.D., Gorlin R., Localized disorders in myocardial contraction. *New Engl. J. Med.* 227: 222-232, 1967.
5. Leighton R.F., Wilt S.M., Lewis R.P., Detection of hypokinesis by quantitative analysis of left ventricular cineangiograms. *Circulation* 50: 121-127, 1974.
6. Harris L.D., Clayton P.D., Marshall H.W., Warner H.R., A technique for the detection of asynergistic motion of the left ventricle. *Comput. Biomed. Res.* 7: 380-394, 1974.
7. Rickards A., Seabra-Gomes R., Thurston P., The assessment of regional abnormalities of the left ventricle by angiography. *Eur. J. Cardiol.* 5: 167-182, 1977.
8. Chaitman B.R., Brnstow J.D., Rahimtoola S.H., Left ventricular wall motion assessed by using fixed external reference systems. *Circulation* 48: 1043-1054, 1973.
9. Ingels N.B. Jr., Daughters G.T., Stinson E.B., Alderman E.L., Evaluation of methods for quantitating left ventricular segmental wall motion in man using myocardial markers as standard. *Circulation* 61: 966-972, 1980.
10. Holman B.L., Wyne J., Idoine J., Neill J., Disruption in the temporal sequence of regional ventricular contraction. I. Characteristics and incidence in coronary artery disease. *Circulation* 61: 1075-1092, 1980.

11. Slutsky R., Karliner J.S., Battler A., Peterson K., Ross J. Jr., Comparison of early systolic and holosystolic ejection phase indexes by contrast ventriculography in patients with coronary artery disease. *Circulation* 61: 1083-1090, 1980.
12. Slager C.J., Hooghoudt T.E.H., Reiber J.H.C., Schuurbiens J.C.H., Booman F., Meester G.T., Left ventricular contour segmentation from anatomical landmark trajectories and its application to wall motion analysis. *Computers in Cardiology* p. 347-350. IEEE Comp. Soc. 1979.
- 12b. Slager C.J., Hooghoudt T.E.H., Reiber J.H.C., Schuurbiens J.C.H., Verdouw P.D., Hugenholtz P.G., Endocardial landmark motion: a new approach to the assessment of regional left ventricular performance. This thesis pp. 30-48.
13. Vine D.L., Hegg T.D., Dodge H.T., Stewart D.K., Frimer M., Immediate effect of contrast medium injection on left ventricular volumes and ejection fraction. *Circulation* 56: 379-384, 1977.
14. Slager C.J., Reiber J.H.C., Schuurbiens J.C.H., Meester G.T., Contouromat - A hard-wired left ventricular angio processing system. I. Design and application. *Comput. Biomed. Res.* 11: 491-502, 1978.
15. Reiber J.H.C., Slager C.J., Schuurbiens J.C.H., Meester G.T., Contouromat - A hard-wired left ventricular angio processing system. II. Performance evaluation. *Comput. Biomed. Res.* 11: 503-523, 1978.
16. Mason D.T., Braunwald E., Covell J.W., Sonnenblick E.H., Ross J. Jr., Assessment of cardiac contractility. The relation between the rate of pressure rise and ventricular pressure during isovolumic systole. *Circulation* 44: 47-58, 1971.
17. Wallace A.G., Skinner N.S. Jr., Mitchell J.H., Hemodynamic determinants of the maximal rate of rise of left ventricular pressure. *Am. J. Physiol.* 205: 30-40, 1963.
18. Brower R.W., Meester G.T., Computer based methods for quantifying regional left ventricular wall motion from cine ventriculograms. *Comput. Cardiol.* 52-62. IEEE Computer Society 1976.
19. Daughters G.T., Ingels N.B. Jr., Jang G.C., Alderman E.L., Stinson E.B., Left ventricular long axis rotation assessed by cinefluoroscopy of implanted myocardial markers. *Fed. Proc.* 36: 447, 1977.
20. Sullivan W., Vlodaver Z., Tuna N., Long L., Edwards J.E., Correlation of electrocardiographic and pathologic findings in healed myocardial infarction. *Am. J. Cardiol.* 42: 724, 1978.
21. Peterson K.L., Skloven D., Ludbrook P., Uther J.B., Ross J. Jr., Comparison of isovolumic and ejection phase indices of myocardial performance in man. *Circulation* 49: 1088, 1974.
22. Gault J.H., Ross J. Jr., Braunwald E., Contractile state of the left ventricle in man. Instantaneous tension-velocity-length relations in patients with and without disease of the left ventricular myocardium. *Circ. Res.* 22: 451-463, 1968.
23. Karliner J.S., Gault J.H., Eckberg D., Mullins C.B., Ross J. Jr., Mean velocity of fiber shortening. A simplified measure of left ventricular myocardial contractility. *Circulation* 44: 323-333, 1971.
24. Dwyer E.M. Jr., Left ventricular pressure-volume alterations and regional disorders of contraction during myocardial ischemia induced by atrial pacing. *Circulation* 42: 1111-1122, 1970.
25. Maddox D.E., Wynne J., Uren R., Parker J.A., Idoine J., Siegel L.C., Neill J.M., Cohn P.F., Holman B.L., Regional ejection fraction: A quantitative radionuclide index of regional left ventricular performance. *Circulation* 59: 1001-1009, 1979.
26. Leighton R.F., Pollack M.E., Welch T.G., Abnormal left ventricular wall motion at mid-ejection in patients with coronary heart disease. *Circulation* 52: 238-244, 1975.
27. Johnson L.L., Ellis K., Schmidt D., Weiss M.B., Cannon P.J., Volume ejected in early

- systole. A sensitive index of left ventricular performance in coronary artery disease. *Circulation* 52: 378-389, 1975.
28. Battler A., Slutsky R., Karliner J., Froelicher V., Ashburn W., Ross J. Jr., Left ventricular ejection fraction and first third ejection fraction after acute myocardial infarction: value for predicting mortality and morbidity. *Am. J. Cardiol.* 45: 197-202, 1980.
 29. Clayton P.D., Bulawa W.F., Klausner S.C., Urie P.M., Marshall H.W., Warner H.R., The characteristic sequence for the onset of contraction in the normal human left ventricle. *Circulation* 59: 671-679, 1979.

CHAPTER VI

QUANTITATIVE ASSESSMENT OF REGIONAL PUMP- AND CONTRACTILE FUNCTION

PART II: CHANGES IN REGIONAL WALL MOTION AND PUMP FUNCTION INDUCED BY PACING IN PATIENTS WITH CORONARY ARTERY DISEASE

T.E.H. Hooghoudt, P.W. Serruys, C.J. Slager, J.H.C. Reiber, J.C.H. Schuurbiens, G.T. Meester, P.G. Hugenholtz. (material contained in this chapter has been submitted in a modified form to *Am.J.Cardiol.*)

Abstract

The applicability of a new method to quantify regional left ventricular wall motion to severely asynergic ventricles was evaluated in this study. Ventriculography was performed in twelve patients with coronary artery disease, at rest (72 ± 12 bpm (mean heart rate \pm standard deviation in beats per minute)) and during atrial pacing (136 ± 11 bpm). Left ventricular wall displacement was determined frame by frame in 20 segments of the 30° RAO ventriculogram. In each segment, displacement and the regional contribution to global ejection fraction (CREF), defined as the ejectional change of volume of a particular segment normalized for end diastolic volume, were determined. CREF decreased in 193 of 240 segments (median value 25%) and increased in 47 segments (median 21%). Six segments in two patients became dyskinetic. Despite pacing induced distortion of the left ventricular silhouette, the sum of CREF values (SUMCREF) for each angiogram correlated well ($r = 0.98$) with global ejection fraction computed according to Simpson's rule. These results suggest that this new method to assess regional left ventricular wall motion provides, even in the case of severe asynergy, realistic displacement data, from which regional pump function may be derived with an acceptable degree of accuracy.

Key words: left ventricular wall motion, atrial pacing, regional pump function.

INTRODUCTION

The purpose of this study is to assess the applicability of a new method to quantify regional wall motion, which is based on the actual motion of endo-

cardial anatomical landmarks in normal individuals (1, 2), to ventriculograms with severe asynergy. Rapid atrial pacing was chosen to induce a spectrum of asynergy in patients with coronary artery disease. Through an increase in myocardial oxygen consumption (3) and without affecting peripheral hemodynamics (4-6) or sympathetic drive (7) rapid atrial pacing challenges the cardiac balance between oxygen supply and demand and is consequently a useful test to assess the reserve capacity of the heart (8). In patients with coronary artery disease, ventriculography during pacing at submaximal heart rate frequently shows a deterioration of regional left ventricular function as expressed by ejection fraction (9, 10). The ejection fraction however describes only global left ventricular function, whereas coronary artery disease often has a regional character which causes regional impairment of left ventricular performance. In contrast, the regional contribution to global ejection fraction (CREF) expresses quantitatively to what extent a particular segment contributes to overall ejection fraction, thus revealing regional dysfunction which could be masked by compensatory motion of other wall segments.

Patient material, cineangiographic and catheterization methods

Twelve patients with coronary artery disease were studied after an overnight fast without premedication. Digitalis and beta-blocking drugs were stopped at least 24 hours before the study. The clinical data of the patients are summarized in table I. A bipolar pacing catheter was introduced in the right atrium

Table I. *Personal and clinical data of the patients in this study. The number of vessels (v) affected by > 50% narrowing due to coronary sclerosis and the number of applied bypasses and their patency is shown.*

Patient	Age (y)	Coronary Sclerosis	Bypasses	
			patent	occluded
1	44	3v	2	
2	48	2v	2	
3	43	3v	4	1
4	48	3v	3	
5	49	2v	2	
6	46	2v	2	
7	44	2v	2	
8	58	2v		1
9	63	3v	no CABG	
10	52	3v	4	
11	54	3v	no CABG	
12	58	3v	2	1

or in the coronary sinus, while a high fidelity tipmanometer* was placed in the left ventricle. From the continuously recorded left ventricular pressure, hemodynamic variables such as end-diastolic pressure, peak rate of change of pressure and contractile element velocity at zero load were derived. Left ventriculography (50 f/sec) was performed in the 30° RAO projection with 0.75 ml/kg Urographin 76** at a flow rate of 18 ml/sec. In all patients the ventriculograms were obtained before coronary arteriography. A cineangiogram was made at resting heart rate and at a heart rate 20 beats below the maximal obtainable heartrate as determined in the atrial pacing stress test performed before the first angiogram. Maximal heart rate was considered to be reached when angina or atrio-ventricular block occurred or at a frequency of 180 bpm. The paced ventriculogram was only made after the values of left ventricular end-diastolic pressure and of isovolumic parameters of contractility were identical with those measured before the resting angiogram, thus eliminating the influence of volume load and contrast toxicity on left ventricular wall performance. In all cases an interval of at least 20 minutes between the two angiograms was observed. Care was taken to preserve the patients' geometrical position relative to the X-ray equipment during the sequential angiograms. Diaphragm movement was excluded by shallow inspiration; care was taken to prevent a Valsalva maneuver.

Calculated variables

From all cineangiograms a complete cardiac cycle was analyzed at resting heart rate and during atrial pacing. End diastolic volume, stroke volume, ejection fraction, regional wall displacement and regional contribution to global ejection fraction were each assessed as described in part I of this study (11).

RESULTS

In 12 patients with coronary artery disease left ventriculography was performed at rest and during rapid atrial pacing. With pacing the heart rate was increased from 72 ± 12 bpm to 136 ± 11 bpm, a change of $92 \pm 32\%$. End-diastolic volume normalized for body surface area decreased from 76.9 ± 12.1 ml/m² to 55.2 ± 9.1 ml/m², while stroke index decreased from 44.6 ± 8.0 ml/m² to 25.7 ± 5.1 ml/m². Ejection fraction (EF) decreased in 11 out of 12 patients with $22.4 \pm 10\%$ of resting EF. Regional wall motion was determined in each patient in both angiograms in 20 segments; in total 480 segments were analysed. From the regional wall displacement data, the regional contribution to global ejection fraction (CREF) was computed for each segment. In 193 out of 240 segments a decrease of CREF occurred under the stress of tachycardia. In 47 of 240 segments an increase of CREF was observed. The median percentage decrease

* Millar Instruments Inc., Houston, Texas, U.S.A.

** Schering A.G., Berlin, Bergkammen, G.B.R.

of CREF amounted to 25% (10th percentile 5%, 90th percentile 76%), whereas the median percentage of those segments which showed an increase of CREF was 21% (10th percentile 5%, 90th percentile 84%). During pacing 6 segments developed overt dyskinesia. In each patient the change of CREF values during atrial pacing showed an individual pattern. In some a decrease of CREF in all wall segments was observed (figure 1), while in others no change of CREF in

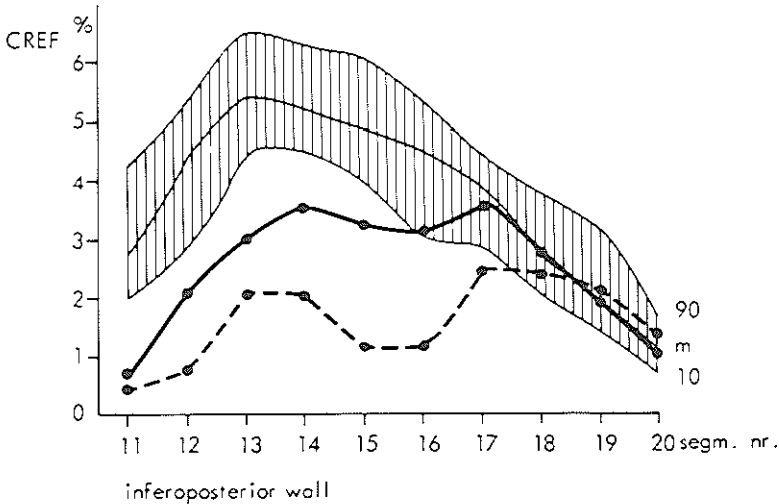
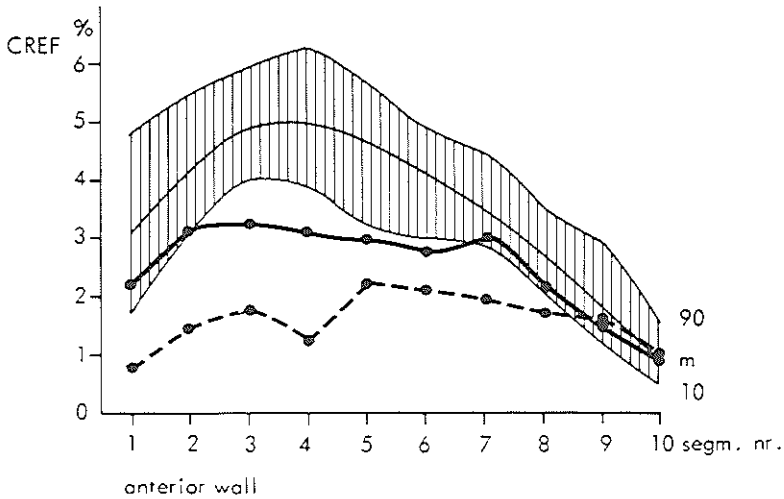


Figure 1. Typical example of a generalized decrease of pump function under the stress of tachycardia. Crosshatched areas show the normal range of CREF (between the 10th and 90th percentile). CREF data determined at resting heart rate (solid line) and during rapid atrial pacing (dashed line) are shown.

one wall region was accompanied by a steep decrease in another (figure 2). In table II global EF, computed according to Simpson's rule is compared with the sum of CREF data (SUMCREF). The relation between the SUMCREF and global EF shows a linear correlation of $r = 0.975$ (figure 3).

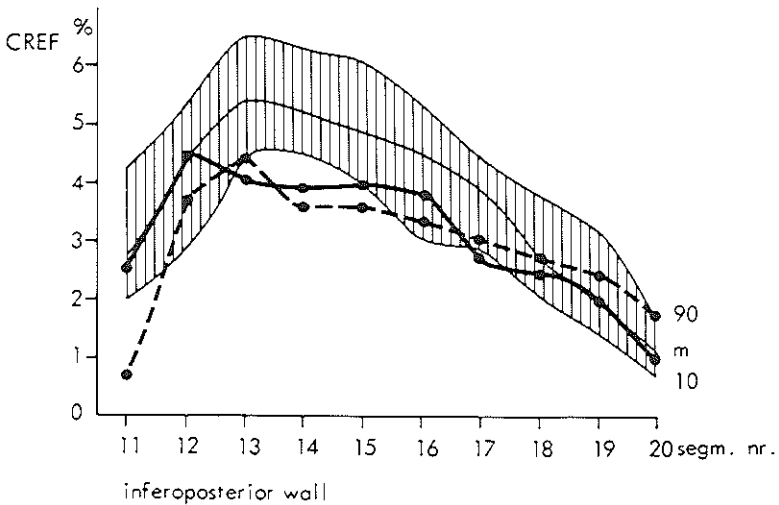
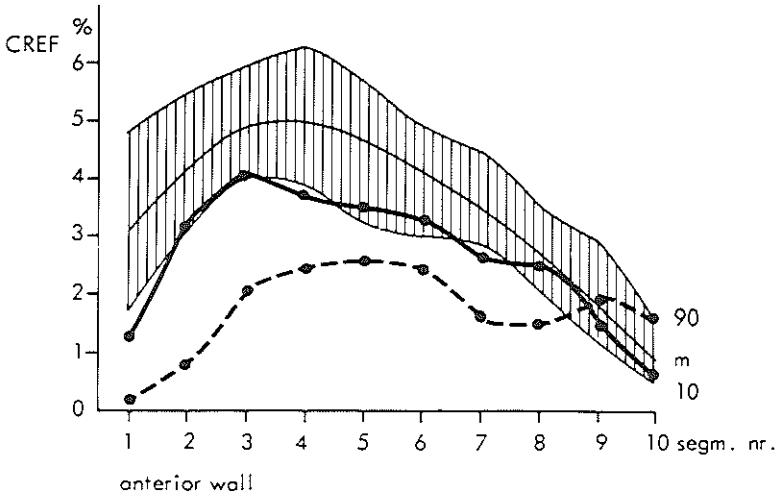


Figure 2. Example of regional functional impairment of the anterior wall due to pacing induced tachycardia. The solid line indicates CREF values at resting heart rate, the dashed line during tachycardia.

Table II. Global ejection fraction determined according to Simpson's rule and sum of CREF values at resting heart rate and during atrial pacing in 12 patients.

	Global EF		sum of CREF (SUMCREF)	
	<i>at rest</i>	<i>during pacing</i>	<i>at rest</i>	<i>during pacing</i>
1.	46.1	32.2	49.9	32.0
2.	48.5	45.0	45.9	42.4
3.	55.9	46.3	54.1	45.8
4.	66.3	75.8	65.6	77.5
5.	57.8	45.4	57.5	46.4
6.	74.4	46.7	75.0	40.5
7.	67.5	51.6	70.9	59.5
8.	63.9	44.9	61.2	38.4
9.	57.2	43.1	59.9	42.6
10.	44.9	38.0	40.5	36.5
11.	48.5	35.4	47.8	32.4
12.	71.4	66.4	72.0	65.6

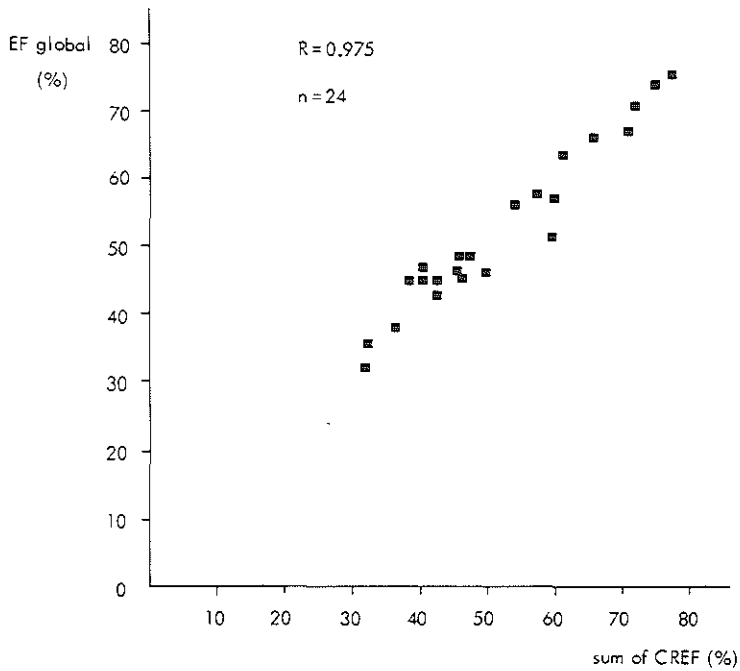


Figure 3. An approximate linear correlation is found between ejection fraction computed as the sum of CREF values and global ejection fraction computed according to Simpson's rule.

DISCUSSION

The applied method to quantify regional wall motion is based on the actual motion of endocardial anatomical landmarks in normal subjects (1, 2). It may thus be objected that in case of asynergy the actual endocardial trajectories do not coincide with the coordinate system of the model. In other words, there is a risk that substantial asynergy may seriously hamper the accurate determination of disturbed endocardial wall motion. If the displacement data are realistic and the wall motion model remains applicable despite malformation of the left ventricular silhouette, an excellent correlation should exist between ejection fraction as calculated from the left ventriculogram according to Simpson's rule and the sum of CREF data (SUMCREF). To test the possible influence of asynergy, patients with normal and abnormal wall motion at rest were submitted to rapid atrial pacing in order to induce additional changes in wall motion. Atrial pacing was also preferred as stress test because it is highly controllable and easy to perform and does not interfere with the acquisition of high quality angiograms, for example, physical exercise would do.

Although in the majority of the patients the stress of tachycardia indeed caused significant malformation of the left ventricular silhouette, a good correlation is observed between the SUMCREF and global ejection fraction. This suggests that the basic regional displacement data, and the derived regional pump function data are accurately assessed. Theoretically this result could also be obtained in the presence of a systematic error which would lead to overestimation of CREF values in one region and complementary underestimation in another region. To exclude this possibility a standard reference method for the assessment of regional left ventricular function would be required. At present no such method is available.

REFERENCES

1. Slager C.J., Hooghoudt T.E.H., Reiber J.H.C., Schuurbiens J.C.H., Booman F., Meester G.T., Left ventricular contour segmentation from anatomical landmark trajectories and its application to wall motion analysis. *Computers in Cardiology* pp 347-350. IEEE Computer Society 1979.
2. Slager C.J., Hooghoudt T.E.H., Reiber J.H.C., Schuurbiens J.C.H., Verdouw P.D., Hugenholtz P.G., Endocardial landmark motion; a new approach to the assessment of regional left ventricular performance. This thesis pp. 30-48.
3. Boerth R.C., Covell J.W., Pool P.E., Ross J. Jr., Increased myocardial oxygen consumption and contractile state associated with increased heart rate in dogs. *Circ. Res.* 24: 725-734, 1969.
4. Ross J. Jr., Linhart J.W., Braunwald E., Effects of changing heart rate in man by electrical stimulation of the right atrium. *Circulation* 32: 549-558, 1965.
5. Linhart J.W., Pacing-induced changes in stroke volume in the evaluation of myocardial function. *Circulation* 43: 253-261, 1971.
6. Brower R.W., Remme W.J., Ten Katen H.J., Van den Brand M., Quantification of the

- atrial pacing stress test: normal values and limits between normal and abnormal for coronary artery disease in man. *Computers in Cardiology* pp. 591-599, Long Beach, California: IEEE Computer Society 1976.
7. Cross D.F., Use of atrial pacing and exercise in studying ventricular function during angina. *Am. J. Cardiol.* 26: 217-218, 1970.
 8. Sowton G.E., Balcon R., Cross D., Frick M.H., Measurement of anginal threshold using atrial pacing. *Cardiovasc. Res.* 1: 301-307, 1967.
 9. Pasternac A., Gorlin R., Sonnenblick E.H., Haft J.I., Kemp H., Abnormalities of ventricular motion induced by atrial pacing in coronary artery disease. *Circulation* 45: 1195-1205, 1972.
 10. Dwyer E.M. Jr., Left ventricular pressure - volume alterations and regional disorders of contraction during myocardial ischemia induced by atrial pacing. *Circulation* 42: 1111-1122, 1970.
 11. Hooghoudt T.E.H., Slager C.J., Reiber J.H.C., Schuurbiens J.C.H., Meester G.T., Hugenholtz P.G., Quantitative assessment of regional pump- and contractile function. Part I: The normal human heart. This thesis pp. 59-81.

CHAPTER VII

“REGIONAL CONTRIBUTION TO GLOBAL EJECTION FRACTION” USED TO ASSESS THE APPLICABILITY OF A NEW WALL MOTION MODEL TO THE DETECTION OF REGIONAL WALL MOTION IN PATIENTS WITH ASYNERGY

T.E.H. Hooghoudt, C.J. Slagter, J.H.C. Reiber, P.W. Serruys, J.C.H. Schuurbiens and G.T. Meester, *Computers in Cardiology*, pp. 253-256, IEEE Computer Society, 1980.

Abstract

In this study the concept of regional contribution to global ejection fraction (CREF), as a parameter of left ventricular pump function, is introduced. This variable can be derived from regional displacement data and will express quantitatively the relative contribution of a particular left ventricular wall segment to global ejection fraction.

Displacement data are assessed with a new model of left ventricular wall motion, based on endocardial landmark trajectories in normal subjects. In order to validate the applicability of this model in patients with asynergy, displacement data and the derived parameter CREF were measured in two groups of patients with heart disease. A strong correlation between the sum of CREF data and global ejection fraction demonstrates that the basic displacement data are accurate. In summary:

- A new parameter for regional left ventricular pump function is introduced.
- The applied wall motion model is effective even when the left ventricular silhouette is malformed by severe asynergy.

INTRODUCTION

The assessment of regional left ventricular function and its response to intervention procedures (1) may elicit both the functional significance of coronary artery stenoses and the viability of myocardium, and may thus be of importance in the selection of patients for bypass surgery. Our efforts to quantify changes in regional left ventricular function due to the stress of tachycardia, were seriously hampered by the virtual absence of an adequate quantitative determinant of regional left ventricular function. The currently available methods to determine

left ventricular pump and contractile function, such as ejection fraction and the isovolumic of contractility, only assess global function and cannot be used when regional dysfunction with compensatory hyperfunction of other segments are present. In order to solve this difficulty the regional contribution to global ejection fraction (CREF) was developed. This parameter of regional pump function is felt to express quantitatively to what extent a particular wall segment contributes to global ejection fraction and is derived from displacement data which are assessed with a wall motion model, based on the actual motion pattern of small anatomical structures at the endocardial border, as established in normal subjects (2). In the present study this new determinant of regional left ventricular pump function is introduced and used to validate the applicability of our new wall motion model in patients with asynergy.

The angio-analysis system, calculated variables

The angio-analysis system consists of a hard-wired video contour detector (3) linked to a mini-computer. The left ventricular cine-angiogram is projected with a Vanguard projector, converted into video format and displayed on a videomonitor. After the 30° RAO ventriculogram has been rotated until the ventricular long axis has a vertical position, the analysis is started a few frames before end diastole by indicating the border points of the aortic valve. The contour detector then automatically traces the endocardial contour (figure 1).

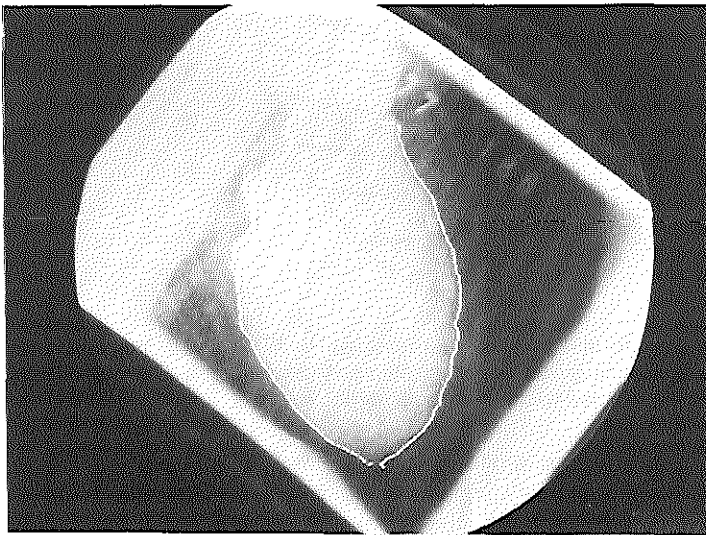


Figure 1. Display of the left ventriculogram with the detected contour.

When the observer disagrees with the contour detector about the position of the detected border, manual correction with a writing tablet is possible.

In this way frame by frame analysis over one entire cardiac cycle is performed. The border information is sent to a PDP 11/34 minicomputer and stored on a RK-05 disk. To analyse these data, the contours of one cardiac cycle are reproduced while the volume of each frame is computed according to Simpson's rule. Instantaneous volume and its first derivative are displayed graphically. This enables the operator to indicate the end diastolic and end systolic frames, which are considered to be the frames with the maximal and minimal volume respectively.

Next, the end diastolic and end systolic contours are displayed, while the calculated volume data, cardiac output and global ejection fraction are displayed. Manual indication of the mitral valve edge initiates the algorithm which generates the wall motion model (figure 2).

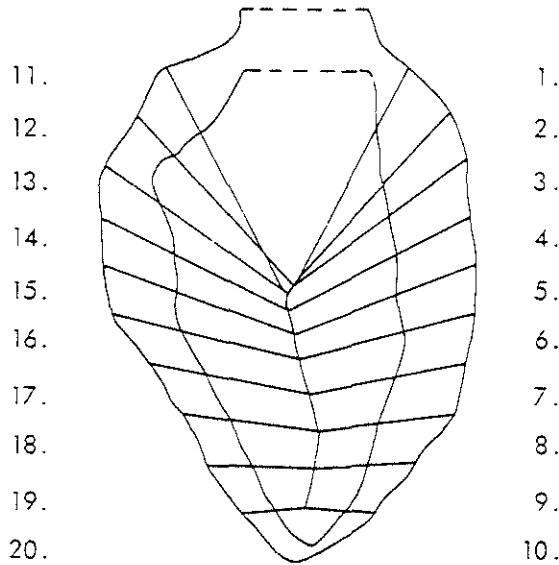


Figure 2. The end diastolic and end systolic contours of a 30° RAO left ventriculogram with the applied wall motion model are shown. Regional wall motion is determined in 20 segments, ten in the anterior and ten in the inferoposterior wall.

Along the trajectories of this model endocardial wall displacement is determined frame by frame in twenty segments (figure 3). Regional wall velocity, the time derivative of regional wall displacement, is also determined and may be observed as a determinant of regional myocardial function reflecting the contractile state. The second parameter which is derived from displacement

data is the regional contribution to global ejection fraction (CREF). For this purpose the left ventricular end diastolic cavity is divided into twenty half

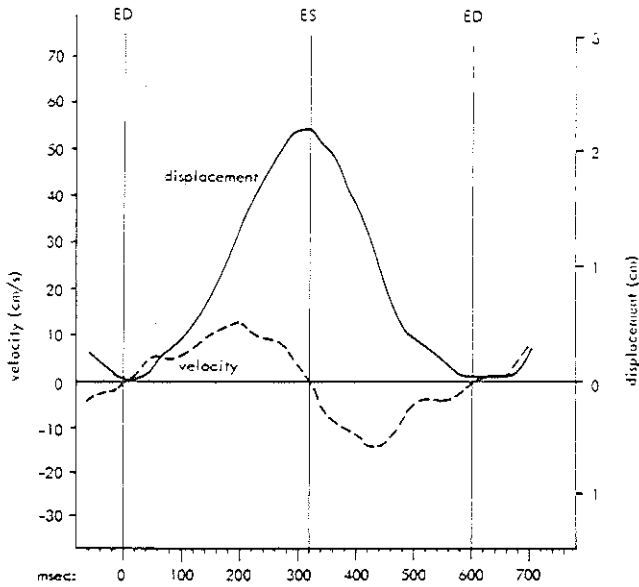


Figure 3. Graphical display of segmental displacement and velocity assessed from frame by frame analysis of the left ventricular contours over one full cardiac cycle.

slices, ten in the anterior and ten in the inferoposterior wall area (figure 4).

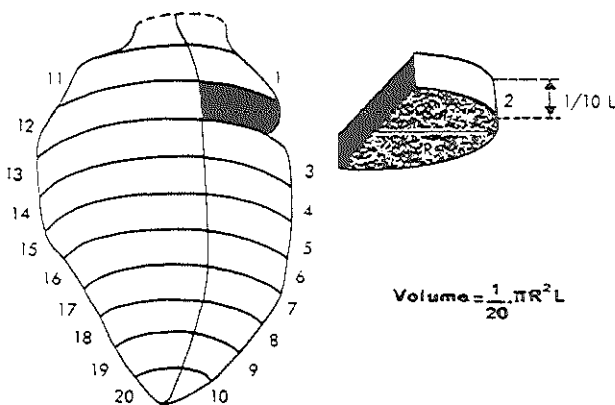


Figure 4. The left ventricular end diastolic cavity is divided into twenty half slices. The volume of each half slice is computed according to the given formula, R is radius and L left ventricular long axis length.

Each half slice corresponds to one of the segments of our wall motion model. The volume of each half slice is computed from the local radius R and the left ventricular long axis length L according to the formula:

$$1/10.L.1/2.\pi R^2 = \frac{1}{20}.\pi R^2 L$$

where L is left ventricular long axis length and R is the radius of the particular slice. The volume change of each slice during systole (ejected volume) is derived from the x-component of regional wall displacement which determines the change in radius of a particular half slice. Normalization for left ventricular end diastolic volume yields the percentage each segment contributes to global ejection fraction (figure 5):

$$\frac{\text{ejected slice volume (ml)}}{\text{global end diastolic volume (ml)}} \times 100 = \text{CREF (\%)}$$

Summation of the CREF-values of all twenty segments should correspond to the global ejection fraction value. This implies that the comparison between the sum of CREF and global ejection fraction is an excellent opportunity to check whether this method to assess regional wall motion tracks wall motion in its actual extent and direction, even in the case of severe asynergy.

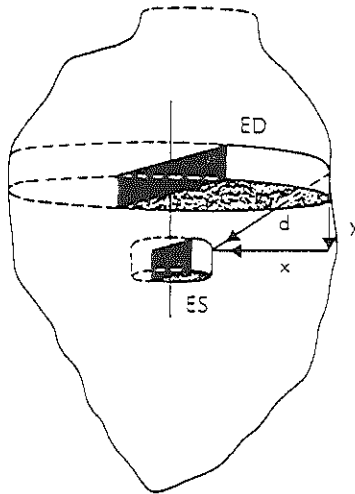


Figure 5. The volume change in each half slice during systole is derived from the x-component (x) of regional wall displacement (d).

Patient population

Two groups of patients were studied. The first group consisted of twelve patients with coronary heart disease (age 43-63 years) who after a first ventriculogram was made at resting heart rate were submitted to a second ventriculogram during atrial pacing at submaximal heart rate, in order to induce additional asynergy.

The second group consisted of 51 consecutive patients (age 21-71, mean 51 years), who were submitted to a diagnostic heart catheterization because of suspected coronary, valvular or congenital heart disease. Ejection fraction ranged between 15 and 68%, which implies that this patient group covers the spectrum from severe wall motion disturbances to normal wall motion.

RESULTS

In the patients who were submitted to a paced ventriculogram, resting heart rate was 72 ± 12 bpm (mean \pm standard deviation). During atrial pacing this was increased to 136 ± 11 bpm. Ejection fraction decreased in 11 of 12 patients with $22.4 \pm 10.0\%$ of resting values. CREF decreased in 193 of 240 segments with a median value of 25 per cent, while six segments became dyskinetic. This implies that the stress of tachycardia induced substantial additional asynergy. Nevertheless an excellent correlation was found between the sum of CREF values and global ejection fraction ($r = 0.975$) (figure 6).

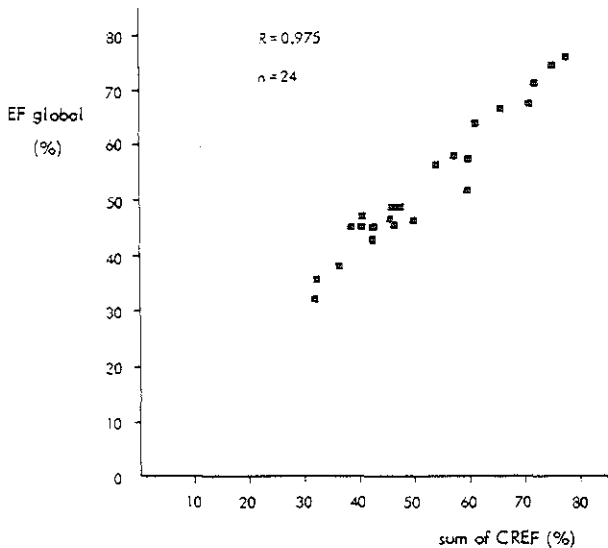


Figure 6. A strong correlation is found between the global ejection fraction and the sum of CREF data in the angiograms of twelve patients at resting heart rate and during rapid atrial pacing.

In the second group of patients ejection fraction was determined with three different methods:

- manual analysis by an experienced technician,
- assessment of global ejection fraction with the computer system, and
- computation of the sum of CREF values for each angiogram.

Manual analysis and automated assessment of global ejection fraction correlated well ($r = 0.96$). Also a good correlation was found between the sum of CREF values and global ejection fraction assessed with the computer system ($r = 0.98$) (figure 7).

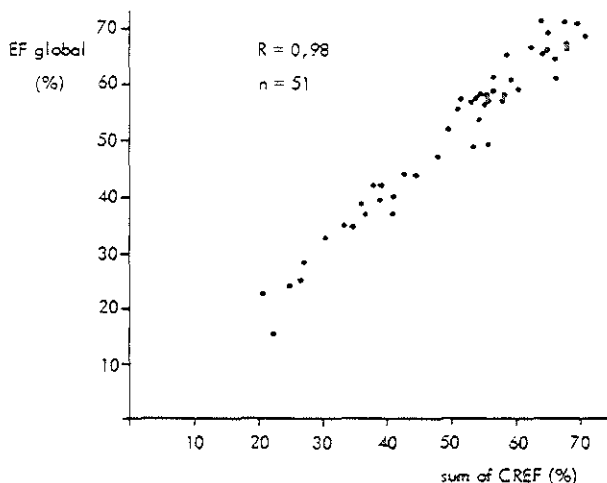


Figure 7. Comparison between global ejection fraction and the sum of CREF data in 51 consecutive patients with heart disease shows an excellent correlation.

DISCUSSION

Regional left ventricular function can be derived from regional wall motion data, provided that the actual motion of the endocardial wall is tracked. A number of methods have been proposed to reach this goal (4 - 7), but almost all introduce a considerable error, both in extent and direction of determined wall motion, as was established recently by Alderman and coworkers (8).

Last year we presented a new wall motion model (2), based on the actual motion pattern of small anatomical structures at the endocardial border, detected in the left ventriculograms of normal subjects with the automated video contourdetector Contouromat (3). This wall motion model is now tested in patients with asynergy causing malformation of the left ventricular silhouette. Assessment of the accuracy of displacement data in a group of patients with

the entire range from normal wall motion to severe asynergy would provide valuable information on the applicability of the model. However at present no "gold standard" exists to test whether displacement is properly assessed. Fortunately this problem could be approached by the advent of a new parameter of regional pump function, derived from displacement data. The analysis of the behaviour of regional left ventricular function during intervention procedures – such as rapid atrial pacing – was hampered by the absence of an adequate parameter to quantify regional pump function. Therefore the regional contribution to global ejection fraction variable was developed, with as a major advantage that it expresses quantitatively the percent contribution of a particular segment to global ejection fraction. As the sum of CREF data in each angiogram should equal global ejection fraction, an easy check can be made whether the basic displacement data are accurate.

The approximate linear correlation found in a heterogenous group with ejection fractions between 15 and 68% is highly suggestive that our model describes regional wall motion in a realistic way, even in the case of severe asynergy. The strong correlation in the group of patients with additional asynergy, induced by rapid atrial pacing, suggests that this model is also applicable to assess the changes in regional wall motion and pump function during stress.

REFERENCES

1. Cohn P.F., Gorlin R., Dynamic ventriculography and the role of the ejection fraction. *Am. J. Cardiol.* 36: 529-531, 1975.
2. Slager C.J., Hooghoudt T.E.H., Reiber J.H.C., Schuurbiens J.C.H., Booman F., Meester G.T., Left ventricular contour segmentation from anatomical landmark trajectories and its application to wall motion analysis. *Computers in Cardiology* pp. 347-350. IEEE Computer Society, 1979.
3. Slager C.J., Reiber J.H.C., Schuurbiens J.C.H., Meester G.T., Contouromat – A hard-wired left ventricular angio-processing system. I. Design and application. *Comput. Biomed. Res.* 11: 491-502, 1978.
4. Leighton R.F., Wilt S.M., Lewis R.P., Detection of hypokinesis by quantitative analysis of left ventricular cineangiograms. *Circulation* 50: 121-127, 1974.
5. Harris L.D., Clayton P.D., Marshall H.W., Warner H.R., A technique for the detection of asynergistic motion of the left ventricle. *Comput. Biomed. Res.* 7: 380-394, 1974.
6. Rickards A., Seabra-Gomes R., Thurston P., The assessment of regional abnormalities of the left ventricle by angiography. *Eur. J. Cardiol.* 5: 167-182, 1977.
7. Chaitman B.R., Bristow J.D., Rahimtoola S.H., Left ventricular wall motion assessed by using fixed external reference systems. *Circulation* 48: 1043-1054, 1973.
8. Ingels N.B. Jr., Daughters G.T., Stinson E.B., Alderman E.L., Evaluation of methods for quantitating left ventricular segmental wall motion in man using myocardial markers as standard. *Circulation* 61: 966-972, 1980.

CHAPTER VIII

OBSERVER VARIABILITY IN THE VISUAL ASSESSMENT OF REGIONAL WALL MOTION AND IN COMPUTER ASSISTED ANALYSIS OF REGIONAL LEFT VENTRICULAR FUNCTION

T.E.H. Hooghoudt, C.J. Slager, J.H.C. Reiber, R.W. Brower, S. Castellanos, I.C.J. Zorn and P.G. Hugenholtz.

Abstract

Regional left ventricular wall motion was graded by an experienced observer as normo-, hypo-, a-, or dyskinetic, and compared with the interpretation of a second observer and with the results of computer assisted analysis of regional left ventricular pump function. With visual inspection the observers agree in only 68% of the readings. In 2% a disagreement of more than one point on a four point scale is observed. There is a major overlap in the assessed regional pump function between wall regions graded as normal (normokinesis) and abnormal (hypo-, a-, or dyskinesis). The median values of pump function in these regions agree well with generally accepted values of normal and abnormal left ventricular pump function respectively. When an ejection fraction of 53.3% is taken to separate normal and abnormal left ventricular function, visual assessment of left ventricular wall motion is incorrect in 22% of the observations. The inter- and intra-observer variability of automated assessment of global and regional left ventricular performance, evaluated with linear regression analysis is small: Global ejection fraction: $58.3 \pm 17.2\%$ (mean \pm SD), standard error of the estimate (SEE): 1.6 - 2.3%; Summed regional contribution to ejection fraction: Anterobasal wall: $17.0 \pm 5.4\%$, SEE: 0.7 - 2.3%; Anterolateral wall: $10.3 \pm 4.5\%$, SEE: 0.8 - 1.4%; Apical wall: $3.1 \pm 1.3\%$, SEE 0.4 - 0.5%; Inferior wall $11.9 \pm 3.6\%$, SEE: 0.4 - 0.9%; Posterobasal wall $16.1 \pm 5.3\%$, SEE: 0.7 - 2.2%. It is concluded that the reproducibility, and thus the accuracy of visual appraisal of regional wall motion is low, whereas automated assessment of regional pump function is reproducible and in this respect preferable.

Keywords: regional left ventricular wall motion, left ventricular regional pump function, reproducibility.

INTRODUCTION

The nature and extent of cardiac disease can be assessed accurately by quantitative analysis of the left ventricular cineangiogram. Many methods have been described to quantitate left ventricular volume (1-4) as well as regional and global performance (5-8). Nevertheless, most cardiologists continue to judge regional left ventricular function by visual inspection, rather than evaluating it with quantitative methods. Little is known about the accuracy of the visual appraisal of left ventricular performance. A few studies (9, 10), which have been performed to assess the inter- and intraobserver variability with Herman et al's (11) method for semiquantitative analysis of left ventricular segmental wall motion, show how variable and inconsistent naked eye observation may be, but such an approach lacks a standard to evaluate the absolute accuracy of the observations.

With an automated endocardial contour detector (12), linked to a system for left ventricular segmental function analysis (13), a comparison between the results of naked eye analysis and quantitative functional data can readily be made. In this study left ventricular regional pump function, expressed as the contribution of a region to global ejection fraction (14), is applied as a quantitative functional standard, to evaluate the results of "eyeball" observation of regional wall motion. We have examined: 1) the variation in results of visual inspection of regional wall motion by two experienced observers; 2) the intra- and interobserver variability of measurements made with the regional function analysis system; 3) the relation between assessment of regional left ventricular performance by visual inspection and with the regional function analysis system.

Material and methods

The left ventricular angiograms of 51 patients (age 21-71, \bar{m} 51 years), submitted to a diagnostic heart catheterization because of suspected coronary, valvular or congenital heart disease, form the basic material for this study. Left ventricular cineangiography was obtained in the 30° right anterior oblique position at 50 frames/sec. using 0.75 ml/kg meglumine diatrizoate. The injection rate varied from 16-18 ml/s. The ventriculogram was evaluated by two experienced observers (A, B), who graded the wall motion of the five left ventricular wall regions shown in figure 1 (anterobasal, anterolateral, apical, inferior and posterobasal) as normo-, hypo-, a-, or dyskinetic. The observers were unaware of the results of automated quantitative analysis, which was performed separately. The reproducibility of visual inspection was determined by comparing the assessments of observers A and B.

To compare the visual readings of wall motion in the five wall regions with quantitative functional data, the angiofilms were processed with an automated

contour detector (12), which performs automated endocardial contour analysis of each cineframe of one or more cardiac cycle. When the observer disagrees with the contour detector about the identification of the left ventricular endocardial border, manual correction with a writing tablet may be performed. Once the computer has determined the left ventricular volume in each of the analyzed

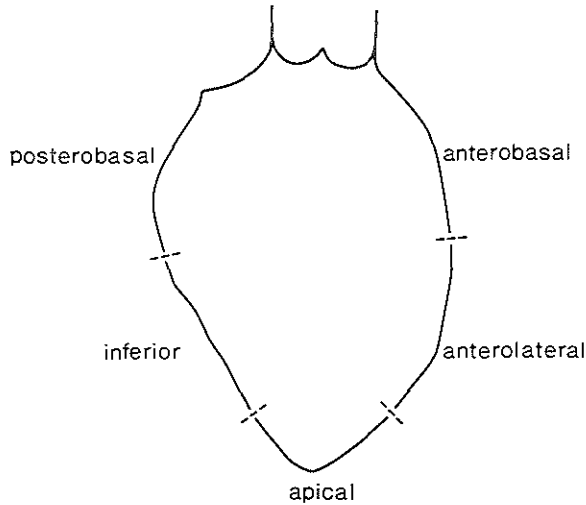


Figure 1. Scheme of the five wall regions in which visual interpretation of regional wall motion is performed.

cineframes, the end diastolic and end systolic cineframes (the frames with maximal and minimal volume respectively) are indicated and ejection fraction is computed. Segmental wall displacement is determined in 10 separate segments in the anterior and 10 segments in the inferoposterior wall, along a system of coordinates as described previously (14, 15) and shown in figure 2. This system

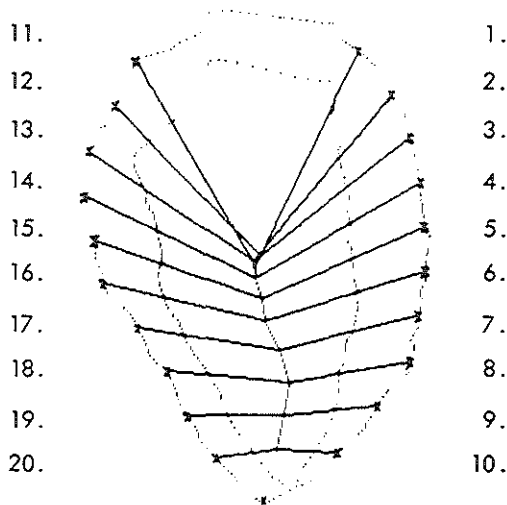


Figure 2. Example of the computer output showing the end diastolic and end systolic contours of a 30° RAO left ventriculogram and the system of coordinates along which left ventricular segmental wall displacement is determined.

of coordinates, which is based on the actual pattern of endocardial wall motion in normal individuals, is generated by the computer after manual indication of the mitral valve edge. The regional contribution to global ejection fraction (CREF), a regional pump function parameter, is derived from the basic displacement data and from left ventricular long axis shortening, which is considered to be 14% (13, 15). Although not specified here, determination of CREF comprises calculation of the systolic volume change of each left ventricular segment and normalization of this volume change for left ventricular and diastolic volume. The sum of the resulting CREF values (SUMCREF) of the 20 segments of a particular left ventricle will equal global ejection fraction (EF) (14). Figure 3 gives an example of the presentation of the data by the computing system. The shaded areas represent the 10th - 90th percentile range of CREF values in normal individuals, while the continuous lines indicate the actual CREF values of the 20 segments in this particular left ventriculogram. To be able to compare the results of automated analysis of regional left ventricular function (CREF) — which is computed in 20 segments — and the results of visual inspection of regional wall motion — assessed in five wall regions — the results of the segments corresponding to each wall region are summated as shown in table I.

Table I. *Relation between the 20 segments and five wall regions used in this study to compare the results of automated assessment of regional left ventricular function with visual interpretation of regional wall motion. The CREF values of the segments 5, 9, 15 and 19 are each allotted half to the neighbouring wall regions.*

<i>Segment</i>	<i>Wall region</i>
1 - 5	Anterobasal
5 - 9	Anterolateral
9, 10, 19 and 20	Apical
15 - 19	Inferior
11 - 15	Posterobasal

The CREF values of segments 5, 9, 15 and 19 are each allotted half to the two neighbouring wall regions. The sum of CREF in each of the five wall regions, which is further referred to as REG-CREF, and the normal range of these data are displayed by the computer as well (figure 3). The 10th percentile border of the REG-CREF in normal individuals (table III, figure 3) is taken to separate normal and abnormal regional left ventricular function. This implies that for the left ventricle as a whole a SUMCREF of 53.3% is considered to be the borderline between normal and abnormal pump function.

For the last part of the study, twenty left ventriculograms coded 1 - 20 were

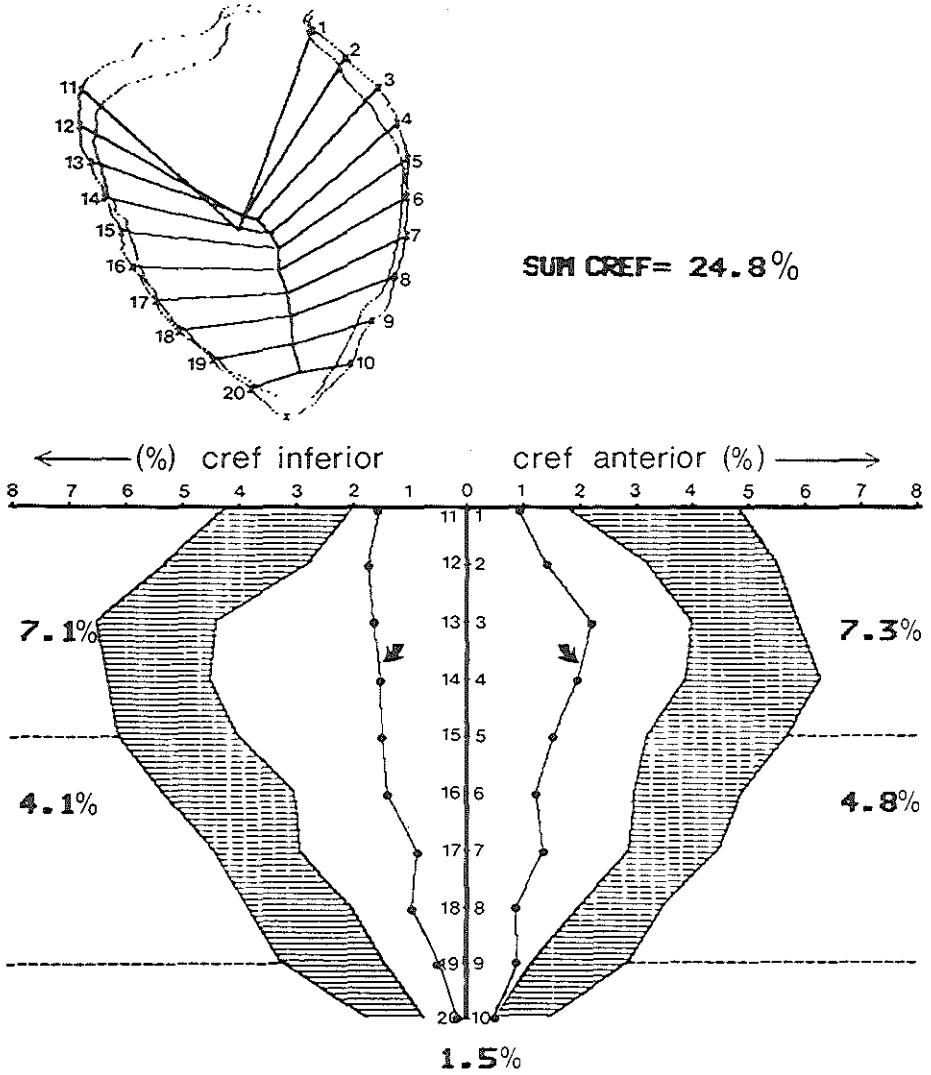


Figure 3. Display of the end diastolic and end systolic left ventricular contours and of the computed CREF values in a patient with a global depression of left ventricular function. On the x-axis the CREF values of the anterior and inferoposterior wall areas are displayed (%), while on the y-axis the segment numbers of the anterior wall (1 - 10) and of the inferoposterior wall (11 - 20) are depicted. The shaded zones represent the 10th - 90th percentile area of CREF values in normal individuals. The continuous lines (arrows) connect the actual CREF values of the individual segments. The sum of CREF in each of the five wall regions (REG-CREF) is indicated in the figure.

processed with the contour detector by two independently working observers X and Y. After an interval of one week to three months, the same films, provided with a new randomly allotted number, were processed for the second time by the same observers. The intra- and interobserver variability in the assessment of global left ventricular volume, EF, REG-CREF and SUMCREF values, was evaluated by computation of the correlation coefficient and the standard error of the estimate (SEE). The relation between EF and SUMCREF was also evaluated twice by each observer.

Table II. Results of visual inspection of regional wall motion in 51 left ventriculograms, performed by two observers (A and B).

		observer A			
		N	H	A	D
observer B	N	78	13	-	-
	H	44	82	3	2
	A	1	5	7	4
	D	1	2	7	6

RESULTS

The result of visual inspection of regional wall motion in 51 left ventriculograms, performed by two experienced observers (A and B) is shown in table II. The observers agree precisely in $173/255 = 68\%$ of the wall regions; 82 are graded differently, half of which are graded as normal by observer A and as hypokinetic by observer B. In $6/255 = 2\%$ the observers disagree more than one grade of this four grade scoring system.

The intraobserver variability in the quantitative assessment of global left ventricular volume and ejection fraction is very small (standard error of the estimate (SEE) of $1.2 - 1.5 \text{ ml/m}^2$ and $1.6 - 1.8\%$ respectively (table IV)). Inter observer variation is only slightly greater (SEE $1.5 - 2.3 \text{ ml/m}^2$ and $1.9 - 2.3\%$ respectively). Computation of SUMCREF is subject to a SEE of $1.8 - 2.5\%$ for the intra-observer variability and $2.2 - 3.6\%$ for the inter-observer variability.

Table III. Relation between the results of automated analysis of regional left ventricular function and visual inspection of regional wall motion in 51 left ventriculograms (see also figure 4).

Wall region	10th percentile REG-CREF border (%)	Number of wall regions scored incorrectly as normal	Number of wall regions scored incorrectly as abnormal (H, A, or D)	Percentage incorrect observations	Specificity (%)	Sensitivity (%)
Anterobasal	14.4	12	2	27	93	46
Anterolateral	10.1	1	8	18	67	96
Apical	2.5	3	8	20	67	89
Inferior	10.6	3	7	20	76	86
Posterobasal	15.7	8	4	24	79	75
SUMCREF	+ 53.3%		\bar{m} 22%			

The 10th percentile of CREF values in normal individuals is taken to separate normal and abnormal regional left ventricular performance.

Specificity: per cent of wall regions with a REG-CREF $>$ 10th percentile, graded as normal. Sensitivity: per cent of wall regions with a REG-CREF \leq 10th percentile, graded as abnormal.

Abbreviations: CREF: regional contribution to ejection fraction, REG-CREF: sum of CREF values in a particular wall region, SUMCREF: sum of CREF values of all five wall regions.

Table IV. Intra- and inter-observer variability in the assessment of left ventricular end diastolic volume, ejection fraction and SUMCREF in 20 patients.

Comparison between observations	LVEDVI (73.1 \pm 27.6 ml/m ²)		Ejection fraction (58.3 \pm 17.2%)		SUMCREF (58.3 \pm 15.6%)	
	Correlation coefficient	SEE (ml/m ²)	Correlation coefficient	SEE (%)	Correlation coefficient	SEE (%)
Xa - Xb	0.99	1.5	0.99	1.8	0.99	2.5
Ya - Yb	0.99	1.2	0.99	1.6	0.99	1.8
Xa - Ya	0.99	1.6	0.99	2.2	0.99	2.2
Xa - Yb	0.99	1.5	0.99	1.9	0.98	2.9
Xb - Ya	0.99	2.2	0.99	2.3	0.98	3.1
Xb - Yb	0.99	2.3	0.99	2.3	0.97	3.6

Abbreviations: LVEDVI: left ventricular end diastolic volume corrected for body surface area; SUMCREF: summated CREF values; SEE: standard error of the estimate; X: observation of observer X; Y: observation of observer Y; a: first observation; b: second observation.

The correlation between EF computed from global left ventricular volume change and SUMCREF is liable to a SEE of 1.9 - 3.9% (table V). The variability in the assessment of REG-CREF is characterized by a SEE of 0.4 - 1.4% when assessed twice by the same observer, and a SEE of 0.4 - 2.3% when determined by two observers (table VI).

Table V. *Correlation between ejection fraction assessed from global left ventricular volume change and the SUMCREF in 20 patients.*

Observations of EF and SUMCREF	Correlation coefficient	SEE (%)
Xa - Xa	0.99	1.9
Xb - Xb	0.97	3.9
Ya - Ya	0.99	2.5
Yb - Yb	0.99	2.6

Abbreviations: EF: ejection fraction; further see table IV.

Table VI. *Intra- and inter-observer variability in the assessment of REG-CREF values of five left ventricular wall regions in 20 patients.*

Comparison between observations	Wall region:									
	Anterobasal (REG-CREF = 17.0 ± 5.4%)		Anterolateral (REG-CREF = 10.3 ± 4.5%)		Apical (REG-CREF = 3.1 ± 1.3%)		Inferior (REG-CREF = 11.9 ± 3.6%)		Posterobasal (REG-CREF = 16.1 ± 5.3%)	
	Correla- tion co- efficient (%)	SEE (%)	Correla- tion co- efficient (%)	SEE (%)	Correla- tion co- efficient (%)	SEE (%)	Correla- tion co- efficient (%)	SEE (%)	Correla- tion co- efficient (%)	SEE (%)
Xa - Xb	0.98	1.2	0.99	0.8	0.95	0.4	0.99	0.5	0.99	0.7
Ya - Yb	0.99	0.7	0.98	1.0	0.98	0.4	0.99	0.4	0.96	1.4
Xa - Ya	0.93	2.0	0.95	1.4	0.95	0.4	0.97	0.9	0.95	1.7
Xa - Yb	0.92	2.2	0.96	1.3	0.95	0.4	0.98	0.8	0.94	1.8
Xb - Ya	0.93	2.0	0.95	1.3	0.94	0.4	0.98	0.7	0.97	1.5
Xb - Yb	0.91	2.3	0.96	1.2	0.92	0.5	0.99	0.6	0.93	2.2

Abbreviations: X: observation of observer X; Y: observation of observer Y; a: first observation; b: second observation; SEE: standard error of the estimate; REG-CREF: sum of CREF values in each of five wall regions.

The relation between the results of automated quantitative assessment of regional performance and of visual interpretation of regional wall motion by

observer A is shown in figure 4. For each of the five wall regions the REG-CREF value is placed in a column corresponding to the qualification given by the observer (N, H, A and D, representing normo-, hypo-, a- and dyskinesis respectively). A considerable overlap is observed between the results of regional function analysis in the four wall motion classes. When the 10th percentile border of REG-CREF in normal individuals is taken to separate normal and abnormal regional left ventricular function, the classification as normal (normokinetic) or abnormal (hypo-, a-, or dyskinetic) by visual inspection is incorrect in 18 - 27, \bar{m} 22 per cent of the observations (table III). The specificity of visual inspection of regional wall motion, defined as the per cent of wall regions with a REG-CREF above the 10th percentile, graded as normal, ranges from 67 - 93 per cent. The sensitivity defined as the per cent of wall regions with a REG-CREF equal to or below the 10th percentile, graded as abnormal (hypo-, a-, or dyskinetic), ranges from 46 - 96 per cent.

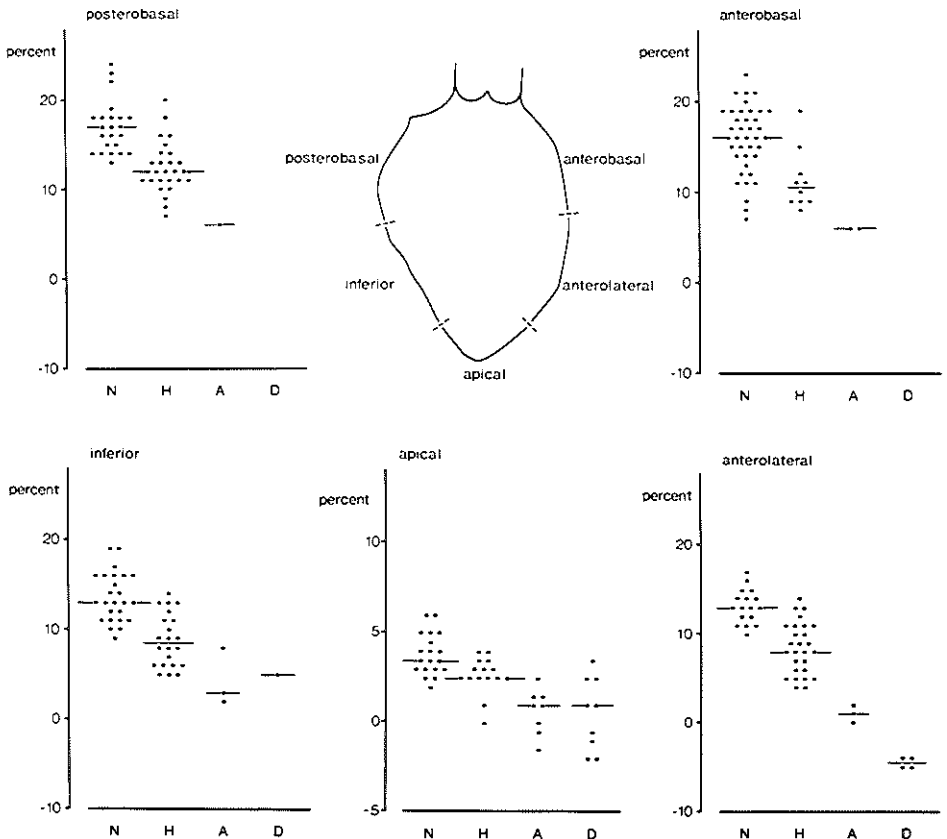


Figure 4. Relation between the results of automated analysis of regional left ventricular function (REG-CREF) and the interpretation of regional wall motion by an experienced observer. The visual interpretation of regional wall motion was classified as normo- (N), hypo- (H), a- (A), or dyskinesis (D). REG-CREF is expressed as percentage; horizontal bars indicate median values of the classified groups.

DISCUSSION

In this study the variability in the assessment of regional left ventricular function by simple visual inspection and with the aid of an automated left ventricular function analysis system is quantified. Currently, analysis of regional (dys)function remains limited largely to subjective interpretation of the left ventriculogram, a method which is subject to a high degree of inter- and intra-observer variability (9, 10, 16). Tzivoni et al. (16) studied the results of three experienced angiographers, who scored wall motion in three left ventricular wall areas (anterior, apical and inferior) with a six-point grading system (from hyperkinetic to dysknetic) and found complete agreement in only 46% of the readings, and partial agreement in another 32% (total 78%). Chaitman et al. (9) found an agreement of 73% between two observers who scored left ventricular wall motion in three wall areas, on a four-point scale. This fits in well with the results from this study, which show an agreement of 68% between observer A and B (table II).

In contrast, quantitative assessment of global left ventricular volume and ejection fraction appears to be highly reproducible, in particular when the second measurement is performed by the same (17), but also when it is performed by another observer (9). Accordingly, in this study left ventricular end diastolic volume and ejection fraction assessed with a computer assisted analysis system, shows a very small intra- and inter-observer variability (table IV). In a previous study (14) also a good agreement was shown between the results of automated assessment of ejection fraction and calculation of ejection fraction from manual tracings (18) of the end diastolic and end systolic contrast silhouette.

Adequate quantification of regional left ventricular function remains a puzzling problem, which has hampered previous attempts to evaluate the accuracy of visual inspection of regional wall motion. To differentiate between normo- and hypokinesis, most methods use the per cent range of systolic shortening of transversal or radial axes, determined in normal individuals (19). Chaitman et al. (9) used for this purpose the systolic percentage decrease in area of parts of the left ventricular contrast silhouette. With these methods it is difficult to test the accuracy of the obtained results, as they are expressed in arbitrary units. The CREF however, expresses quantitatively the contribution of each of 20 left ventricular segments to global ejection fraction, even if the ventricle is severely asynergic and malformed (14). Comparison of SUMCREF and EF values shows a good correlation and a small SEE (table V), which implies that the sum of segmental values practically equals global ejection fraction. The intra- and inter-observer variability of the assessed SUMCREF values is small, as reflected by a SEE which is hardly greater than that of ejection fraction determined from global volume (table IV). The REG-CREF values show also a high reproducibility and an acceptable SEE (table VI). The intra- and inter-

observer variation is mainly caused by human interference in the detection process. Although in adequately opacified ventriculograms most left ventricular contours are detected without human interference (20), manual indication of the mitral and aortic valve in the first analyzed cineframe and indication of the place of the aortic valve during its systolic descent remain factors which introduce observer variation. Especially the definition of the mitral valve edge is important, as this point is one of the determinants of the coordinate system: variation in the indicated place of the mitral valve edge will influence in particular the assessment of wall displacement and consequently regional pump function in the basal segments. This explains the relatively high variability in the assessment of REG-CREF in the antero- and posterobasal regions.

In this study the 10th percentile border of CREF values assessed in normal individuals (13) is taken to separate normal and abnormal regional left ventricular pump function. The border between normal and abnormal global left ventricular pump function is thus drawn at an ejection fraction of 53.3%, which is an arbitrary value, but is well in agreement with the range of 56 - 78% considered as normal in our laboratory and with generally accepted values (21-23). In figure 4 the relation between the results of visual interpretation and of automated assessment of regional left ventricular function is shown. Addition of the median REG-CREF values of wall regions graded as normal yields an ejection fraction of 62%, while addition of the median REG-CREF values of segments graded hypokinetic, gives 41%. These values are well in agreement with ejection fraction values considered as normal and abnormal respectively. There is however a considerable overlap between the results of quantitative regional function analysis in the four wall motion classes. Using the 10th percentile of CREF in normal subjects as border between normal and abnormal regional function, about a quarter of the "eyeball" readings must be judged incorrect, which is also reflected by the specificity and sensitivity values (table III). The 10th percentile border is an arbitrary choice. Although upward and downward shift of this borderline will cause a change in observed specificity and sensitivity values, it will however not significantly influence the percentage of incorrect observations.

From these data we conclude that the reproducibility, and thus the accuracy of visual appraisal of regional wall motion is low, while automated analysis of left ventricular performance with this method shows a good reproducibility. To answer the question whether quantitative analysis of regional left ventricular function is more accurate than visual reading further research will be needed.

REFERENCES

1. Sandler H., Dodge H.T., The use of singleplane angiocardiograms for the calculation of left ventricular volume in man. *Am. Heart J.* 75: 325, 1968.

2. Dodge H.T, Sandler H., Ballew D.W., Lord J.D. Jr., The use of biplane angiocardio-graphy for measurement of left ventricular volume in man. *Am. Heart J.* 60: 762, 1960.
3. Chapman C.B., Baker O., Reynolds J., Bonte F.J., Use of biplane cinefluorography for measurement of ventricular volume. *Circulation* 18: 1105, 1958.
4. Greene D.G., Carlisle R., Grant C., Bunnell I.L., Estimation of left ventricular volume by one plane cineangiography. *Circulation* 35: 61, 1967.
5. Leighton R.F., Wilt S.M., Lewis R.P., Detection of hypokinesia by quantitative analysis of left ventricular cineangiograms. *Circulation* 50: 121, 1974.
6. Harris L.D., Clayton P.D., Marshall H.W., Warner H.R., A technique for the detection of asynergistic motion of the left ventricle. *Comput. Biomed. Res.* 7: 380, 1974.
7. Rickards A., Seabra-Gomes R., Thurston P., The assessment of regional abnormalities of the left ventricle by angiography. *Eur. J. Cardiol.* 5: 167, 1977.
8. Chaitman B.R., Bristow J.D., Rahimtoola S.H., Left ventricular wall motion assessed by using fixed external reference systems. *Circulation* 48: 1043, 1973.
9. Chaitman B.R., DeMots H., Bristow J.D., Roesch J., Rahimtoola S.H., Objective and subjective analysis of left ventricular angiograms. *Circulation* 52: 420, 1975.
10. Zir L.M., Miller S.W., Dinsmore R.E., Gilbert J.P., Harthorne J.W., Interobserver variability in coronary angiography. *Circulation* 53: 627, 1976.
11. Herman M.V., Heinle R.A., Klein M.D., Gorlin R., Localized disorders in myocardial contraction. Asynergy and its role in congestive heart failure. *New Engl. J. Med.* 277: 222, 1967.
12. Slager C.J., Reiber J.H.C., Schuurbiens J.C.H., Meester G.T., Contouromat – A hard-wired left ventricular angio processing system. I. Design and application. *Comput. Biomed. Res.* 11: 491, 1978.
13. Hooghoudt T.E.H., Slager C.J., Reiber J.H.C., Schuurbiens J.C.H., Meester G.T., Hugenholtz P.G., Quantitative assessment of regional pump- and contractile function. Part I: The normal human heart. This thesis pp. 59-81.
14. Hooghoudt T.E.H., Slager C.J., Reiber J.H.C., Serruys P.W., Schuurbiens J.C.H., Meester G.T., Regional contribution to global ejection fraction used to assess the applicability of a new wall motion model to the detection of regional wall motion in patients with asynergy. *Computers in Cardiology* pp. 253-256. IEEE Computer Society, 1980.
15. Slager C.J., Hooghoudt T.E.H., Reiber J.H.C., Schuurbiens J.C.H., Booman F., Meester G.T., Left ventricular contour segmentation from anatomical landmark trajectories and its application to wall motion analysis. *Computers in Cardiology* pp. 347-350. IEEE Computer Society, 1979.
16. Tzivoni D., Diamond G., Pichler M., Stankus K., Vas R., Forrester J., Analysis of regional ischemic left ventricular dysfunction by quantitative cineangiography. *Circulation* 60: 1278, 1979.
17. Cohn P.F., Levine J.A., Bergeron G.A., Gorlin R., Reproducibility of the angiographic left ventricular ejection fraction in patients with coronary artery disease. *American Heart J.* 88: 713, 1974.
18. Brower R.W., Meester G.T., Hugenholtz P.G., Quantification of ventricular performance: A computer-based system for the analysis of angiographic data. *Catheterization Cardiovascular Diagn.* 1: 133, 1975.
19. Brower R.W., Meester G.T., Computer based methods for quantifying regional left ventricular wall motion from cine ventriculograms. *Computers in Cardiology*, pp. 55-62. IEEE Computer Society, Long Beach, Cal., 1976.
20. Reiber J.H.C., Slager C.J., Schuurbiens J.C.H., Meester G.T., Contouromat – A hard-wired left ventricular angio processing system. II. Performance evaluation. *Comput. Biomed. Res.* 11: 503, 1978.

21. Dodge H.T., Baxley W.A., Left ventricular volume and mass and their significance in heart disease. *Am. J. Cardiol.* 23: 528, 1969.
22. Kennedy J.W., Baxley W.A., Figley M.M., Dodge H.T., Blackmon J.R., Quantitative angiocardiology. I. The normal left ventricle in man. *Circulation* 34: 272, 1966.
23. Bunnell I.L., Grant C., Greene D.G., Left ventricular function derived from the pressure-volume diagram. *Am. J. Med.* 39: 881, 1965.

CHAPTER IX

INFLUENCE OF INTRACORONARY NIFEDIPINE ON LEFT VENTRICULAR FUNCTION, CORONARY VASOMOTILITY AND MYOCARDIAL OXYGEN CONSUMPTION

Patrick W. Serruys, Ton E.H. Hooghoudt, Johan H.C. Reiber, Cornelis Slager, Ronald W. Brower, Paul G. Hugenholtz. Technical assistance: Johan C.H. Schuurbiens, Inge C.J. Zorn. (Submitted for publication in *Am. J. Cardiol.*).

Abstract

The present study provides quantitative data on the effects of intracoronary nifedipine (ICN) on regional and global left ventricular performance, coronary vasomotility and myocardial oxygen consumption. Left ventricular pressures (tip manometry) and volumes (angiography), indices of contractility (V_{max}) and relaxation (time constant: TCR) were simultaneously recorded before and 30 seconds after ICN in 5 patients without coronary artery disease. In these patients, frame to frame analysis of regional wall motion shows that ICN in the left main coronary artery not only delays (+ 115 msec) anterior wall contraction but also slows (3.5 vs 1.9 cm/sec) and depresses it (- 26%), resulting in a depression of the global left ventricular ejection. This asynchrony and depression of the regional contraction is considered to be responsible for the slowed isovolumic contraction (V_{max} , - 21%) and relaxation (TCR, + 78%) of the whole ventricle.

In 10 other patients with coronary artery disease, coronary sinus blood flow and myocardial oxygen consumption were measured before and after ICN. The observed decrease in myocardial oxygen consumption (- 28%) depends primarily on a decrease in contractility and left ventricular performance. In a third study group of 12 patients with coronary artery disease, the effects of ICN on the coronary vasomotility of 40 coronary segments (normal, prestenotic, stenotic, poststenotic) were determined quantitatively with a computer based image analysis system. Left ventricular hemodynamics (LVP, EDP, V_{max}) and coronary sinus saturation were monitored during the cineangiograms performed before and after nifedipine. It is demonstrated that nifedipine provokes a vasodilation of the normal (+ 10.3%), prestenotic, stenotic (+ 4 to 30%) and poststenotic (+ 16.4%) coronary segments which persist after the disappearance of its direct effects on the myocardium.

In conclusion, it is suggested that the transient regional "cardioplegic" effect of nifedipine, associated with an increase in coronary blood flow, a reduction in MVO₂ and a vasodilatation of the epicardial vessels is likely to be beneficial during temporary coronary occlusion.

INTRODUCTION

Nifedipine is increasingly employed by direct intracoronary injection in an effort to reverse spontaneously occurring or induced spasm (1, 2) in order to restore coronary bloodflow. Recently introduced techniques, such as transluminal angioplasty (3, 4), fibrinolytic recanalization of coronary artery thrombosis (5, 6) have also become indications to inject nifedipine directly in the affected coronary artery, since it is believed that the specific inhibitory action of nifedipine on contractile energy expenditure may provide significant support for ischemic or potentially ischemic cardiac cells in that region.

In a recent study from this laboratory Verdouw (7) was able to show that nifedipine, administered after a 30 minutes ischemic period but just before reperfusion, allowed the mechanical function of the heart, measured in terms of systolic wall thickening to return to within 80% of baseline values immediately after reperfusion. Untreated animals only recovered to 50% of control values.

It appeared of interest therefore, to explore further the effect of this drug, selectively administered by an intracoronary bolus injection, and to determine to what extent it depresses left ventricular performance or reduces the myocardial oxygen consumption whilst at the same time dilating the coronary artery system. Regional and global left ventricular performance were intermittently studied together with the epicardial coronary artery dimensions, the coronary sinus blood flow and the myocardial oxygen consumption.

PATIENT POPULATION AND METHODS

A. Patient population, design of the study

For the first part of the study, data were collected from 5 patients (32 - 55 years) catheterized because of suspected coronary artery disease. Four of them with atypical chest pain and one with exertional angina. All of them proved to have normal coronary arteries with an ejection fraction well within the normal range; however, one of them proved to have an asymmetric septal hypertrophy without outflow obstruction and one showed on his ECG light ventricular hypertrophy without strain. With a tipmanometer on a 8 F catheter*

* Millar Instruments Inc. Houston, Texas, U.S.A.

pressures were recorded and derived variables were calculated on line by a computer system (8, 9). A 30° RAO ventriculogram was obtained by injection of 0.75 ml/kg 76% Urografin* at a rate of 50 frames per second. When the diagnostic coronary arteriography by Sones' technique revealed that the coronary arteries were normal, informed consent was obtained from the patient to participate in the remainder of the study. This included an additional left ventricular cineangiogram 30 seconds after a bolus injection of 0.075 to 0.175 mg nifedipine into the left main coronary artery. The injection was made only after the values for left ventricular end diastolic pressure and the various isovolumic parameters of contractility were again identical with those recorded before the initial angiogram. It was thus possible to eliminate any influence of volume load and possible contrast material toxicity on left ventricular wall performance (10). In all cases the interval between the two angiograms was at least twenty minutes. Care was taken to maintain the patients' position constant in relation to the X-ray equipment during both angiograms. Diaphragm movement was excluded by shallow inspiration taking care to prevent Valsalva manoeuvre.

B. Analysis of isovolumic indices during ventriculography

After identification of the isovolumic contraction period the on-line computer system provides the following data: peak left ventricular pressure (LVP in mmHg), left ventricular end diastolic pressure (LVEDP in mmHg), peak positive rate of change of pressure ($pk + dP/dt$ in mmHg/sec). In addition isovolumic relaxation phase variables were calculated: peak negative rate of change of pressure ($pk - dP/dt$) and the time constant of relaxation (T) by the least squares fit of $P = e^{At} + B$ ($T = -1/A$) from the moment of $pk - dP/dt$ to the opening of the mitral valve (MVO) (11, 12). The opening of the mitral valve was defined from the angiographic frame preceding that in which non-opacified blood first entered the left ventricle. In all cases MVO was recognized in the same frame by two independent observers.

C. Analysis of global and regional left ventricular function, during systole and diastole

From all cineangiograms a complete cardiac cycle was analyzed frame by frame. Films were projected with a 35 mm film projector and converted into video format with a videocamera**. The ventricular contour was detected automatically with a dedicated hard-wired system, the Contouromat, earlier developed in

* Schering A.G., Berlin, Bergkammen, G.B.R.

** Philips, Eindhoven, The Netherlands.

our laboratory (13, 14, 15). All contour data were coded in a special interface and stored with a PDP 11/34 minicomputer onto a RK-05 disk*. For each analyzed cineframe left ventricular volume was computed according to Simpson's rule. Every videoline in the RAO image is taken to represent a circular slice of the left ventricular lumen. After the end diastolic and end systolic frames are determined, stroke volume, global ejection fraction and total cardiac index are computed. End diastolic (ED) was defined with reference to the point in the pressure trace at which the derivative of pressure first exceeded 200 mmHg/sec. In all cases this point coincided with the maximal volume measured. End systole (ES) was defined, with reference to the pressure tracing, at the occurrence of the incisura of the central aortic pressure. Early diastole was defined as the interval between the opening of the mitral valve and minimal ventricular diastolic pressure. This is the pressure at which the rate of change of pressure first reaches 0. Early diastolic left ventricular inflow volume was measured as an absolute value (ml) and early diastolic mean inflow rate was calculated as the ratio between the difference of ventricular volumes at minimal pressure and opening of the mitral valve and the time interval corresponding to the number of frames between them.

To analyze the regional left ventricular function, the computer generates a system of coordinates along which the left ventricular displacement is determined frame by frame in 20 segments (figure 1). This method of left ventricular

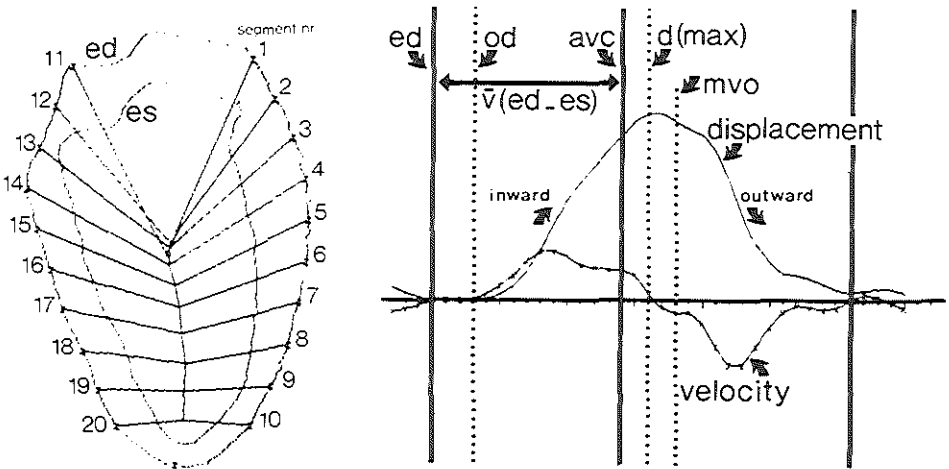


Figure 1. End diastolic and end systolic left ventricular contours, as detected with the automated analysis system. On these silhouettes is superimposed a system of coordinates along which segmental left ventricular wall displacement is detected. Left ventricular wall velocity – first derivative of wall displacement – is derived from these data.

Abbreviations: ed: end diastole; es: end systole; od: onset of displacement; $\bar{v}(ed-es)$: mean systolic wall velocity; d(max): maximal inward wall displacement; mvo: mitral valve opening.

* Digital Equipment Corporation.

wall motion analysis is based on the motion pattern of specific endocardial sites which could be traced through the cardiac cycle with the automated contour detector (13). The directions of the 20 segmental coordinates were derived from the mean directions of motion of these endocardial sites in 23 normal individuals (14). These mean directions of motion have been formulated in a generalized mathematical expression which makes it amenable to automated data processing (14, 15).

Regional wall velocity is computed as the first derivative of the instantaneous displacement function. Mean wall velocity (\bar{v}) was calculated from end diastole to end systole (\bar{v}_{ed-es}) (fig. 1).

For each segment, segmental volume is computed from the local radius (R) and the height of each segment (1/10 of left ventricular long axis length L)

according to the formula: $\frac{1}{20} \pi R^2 L$. When normalized for end diastolic volume,

the systolic segmental volume change can be considered as a parameter of regional pump function (figure 2). During systole this parameter expresses

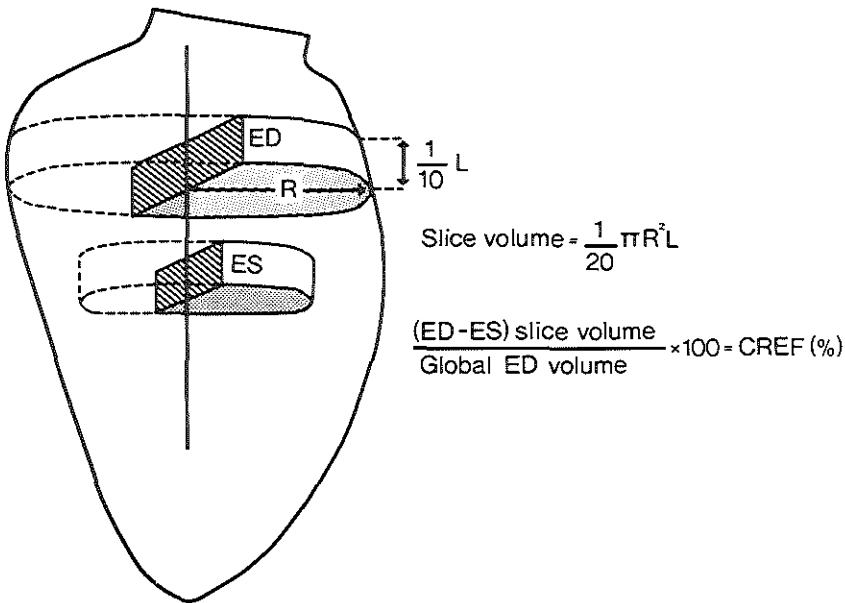


Figure 2. Method for computing regional contribution to ejection fraction (CREF): volume of each segment (slice volume) is computed according to the formula, shown in the figure. The systolic volume change is normalized for left ventricular end diastolic volume.

quantitatively the contribution of a particular segment to global ejection fraction. This was termed regional contribution to global ejection fraction or CREF (15). Obviously, the sum of the values for all 20 segments must equal the global ejection fraction.

Diastolic function was analyzed in terms of volume stiffness. Pressure-volume relations were determined from the lowest diastolic pressure to the beginning of the "a" wave. The natural logarithm of pressure was used in a linear regression analysis of pressure and volume from which a slope k was derived. Changes in k were taken as changes in volume stiffness (16).

D. Coronary sinus blood flow measurement and myocardial oxygen consumption

For this second part of the study, data were collected from 10 other patients (54 - 68 years), who all proved to have significant coronary heart disease. In these patients measurement of coronary sinus blood flow was obtained via the continuous thermodilution method (17). The main objective of this measurement was to detect changes in the coronary blood flow and myocardial oxygen consumption after the intracoronary injection of 0.1 mg of nifedipine (18). The position of the external thermistor was assessed by injection of 3 ml of contrast material before the pharmacological intervention. The computation of flow was based on the original formula as described by Ganz (17). As demonstrated by Ganz et al., the time constant of the method varies between 0.8 and 0.4 s in the range of flow between 100 and 200 ml/min. Since a time interval equal to three time constants is necessary to record 95% of a sudden change of flow, the effects due to nifedipine can be detected within 2.4 s. Before the intracoronary injection of nifedipine, the blood oxygen content in the aorta and in the coronary sinus was determined* and baseline data for flow and aortic pressures were obtained during 60 seconds. Thirty seconds and three minutes after the intracoronary administration of nifedipine these measurements were repeated and changes in myocardial oxygen consumption computed.

E. Quantitative coronary angiography

For the third part of the study, data were collected from 12 patients (33 - 59 years), again catheterized for suspected coronary artery disease. Two patients had entirely normal coronary arteries, there was one patient with one vessel disease, 6 patients had two vessels involved, 3 patients had three vessels affected,

* Lex-O₂-CON, Lexington Instruments Corporation.

all with obstruction of 70% or more. The effects of intracoronary injection of nifedipine on coronary vasomotility were studied in four consecutive coronary cine-angiograms. Before the angiographic study, a fiberoptic catheter* was inserted into the coronary sinus and the O₂ saturation was continuously measured (19). The left ventricular pressure was also continuously recorded with a dual tipmanometer** and analyzed for changes in left ventricular contractility, reflected by peak dP/dt, peak VCE and V_{max} (8, 9). A total of 40 segments were selected for quantitative angiographic analysis. Eight were stenotic in nature, 5 were prestenotic, 17 were poststenotic, and 10 were normal. Before the pharmacological intervention, two baseline coronary angiograms (C1, C2) were performed with a 5 minute interval. The second control angiogram (C2) was carried out to study the effect of the contrast agent itself on the artery. Five minutes later, 0.15 mg of nifedipine was injected within 20 seconds into the left main coronary artery. Hereafter, a third arteriogram (N1) was obtained as soon as the coronary sinus saturation reached its maximum value, usually within 30 seconds. The final coronary angiogram (N2) was recorded when the coronary sinus saturation had returned to its control values, usually within five minutes. All arteriograms were obtained via the Sones technique and recorded on Kodak 35 mm cinefilm at a rate of 50 frames per second with the biplane Cardioskope U***. As for the contrast medium, 76% Urografin**** was injected at a flow rate of 3 ml/sec with a Medrad injector*****. The quantitative analysis of selected coronary segments was carried out with the help of a computer (PDP 11/34) based Coronary Angiography Analysis System (CAAS), developed and implemented at the Thoraxcenter. The basic principles of the system have been described in detail elsewhere (20, 21). To analyze a coronary segment, the 35 mm cinefilm is mounted on a Tagarno***** projector and the selected frame converted into video format with a high resolution video camera. The user communicates with the system by means of a keyboard and a writing tablet. To automatically detect the contours of a selected coronary segment the user must indicate a number of center positions within the segment with the writing tablet. Straight lines connecting these positions function as tentative centerlines. Regions of interest are digitized with the video A/D converter and stored in memory of the minicomputer for subsequent processing. The contours of the arterial segment are detected automatically by means of an averaging first derivative function applied to the digitized video brightness levels along scanlines perpendicular to the corresponding centerline segments. Detected contours, graphics and patient data are superimposed on the original video image with

* American Optical Company, Southbrige, Massachusetts, U.S.A.

** Millar Instruments Inc. Houston, Texas, U.S.A., Millar PC 471 or 481, PC 770 or 880.

*** Siemens AG, Henkesstrasse, Erlangen, GBR.

**** Schering AG, Berlin, Bergkammen, GBR.

***** Medrad Inc., Pittsburgh, Pennsylvania, U.S.A.

***** Tage Arno Hoserns, Denmark.

a refresh memory and displayed on the monitor. The final output of the system for a segment of the left anterior descending in the right anterior oblique orientation is given in figure 3. From the detected contour positions a diameter function is computed which is also shown in figure 3.

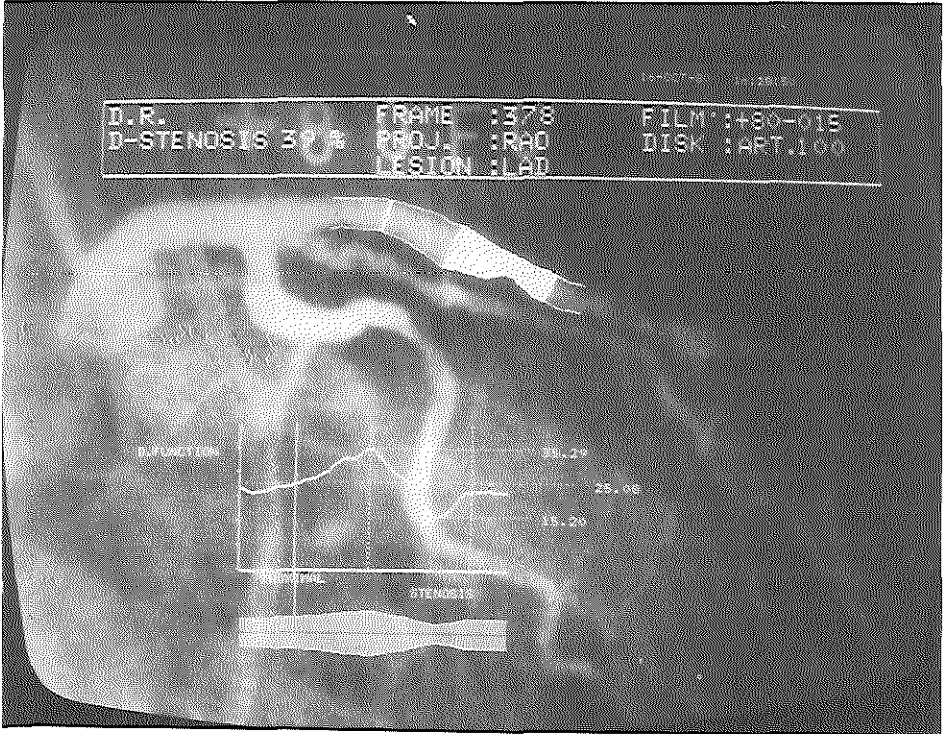


Figure 3. Cineangiogram of the left anterior descending coronary artery in the right anterior oblique projection. The detected contours are superimposed on the original video image. Administrative data are displayed at the top. The diameter function along this coronary segment is also displayed on the video screen.

The diameter values are plotted along the ordinate in arbitrary units (pixel elements) and the positions along the centerline of the arterial segment from proximal to distal along the abscissa. To determine the mean diameter of a part of the processed arterial segment the user must indicate the boundaries of the part in question with the writing tablet. It is emphasized that the X-ray system settings were not changed during consecutive filming after drug injection. Therefore calibration of the diameter values in mm is not necessary. The results

after nifedipine administration are then expressed as relative changes in diameter values, with respect to the control situation.

The accuracy and precision of the quantitation method has been validated with ten copper models of obstructed coronary arteries with circular cross sections. The percentages diameter narrowing for the set of models range from 0% through 90% in steps of approximately 10%. The proximal and distal diameters of the models equal 4.0 mm and all diameters are produced with an accuracy of 0.01 mm. Cinefilms were made of the models immersed in a water-bassin with 10 cm of water, with the same X-ray system settings as during coronary angiography. The cinefilms were repeatedly analyzed as described above. The accuracy was found to be 1.9% and the precision (variability) 1.6%.

RESULTS

A. Global systolic and diastolic left ventricular function

Left ventricular pressures and volume measurements before and after nifedipine are shown in table Ia and Ib. In all but one patient (case 4) the heart rates remained essentially unchanged during the two consecutive cineangiographic investigations, while peak systolic pressure, peak positive dP/dt , peak negative dP/dt , peak V_{CE} and V_{max} decreased significantly. Also the end diastolic pressure became elevated and the time constant of relaxation lengthened. End diastolic volumes did not show a significant increase 30 seconds after the bolus injection of nifedipine, but there was an increase in the residual volume, with a consistent decrease in stroke index and ejection fraction. In four of five patients, the mean rate of flow measured during the early diastolic filling period (EDIR), between the mitral valve opening and the point of minimal pressure, declined.

The relationship between left ventricular diastolic pressure and volume after nifedipine is illustrated by one example (figure 4). It is evident that the entire diastolic pressure-volume relationship is shifted upward and to the right so that at any given volume, pressure is higher. This effect was consistently observed after each nifedipine administration. Furthermore, the k constant – considered as a good index of volume stiffness – was considerably reduced in all patients.

B. Regional left ventricular function

The profound effect of intracoronary nifedipine on left ventricular wall motion and its time sequence is shown in figure 5. The delay in onset of displacement with respect to the end diastole (table II) is illustrated in figure 6 for each of the 20 segments. Prior to administration of nifedipine, the onset of displacement

Table Ia. *Left ventricular volume measurements and derived indices.*

Case	Dosage IC nifedipine mg.	HR bpm		EDVI ml/m ²		ESVI ml/m ²		SI ml/m ²		EF %		EDI ml/m ²		mean EDIR ml/m ² /s	
		C	N	C	N	C	N	C	N	C	N	C	N	C	N
1	0.075	75	74	75.1	79.1	21.4	29.9	53.6	49.2	71.4	62.1	11.1	16.7	318	305
2	0.15	67	72	92	89.1	26.4	43.6	65.5	45.5	71.3	51	14.5	4.6	486	84
3	0.175	66	66	80.4	88.4	27.3	47.2	53.1	41.1	65.9	46.5	8.8	3.7	247	204
4	0.125	70	86	122.6	101.5	34.4	51.5	88.1	50	71.9	49.2	24.3	25.6	610	641
5	0.1	66	71	69.2	60.6	11.7	26.1	57.5	34.4	83	56.8	8.2	4.6	321	220
mean ± SD		69 ± 4	74 ± 7	88 ± 21	84 ± 15	24 ± 8	40 ± 11	64 ± 15	44 ± 6	73 ± 6	53 ± 6	13 ± 7	11 ± 10	396 ± 148	291 ± 94
		ns		ns		p<.002		p<.03		p<.005		ns		ns	

Abbreviations: EDVI: end diastolic volume index; ESVI: end systolic volume index; SI: stroke index; EF: ejection fraction; EDI: early diastolic inflow volume; EDIR: early diastolic inflow rate; C: control; N: nifedipine.
Values expressed as means ± SD; p = p value. Student's t-test (paired data).

Table Ib. *Left ventricular pressure measurements and derived indices.*

Case	Pmin mm Hg		k _p ml ⁻¹		EDP mm Hg		peak (+) dP/dt mmHg/s		peak VCE sec ⁻¹		Vmax sec ⁻¹		peak LVP mmHg		ESP mmHg		peak (-) dP/dt mmHg/s		TCR msec	
	C	N	C	N	C	N	C	N	C	N	C	N	C	N	C	N	C	N	C	N
1	0.3	6.5	0.125	0.045	8.7	17.4	1830	1460	47	39	59	50	138	132	71	70	2081	1454	35.4	60.8
			<i>r=0.88</i>		<i>r=0.96</i>															
2	6	13.1	0.029	0.007	20.8	23	1440	1110	29	24	41	31	98	91	79	59	1367	1073	51.5	70.3
			<i>r=0.97</i>		<i>r=0.72</i>															
3	1.4	14	0.048	0.012	9.9	21	1410	1020	36	20	41	26	101	95	81	59	1792	825	35.1	84.2
			<i>r=0.97</i>		<i>r=0.97</i>															
4	0	13	0.061	0.031	12.1	22.8	1470	1130	38	25	48	30	120	113	94	82	1520	1248	43.2	68.2
			<i>r=0.96</i>		<i>r=0.97</i>															
5	0.3	8.1	0.158	0.049	10.4	21.6	1730	1020	54	22	58	34	135	91	102	58	2164	1310	21.0	47.5
			<i>r=0.89</i>		<i>r=0.98</i>															
mean	1.6	11	0.084	0.029	12	21	1576	1148	41	26	50	34	118	105	86	66	1785	1182	37	66
S.D.	±2.5	±3	±0.054	±0.019	±5	±2	±191	±182	±10	±8	±9	±9	±19	±18	±12	±10	±345	±242	±11	±13
p-value	<.005		<.03		<.01		<.005		<.05		<.005		ns		<.05		<.02		<.01	

Abbreviations: Pmin: left ventricular minimal diastolic pressure; R: slope of diastolic logarithmic pressure-volume relation; EDP: end diastolic pressure; dP/dt: rate of change of pressure; VCE: velocity of contractile elements dP/dt/P; Vmax: VCE linearly extrapolated to P = 0 mmHg; LVP: left ventricular pressure; ESP: pressure at aortic valve closure; TCR: time constant of relaxation; C: control; N: nifedipine. Values expressed as means ± SD; p = p-value, Student's t-test (paired data).

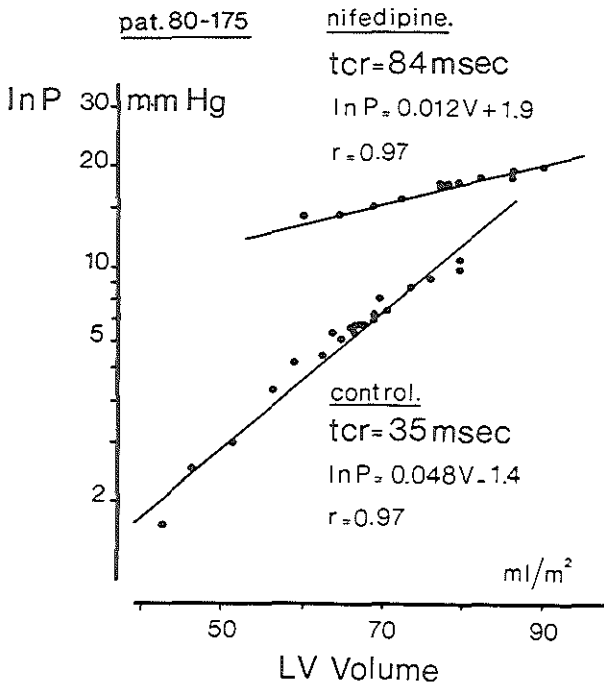


Figure 4. Pressure - volume relationship during diastole before (control) and after nifedipine (N). Linear regression equation of the relation between the natural logarithm of left ventricular pressure (ln P) and left ventricular volume is shown. Intracoronary nifedipine results in a reduction in the slope (kp) of the regression line.

Abbreviation: tcr = time constant of relaxation.

Table II. Regional contractile- and pump function and time-relationship.

	delay of onset of displacement in msec.		temporal relation between AVC and max. wall displ. (msec.)		\bar{V}_{ed-es} cm / sec.		CREF %	
	C	N	C	N	C	N	C	N
anterior wall segments	29 ± 27	144 ± 95	-11 ± 31	60 ± 56	3.5 ± 1.2	1.9 ± 1.2	3.33 ± 1.46	2.46 ± 1.29
	p < 10 ⁻¹⁰		p < 10 ⁻¹⁰		p < 10 ⁻¹⁰		p < 10 ⁻⁸	
inferior wall segments	28 ± 27	72 ± 70	10 ± 44	22 ± 76	3.5 ± 1.1	2.3 ± 1.0	3.32 ± 1.34	2.85 ± 1.26
	p < 10 ⁻⁴		ns		p < 10 ⁻⁸		p < 10 ⁻⁴	

Abbreviations: C: control values; N: values 30 sec. after nifedipine; \bar{V} : mean velocity; ed: end diastolic (based on pressure measurement); es: end systolic (based on pressure measurement); CREF: regional contribution to global ejection fraction.

Values expressed as means ± S.D. p: p-value Student's t-test (paired data).

of the anterior and inferior wall are observed respectively 29 and 28 msec after end diastole. After injection of nifedipine into the main stem of the left coronary artery, the onset of displacement of the anterior wall is delayed by 115 msec ($p < 0.001$), while the inferior wall is delayed by only 44 msec ($p < 0.001$).

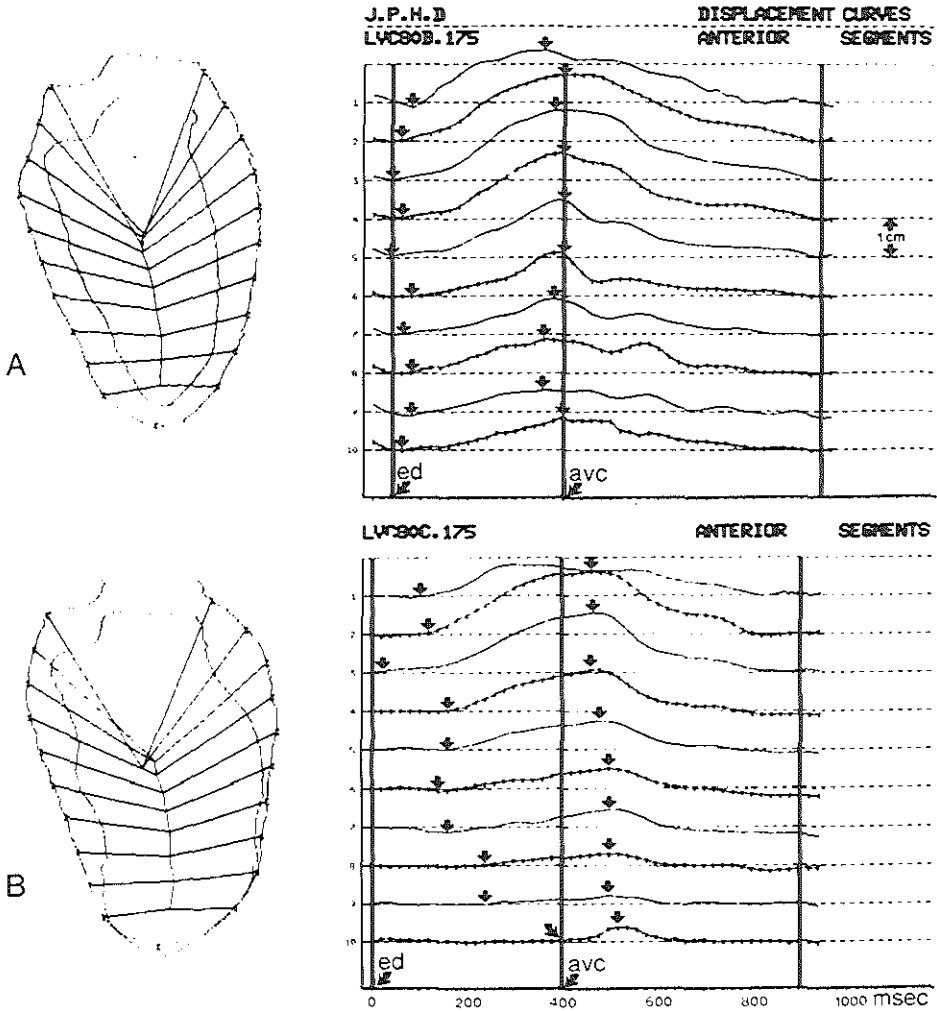


Figure 5. Effect of nifedipine into the left main coronary artery on left ventricular anterior wall motion and its time sequence. Arrows indicate onset and the moment of maximal segmental wall displacement. Nifedipine induces a delay in onset of displacement, a decrease in the extent of segmental wall motion and a delay of the maximal wall displacement. A: control left ventriculogram. B: post nifedipine left ventriculogram.

Abbreviations: ED = end diastole, AVC: aortic valve closure.

For each segment the timing relationship between the aortic valve closure and the occurrence of the maximal wall displacement is demonstrated in figure 7.

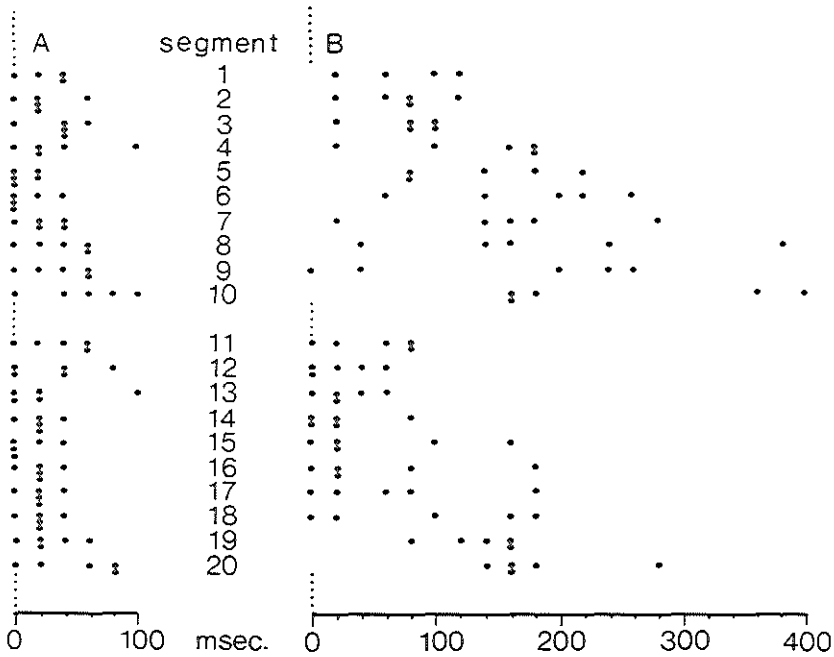


Figure 6. Delay (msec) in onset of displacement for the 20 individual wall segments with respect to end diastole (time zero) before (A) and after (B) intracoronary nifedipine. In 2 (segment 1) of 200 segments the moment of onset of displacement could not be determined accurately. These data are omitted in the figure.

Before nifedipine, the maximal displacement of the anterior wall occurs 11 msec before the aortic valve closure (AVC). In contrast with the anterior wall segments, the infero-posterior wall segments do not reach their maximal wall displacement synchronously. The maximal displacement of the five posterobasal segments (no. 11-15) occurs between 20 and 100 msec after the aortic valve closure so that the maximal wall displacement of the entire inferior wall falls, on average, 10 msec after the aortic valve closure. After nifedipine, the moment of maximal wall displacement for the anterior wall shifts from end systole (11 msec before AVC) to early diastole (60 msec after AVC). The anterolateral and the apical segment of the anterior wall, as well as the apical segment of the

inferior wall appear to be the most affected. On the contrary, the posterobasal wall segments reach their maximum in end systole, instead of early diastole.

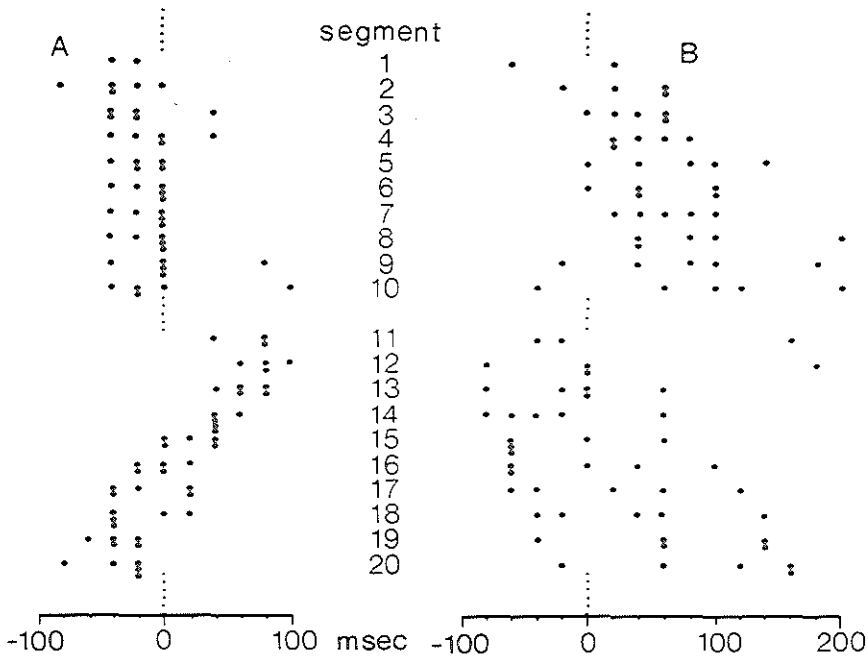


Figure 7. Time relationship between aortic valve closure (time zero) and the occurrence of maximal wall displacement before (A) and after (B) intracoronary nifedipine. In 13 of 200 segments the moment of maximal wall displacement could not be determined accurately. These data are omitted in the figure.

The measurement of mean systolic wall velocity shows after nifedipine a decrease which is again more pronounced in the anterior wall segments (table II) than in the inferior wall segments. Figure 8 shows a typical example of such a regional depression of contractility. The individual regional pump function data for all twenty segments before and after the intracoronary administration of nifedipine, are given in figure 9. Although these data demonstrate a myocardial depression affecting the whole ventricle, the anterolateral and apical segments are the most severely affected. Two patients with a left dominant coronary artery exhibit an impressive reduction of the pump function of their posterobasal wall segments as well. Under the influence of nifedipine, the mean CREF values decrease from 3.33 to 2.46% ($p < 10^{-8}$) for the anterior wall and from 3.32 to 2.85% ($p < 10^{-4}$) for the inferior wall.

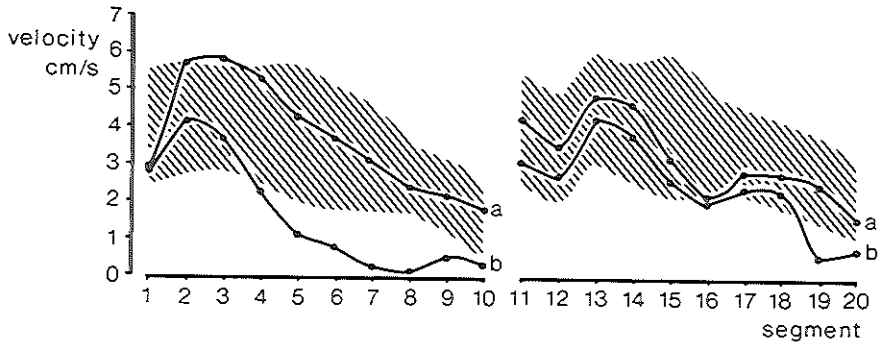


Figure 8. Mean systolic wall velocity (patient no. 3) in 20 wall segments before (A) and after (B) nifedipine. Shaded areas indicate the normal range. After injection of nifedipine into the left main coronary artery, a reduction of wall velocity is observed in the anterior (1-8) and apical (9, 10 and 19, 20) segments.

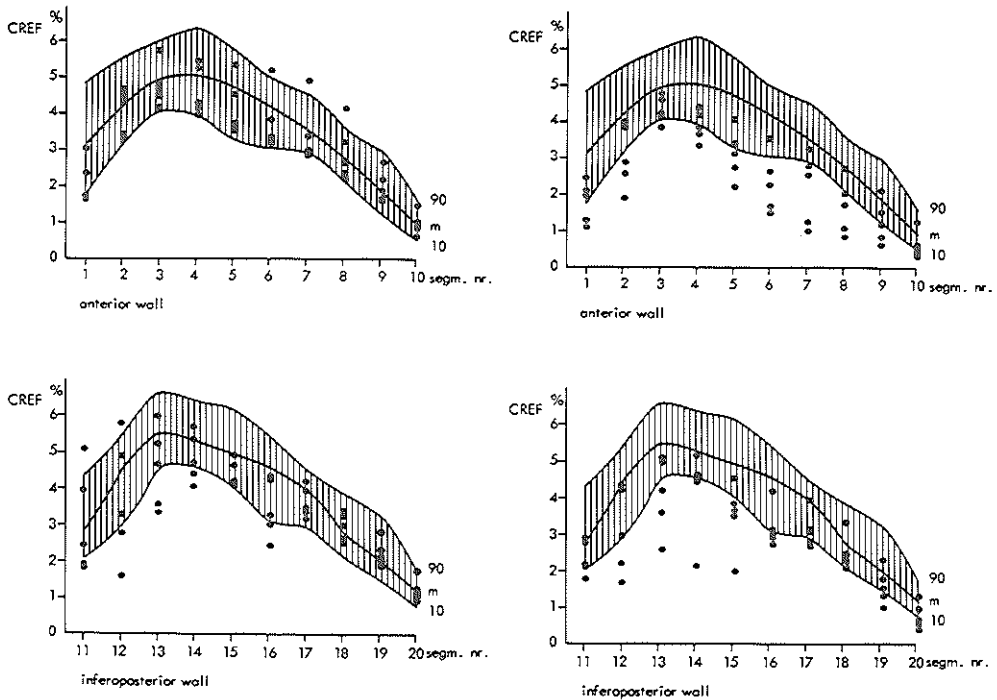


Figure 9. Effect of nifedipine injection into the left main coronary artery on regional contribution to global ejection fraction (CREF). Left side of the figure: Individual CREF values (five patients) in the anterior and infero-posterior wall segments before nifedipine injection. Shaded areas represent the normal range of CREF-values. Right side of the figure: After nifedipine an overall depression of regional pump function is observed which is more pronounced in the anterior (segment 1-8) and apical (9, 10, 19, 20) areas.

C. *Coronary sinus blood flow and myocardial oxygen consumption (table III).*

Thirty seconds after intracoronary administration of nifedipine, coronary sinus blood flow increases significantly ($p < 0.005$) from $103 \text{ ml}\cdot\text{min}^{-1}$ to $155 \text{ ml}\cdot\text{min}^{-1}$ but returns to the pre-administration values within three minutes. Simultaneously, mean aortic blood pressure drops from 111 mmHg to 98 mmHg and comes back to control values after three minutes. Despite this transient decrease in perfusion pressure, coronary vascular resistance is significantly reduced (1.15 versus $0.66 \text{ mmHg/ml}\cdot\text{min}^{-1}$; $p < 0.0002$). Thirty seconds after nifedipine, there is almost a doubling of the coronary sinus oxygen content (from 6.0 to 11.9 ml/100 ml; $p < 10^{-5}$), which is reflected by a considerable narrowing of the aortic – coronary sinus oxygen difference (from 12.7 to 6.3 ml/100 ml; $p < 10^{-5}$). In this group of patients, the net increase in myocardial blood flow is smaller than expected from the narrowing of the aortic – coronary sinus oxygen difference, reflecting a reduced myocardial oxygen consumption (from 13.4 to 9.6 $\text{ml}\cdot\text{min}^{-1}$; $p < 0.01$).

D. *Quantitative coronary cineangiography*

Hemodynamic data collected from the patients studied to assess the effects of nifedipine on the epicardial coronary arteries are shown in table IV. Peak systolic pressure remains constant during both control cineangiograms, but decreases by 14 mmHg immediately after the intracoronary injection of nifedipine ($p < .05$). This acute change is transient so that by the time the fourth coronary angiogram is recorded, the LV pressure has already returned to its control value of 135 mmHg. End diastolic pressure shows a significant increase from 19 to 25 mmHg ($p < .001$), 30 s after the nifedipine administration. During the fourth cinefilm, the end diastolic pressure is still slightly, but not significantly, elevated. After the intracoronary injection of nifedipine, peak dP/dt and V_{\max} decrease simultaneously by 17 and 18% and both parameters have returned to their control values by the time of the fourth coronary cineangiogram. As for the coronary sinus saturation, thirty seconds after the intracoronary administration of nifedipine there is a marked increase from 36% to 63% occurring simultaneously with the drop in V_{\max} . It must be emphasized that 5 min after the intracoronary injection of nifedipine, there is no detectable effect of nifedipine on the coronary sinus O_2 saturation or on contractility measurements left.

The effects of nifedipine on the mean diameter of 10 normal, 5 prestenotic and 16 poststenotic segments are given in table V and shown in figure 10. One of the 17 poststenotic segments was excluded from the statistical analysis because it showed a paradoxical reduction of 60% in diameter after nifedipine. There is no significant difference in the mean diameter between the first and the

Table III. Effect of intracoronary nifedipine (0.1 mg) on coronary sinus blood flow and myocardial oxygen consumption in 10 patients with coronary artery disease.

	HR			mean Ao P			CSBF			CVR			(Ao-Cs)O ₂			CS O ₂ content			MVO ₂		
	C	N1	N2	C	N1	N2	C	N1	N2	C	N1	N2	C	N1	N2	C	N1	N2	C	N1	N2
mean	65	74	65	111	98	112	103	155	109	1.15	0.66	1.12	12.7	6.3	11.9	6.0	11.9	6.6	13.4	9.6	13.7
SD	±8	±8	±9	±13	±13	±10	±30	±40	±36	±0.31	±0.15	±0.35	±1.5	±1.6	±1.1	±1.1	±1.4	±0.7	±4.9	±3.1	±6.1
C vs N1	p < 0.002			p < 0.0005			p < 0.0005			p < 0.0002			p < 10 ⁻⁵			p < 10 ⁻⁵			p < 0.01		
C vs N2	ns			ns			ns			ns			p < 0.0005			p < 0.02			ns		
N1 vs N2	p < 0.0005			p < 0.0005			p < 0.001			p < 0.0005			p < 10 ⁻⁵			p < 10 ⁻⁵			p < 0.01		

Abbreviations: C = control values; N1 = values 30 seconds after nifedipine; N2 = values 3 minutes after nifedipine; HR = heart rate; Ao P = aortic pressure; CSBF = coronary sinus blood flow; CVR = coronary vascular resistance; (Ao-Cs)O₂ = aortic/coronary sinus O₂ difference; MVO₂ = myocardial oxygen consumption.

Values expressed as means ± SD; p = p-value, Student's t-test (paired data).

Table IV. Pressure derived variables and coronary sinus saturation during the two control (C1, C2) and the two post-nifedipine cine-angiograms (N1, N2). (Mean \pm s.e.m.).

	Peak LVSP mmHG	LVEDP mmHg	V _{max} s ⁻¹	Peak dP/dt mmHg.s ⁻¹	Peak VCE s ⁻¹	CS _{O₂} sat
C1	135 \pm 11.5	18 \pm 2.6	47.8 \pm 2.3	1722 \pm 191	35.5 \pm 3.8	36 \pm 3.0
C2	137 \pm 11.6	19 \pm 2.6	45 \pm 2.1	1607 \pm 120	32 \pm 2.5	36 \pm 3.2
N1	123 \pm 8.4	25 \pm 3.1	36.7 \pm 2.8	1333 \pm 139	24.3 \pm 2.4	63 \pm 4.7
N2	135 \pm 11	22 \pm 2.6	47.5 \pm 1.9	1629 \pm 139	31.3 \pm 2.6	35.3 \pm 1.1
C1 vs N1	p < 0.05	p < 0.002	p < 0.005	p < 0.02	p < 0.02	p < 0.01
C1 vs N2	ns	ns	ns	ns	ns	ns
C2 vs N1	p < 0.005	p < 0.001	p < 0.002	p < 0.05	p < 0.01	p < 0.005
C2 vs N2	ns	ns	ns	ns	ns	ns
N1 vs N2	p < 0.03	ns	p < 0.002	p < 0.02	p < 0.01	p < 0.005

Abbreviations: Peak LVSP: peak left ventricle systolic pressure; LVEDP: left ventricle end-diastolic pressure; V_{max}: maximal velocity of contractile element; peak dP/dt: first derivative LV pressure; peak VCE: peak velocity of contractile element; CS_{O₂} sat: coronary sinus oxygen saturation; p: p-value Student's t-test (paired); ns: not significant.

Table V. Effect of intracoronary nifedipine on the mean diameter of normal, prestenotic and poststenotic coronary segments; percentage diameter change is defined as: $(B - A) / A \times 100$.

A	vs	B	normal segment n = 10		prestenotic segment n = 5		poststenotic segment n = 16	
			$\bar{m} \pm SD$ %	p	$\bar{m} \pm SD$ %	p	$\bar{m} \pm SD$ %	p
C1	vs	C2	-2 ± 6	ns	$+1 \pm 4$	ns	-1 ± 7	ns
C1	vs	N1	$+6 \pm 6$	<.02	$+6 \pm 4$.04	$+8 \pm 10$	<.002
C1	vs	N2	$+10 \pm 7$	<.002	$+10 \pm 10$	ns	$+16 \pm 11$	<.0001
C2	vs	N1	$+8 \pm 6$	<.05	$+5 \pm 4$	ns	$+9 \pm 10$	<.001
C2	vs	N2	$+12 \pm 7$	<.001	$+9 \pm 10$	ns	$+16 \pm 11$	< 10^{-5}
N1	vs	N2	$+4 \pm 7$	ns	$+4 \pm 10$	ns	$+8 \pm 11$	<.005

p = p value, Student's t-test (paired data).

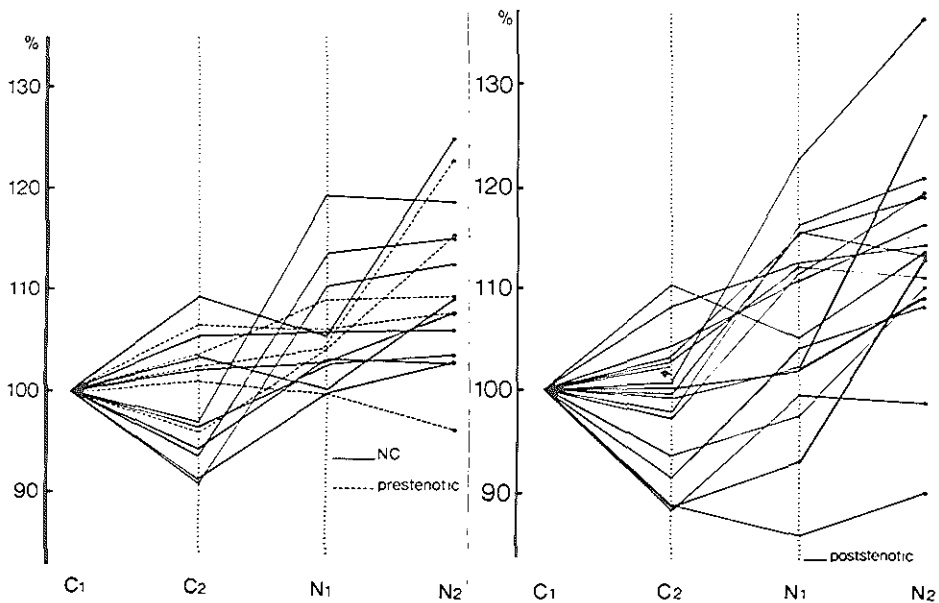


Figure 10. Effect of intracoronary nifedipine on the mean diameter of 10 normal (NC), 5 prestenotic and 17 poststenotic coronary segments during two control cineangiograms (C1, C2) and two post-nifedipine cineangiograms (N1, N2). The individual diameter measurements are expressed as percentage with respect to C1 = 100%. Arrow indicates a segment which shows paradoxical reduction of 60% after nifedipine injection (see text).

second control cinefilm. After the nifedipine administration (film N2), all segments ($N = 29$) show an increase of 12%, ($p < 10^{-7}$) in mean diameter, except for 3 coronary segments (one prestenotic, two poststenotic in series in the same artery). These changes can be detailed as follows:

– Thirty seconds after the intracoronary injection of nifedipine, there is already a small, but significant vasodilation (C1 vs N1, 6.2%, $p < .02$; C2 vs N1, 7.9%, $p < 0.05$) of the normal coronary segments. Five minutes later, on the last film (N2), there is an additional increase in mean diameter so that an overall increase of 10.3% ($p < .002$) in mean diameter is observed between C1 and N2 and a 12.0% increase ($p < .001$) between film C2 and N2. Similar changes are observed in the prestenotic coronary segments (table V). As for the poststenotic segments, at 30 s after the nifedipine administration there is also a significant increase of the luminal diameter (C1 vs N1, 8.3%, $p < .002$ and C2 vs N1, 9%, $p < .001$). This vasodilation persists and increases further: all 16 segments show an increase in mean diameter with an average of 15.7% ($p < 10^{-4}$) between films C1 and N2 and an average increase of 16.4% ($p < 10^{-5}$) between films C2 and N2.

– Seven of the eight stenotic areas also dilated with nifedipine and their luminal diameters increase in absolute terms over a range of 4 to 30% (table VI). There is a slight reduction in diameter in one segment. It is clear that the normal, prestenotic, stenotic and poststenotic segments all remain in a state of vasodilation even when V_{\max} and the coronary sinus saturation have returned to their control values. In other words, nifedipine provokes a coronary vasodilation which persists after the disappearance of its direct effects on the myocardium.

Table VI. Luminal diameters of eight stenotic lesions during the control cineangiogram (C1) and after (N2) intracoronary administration of nifedipine; luminal diameters are expressed in pixels. Luminal diameter change is defined as: $(N - C) / C \times 100$, and expressed as a percentage.

Control C1	Nifedipine N2	Luminal diameter change (%)
4.73	6.18	31
9.92	12.59	27
10.93	13.67	25
10.31	12.63	22.5
13.75	16.10	17
13.97	15.29	9.4
8.32	8.68	4.3
9.84	8.90	-9.5

DISCUSSION

A. Global and regional left ventricular function

Earlier studies of the direct effect of nifedipine on the myocardium were carried out in this laboratory in patients in whom radiopaque markers had been implanted on the epicardium at the time of bypass surgery (12).

The question remained however, to what extent regional endocardial movement was affected. In order to investigate this aspect, frame by frame analysis of the left ventricular cavity outline provided the opportunity to investigate the relationship between changes in regional endocardial wall motion and the alterations of left ventricular isovolumic contraction and relaxation, which have been described, after intracoronary administration of nifedipine (22, 23, 24). Asynchrony in regional wall motion by itself could explain the disturbance in isovolumic contraction, the depressed systolic function and the abnormalities in relaxation (25, 26, 27, 28). In other words, the teamwork which must exist between the different parts of a ventricle to provide maximal mechanical efficiency during ejection might be simply disrupted by the regional administration of nifedipine, without implying a true reduction of regional myocardial performance. It has been suggested that the primary abnormality induced by intracoronary nifedipine could be a delayed onset of contraction without abnormal function. If this theory was correct, all disturbances described above could be due to a electrophysiological delay in the activation of the Purkinje fibers. Recent work of Hoffman and coworkers (29) has all but excluded this possibility. It is more likely therefore that the changes in isovolumic contraction and relaxation may reflect globally altered myocardial contractile behaviour or dyssynchronisation of the electro-mechanical coupling within the sarcomere population. In favour of this hypothesis the data are obtained from the analysis of endocardial wall motion. These consisted of a delay in the onset of wall displacement (figure 6; table II) and a profound change in the timing relation between aortic valve closure and peak inward displacement of the individual wall segments. Normally contraction ends in a synchronous manner, except for some physiological late contraction of the inferobasal area (figure 7). After nifedipine a considerable delay (table II) of the anterior segments (4-8) and apical segments (8-10, 18-20) is observed, while on the contrary, contraction of the inferobasal segments (11-15) ends earlier.

The mean velocity of systolic wall displacement (V_{ed-es}) was significantly reduced (table II). Furthermore, after intracoronary administration of nifedipine, the regional contribution to ejection fraction (CREF) of the anterior and inferior wall segments decreased respectively by 26 and 14%.

It is thus concluded that intracoronary nifedipine not only slows and depresses the segmental contraction, but also delays and prolongs it. This latter observation brought us to analyze another phenomenon. Since the volume of the

ventricle is per definition constant during the relaxation period – defined in terms of valve movement – inward movement in one area must be compensated for by outward movement elsewhere. This is illustrated and demonstrated quantitatively in figure 11. Displacement 1 (D1) expresses for the individual segments (S) the systolic inward wall displacement from end diastole (ED) to aortic valve closure (AVC). Between AVC and mitral valve opening (MVO) the majority of the anterior and infero-apical segments exhibit a persisting inward wall motion, in contrast with the inferobasal segments which move outward. Column D2 (displacement 2) expresses the net effect of inward and outward wall displacement as computed just before MVO. From the displacement 1 and 2 the segmental volume displacement VD1 and VD2 are computed. The sum of VD1, the volume displaced between ED and AVC equates VD2, the volume displaced between ED and MVO. Thus the ventricular volume remains constant while a variety of segmental wall motion in opposite direction takes place. In studying this figure it becomes obvious that changes in the rate of pressure relaxation may not only reflect a globally altered myocardial relaxation but also heterogeneity in activation and performance within the ‘sarcomere population’, with continuation of contraction and tension development extending into the isovolumic period. In other words, impaired relaxation of the ventricle as a whole must not automatically be equated with impaired relaxation at a cellular level.

Fleckenstein et al. (30) have indicated that electromechanical decoupling occurs after nifedipine which leads to a decrease in actin-myosin interaction. The negative inotropic effect on the heart which was recorded and the upward shift in left ventricular diastolic pressure-volume curves observed in this study are probably an expression of that fundamental biochemical effect: nifedipine interrupts the normal process by which calcium is transported to the cell, lowers the cytosolic calcium, inhibits and delays contraction of the myocardial wall so that there is delay in diastolic interaction of contractile elements. This could be a reasonable explanation for the upward shift in left ventricular diastolic pressure volume curves. Residual diastolic interaction between contractile elements has also been proposed by Grossman and coworkers as a possible explanation for the upward shift in diastolic pressure volume relations seen during angina (31). They have proposed that myocardial ischaemia increases the net calcium influx, leads to a rise in cytosolic calcium impairs the relaxation and provokes diastolic interaction of contractile elements (32). In other words, a delayed contraction due to an decreased cytosolic calcium or conversely, a persistent contracture due to an increased cytosolic calcium (33) could both induce residual diastolic interaction and alteration of the pressure volume curve.

Lorell and Barry (34) of Harvard Medical School have conducted in vitro research with calcium antagonist that may shed light on these apparently conflicting observations and hypotheses. They have demonstrated that cultures of

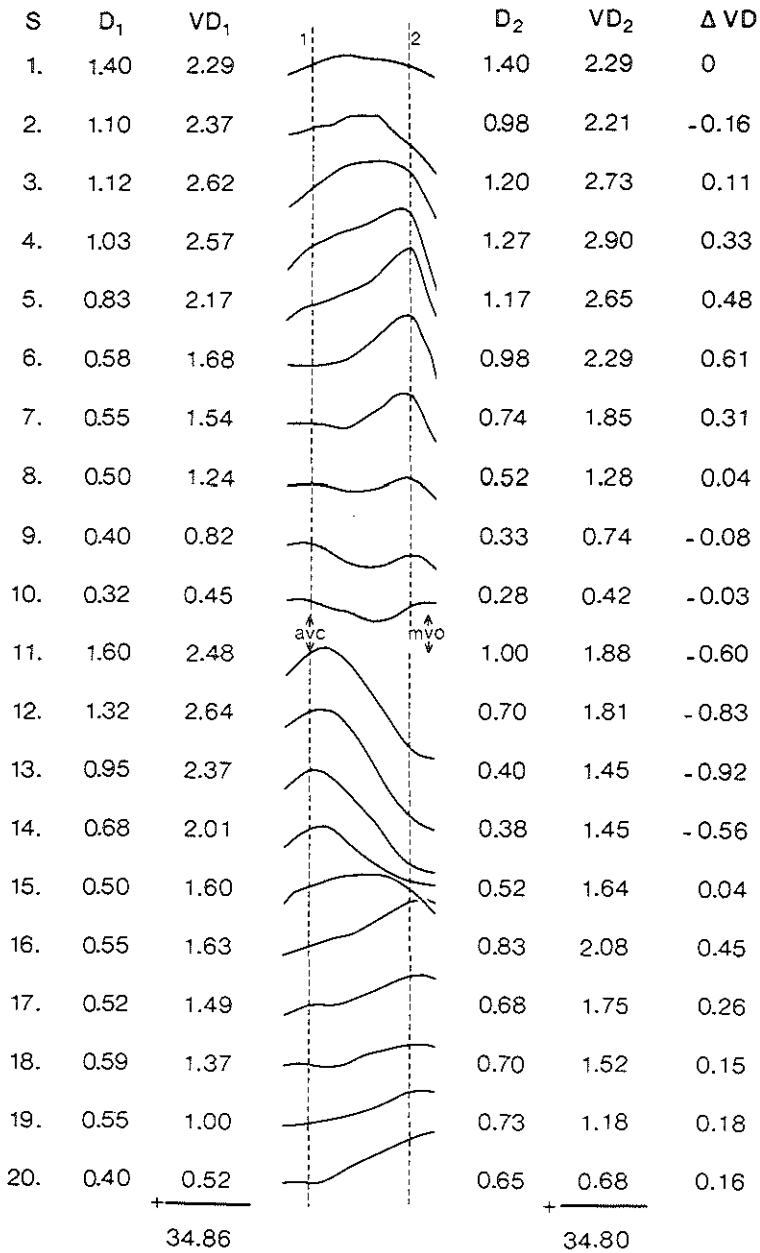


Figure 11. Segmental wall motion after intracoronary nifedipine during the isovolumic relaxation phase, between the closure of the aortic valve (AVC) and the opening of the mitral valve (MVO). See also figure 1.

Abbreviations: S: segment number; D₁: segmental wall displacement (cm) between end diastole (ED) and AVC; D₂: segmental wall displacement (cm) between ED and MVO; VD₁: segmental volume displacement (ml) between ED and AVC; VD₂: segmental volume displacement (ml) between ED and MVO; Δ VD: changes in segmental volume between AVC and MVO, expressed in ml.

dissociated beating ventricular cells from chick embryos manifested a negative inotropic response to a calcium antagonist. That is, amplitude and velocity of contraction of the individual cells decrease in the presence of the drug. Conversely, the calcium antagonist has no effect on velocity of cell wall motion during relaxation. On the other side, high calcium concentrations also cause abnormalities in the cultured cells: a slowing in the rate of relaxation and a decrease in the amplitude of cell contraction as though the cells were in a constant state of partial contracture. Their ultimate experiments reconcile these apparently conflicting observations by showing that the changes induced in cultured cells by high calcium concentrations are reversed by calcium antagonist indicating "that calcium antagonist can dramatically improve systolic and diastolic function of a calcium-overloaded myocardial cell".

B. Coronary blood flow and myocardial oxygen consumption

In our patients the myocardial oxygen consumption decreased by 28% after intracoronary injection of nifedipine. From our hemodynamic and angiographic data we assume that the decrease in myocardial oxygen consumption depends primarily on a decrease in contractility and left ventricular performance. However, this interpretation is open to question since despite an increase in global coronary blood flow, an endocardial decrease in flow and oxygen supply could make the endocardium ischemic and consequently alter its mechanical performance. Others have pointed to the fact that after administration of a coronary vasodilator endocardial capillary blood flow may actually decrease owing to an epicardial coronary 'steal' phenomenon (35, 36). This difference in regional blood flow response is particularly observed when CBF is increased in the presence of a critical stenosis of a large coronary artery (37, 38, 39). In these circumstances when flow is elevated as a result of arteriolar dilatation distal to the stenosis, transmural perfusion becomes heterogeneous because of the greater increase in epicardial flow. In the present study we do not have any experimental evidence which would allow us to rule out this hypothesis, but Henry et al. (40) have demonstrated that, in dogs subjected to coronary occlusion, nifedipine increases collateral flow to the ischemic myocardium. This increase was accompanied by a relative increase in endocardial perfusion, a phenomenon that was particularly prominent in the ischemic zone (40). Microsphere studies in our laboratory (Piet Verdouw; personal communication) revealed that, in pigs with unobstructed coronary arteries, epicardial as well as endocardial flow increased after intracoronary administration of nifedipine, although the increase in epicardial blood flow was slightly larger than the increase in the endocardium.

Recently, the effect of intracoronary nifedipine on myocardial blood flow at various grades of coronary stenosis has been studied (41); for certain degrees

of occlusion, redistribution of blood flow from endocardium to epicardium has been shown to occur.

C. Quantitative coronary angiography

Although it has been proven that nifedipine has a strong coronary dilatory effect and is very effective in patients with variant angina in particular, there have been few studies (42, 43) which show whether this drug actually dilates the coronary artery at the point of the stenotic lesions or at points distal to the fixed obstructions.

The present study provides quantitative measurements of the effects of nifedipine on the epicardial coronary artery after direct intracoronary administration. Absolute stenosis diameter was obtained in order to compare the geometric severity of the same area in the same artery before and after the intracoronary administration of nifedipine. This route of administration was employed in order to dissociate its coronary vasodilatory effect from its direct myocardial action and its peripheral afterload reduction effect (12, 23, 44). The data from our hemodynamic studies indicate that when nifedipine is regionally administered, it has a transient negative inotropic effect, associated with a transient increase in coronary blood flow and decrease in myocardial oxygen consumption. However, the vasodilation of all three, the prestenotic, stenotic and poststenotic coronary segments persists much longer than the hemodynamic effects, at least during the period of observation in this study. This observation raises the possibility that there exist marked differences in the regulation of the electro-mechanical coupling between the myocardial cells and the smooth muscle cells in the coronary vascular wall.

Another essential question is: What effect do large vessel vasomotor tone and distal arteriolar resistance have on a proximal lesion? Logan (45) has showed in isolated perfused human coronary arteries that a decrease in perfusion pressure leads to a "dynamic" increase in resistance to flow across an elastic and eccentric stenosis.

Walinsky et al. (46), Santamore et al. (47) and Schwartz et al. (48) have even demonstrated experimentally that the administration of a coronary vasodilator could induce a fall in distending pressure of the poststenotic coronary segment, resulting in a passive collapse of the wall of the stenotic segment, with a decrease in stenosis area and an increase in resistance to flow. In contrast to these experimental data, Brown et al. (49), Doerner et al. (50) and Ovaretz et al. (51) described a significant decrease in severity of stenosis after the administration of nitroglycerine, as seen on coronary arteriograms. Their approach, using theoretical flow equation and measurements of absolute stenosis diameter was appropriate because they examine changes in stenosis after an intervention in comparison with the same stenosis under control condition. A comprehensive ex-

planation for these conflicting results is, as suggested by Gould, "that in the experimental studies the vasodilatory stimulus affected primarily the distal arteriolar coronary bed leading to a reduction in intraluminal pressure in the poststenotic coronary segment whereas in the clinical studies the vasodilatory drug (nitroglycerine) affected primarily the epicardial large coronary arteries in their prestenotic as well as in their poststenotic segment" (52).

CONCLUSION

From our angiographic study, we conclude that intracoronary nifedipine not only delays and prolongs the segmental contraction, but also slows and depresses it. It is suggested that a decreased cytosolic calcium might induce delayed diastolic interaction between contractile elements which could be a reasonable explanation for alteration of the isovolumic relaxation and for the upward shift in the left ventricular pressure volume curve after intracoronary administration of nifedipine. From our hemodynamic data we assume that the decrease in myocardial oxygen consumption depends primarily on a decrease in contractility and left ventricular performance. Finally we demonstrated that the vasodilatation of the epicardial vessels after intracoronary nifedipine persists longer than its direct effects on the myocardium.

In conclusion, it is suggested that the transient regional "cardioplegic" effect of nifedipine, associated with an increase in coronary blood flow, a reduction in MVO_2 and a vasodilatation of the epicardial vessels is likely to be beneficial during temporary coronary occlusion.

REFERENCES

1. Hugenholtz P.G., Michels H.R., Serruys P.W., Brower R.W., Nifedipine in the treatment of unstable angina, coronary spasm and myocardial ischemia. *Am. J. Cardiol.* 47: 163, 1981.
2. Bertrand M.E., Lablanche J.M., Tilmant P.Y., Treatment of Prinzmetal's Variant Angina. Role of medical treatment with nifedipine and surgical coronary revascularization combined with Plexectomy. *Am. J. Cardiol.* 47: 174, 1981.
3. Gruentzig A., Transluminal dilatation of coronary artery stenosis. *Lancet* 1: 263, 1978.
4. Serruys P.W., Booman F., Reiber J.H.C., Cherrier F., Hugenholtz P.G., Computerized quantitative coronary angiography applied to the PTCA procedure: advantages and limitations. (abstract) 4th Symposium on Coronary Heart Disease. Frankfurt/Main, 18-20 May 1981.
5. Rentrop P., Blanke H., Koesterling K., Karsch K.R., Acute myocardial infarction: intracoronary application of nitroglycerin and streptokinase in combination with transluminal recanalization. *Clin. Cardiol.* 5: 354, 1979.

6. Rutsch W., Methods of nonsurgical recanalization (abstract). 4th Symposium on Coronary Heart Disease, Frankfurt/Main, 18-20 May 1981.
7. Verdouw P.D., ten Cate F.J., Hartog H.M., Hugenholtz P.G., Does nifedipine protect against reperfusion damage? *Am. J. Cardiol.* 47: 461, 1981.
8. Meester G.T., Bernard N., Zeelenberg C., Brower R.W., Hugenholtz P.G., A computer system for real time analysis of cardiac catheterization data. *Cath. & Cardiovasc. Diagn.* 1: 113, 1975.
9. Meester G.T., Zeelenberg C., Corter S., Miller A.C., Hugenholtz P.G., Beat-to-beat analysis of left ventricular function parameters. *Eur. J. Cardiol.* 1: 279, 1974.
10. Vine D.L., Hegg T.D., Dodge H.T., Stewart D.K., Frimer M., Immediate effect of contrast medium injection on left ventricular volumes and ejection fraction. *Circulation* 56: 379, 1977.
11. Fioretti P., Brower R.W., Meester G.T., Serruys P.W., Interaction of left ventricular relaxation and filling during early diastole in human subjects. *Am. J. Cardiol.* 46: 197, 1980.
12. Serruys P.W., Brower R.W., ten Katen H.J., Bom A.H., Hugenholtz P.G., Regional wall motion from radiopaque markers after intravenous and intracoronary injections of nifedipine. *Circulation* 63: 584, 1981.
13. Slager C.J., Reiber J.H.C., Schuurbijs J.C.H., Meester G.T., Contouromat - a hard-wired left ventricular angio processing system. Design and application. *Comp. Biomed. Res.* 11: 491, 1978.
14. Slager C.J., Hooghoudt T.E.H., Reiber J.H.C., Schuurbijs J.C.H., Booman F., Meester G.T., Left ventricular contour segmentation from anatomical landmark trajectories and its application to wall motion analysis. *Computers in Cardiology*: 347, 1979.
15. Hooghoudt T.E.H., Slager C.J., Reiber J.H.C., Serruys P.W., Schuurbijs J.C.H., Meester G.T., Hugenholtz P.G., "Regional contribution to global ejection fraction" used to assess the applicability of a new wall motion model to the detection of regional wall motion in patients with asynergy. *Computers in Cardiology*: 253, 1980.
16. Gaasch W.H., Levine H.J., Quinones M.A., Alexander J.K., Left ventricular compliance: mechanisms and clinical implications. *Am. J. Cardiol.* 38: 645, 1976.
17. Ganz W., Tamura K., Marcus H.S., Donoso R., Yoshida S., Swan H.J.C., Measurement of coronary sinus blood flow by continuous thermodilution in man. *Circulation* 44: 181, 1971.
18. Serruys P.W., Brand M. v.d., ten Katen H.J., Brower R.W., Regional wall motion following intra-bypass injection of nifedipine: design of a protocol and initial experience. In: *Calcium-Antagonismus*, edited by Fleckenstein A., Roskamm H., Berlin-Heidelberg-New York, Springer Verlag 1980, p. 282.
19. Hugenholtz P.G., Verdouw P.D., Meester G.T., Fiberoptics in cardiac catheterization II. Practical applications. In: *Dye curves: the theory and practice of indicator dilution*, edited by Bloomfield D.A., Baltimore, London, Tokyo: University Park Press 1974, 28.
20. Reiber J.H.C., Booman F., Tan H.S., A cardiac image analysis system, objective quantitative processing of angiocardiograms. *Proc. Comp. Cardiol.* 239, 1978.
21. Booman F., Reiber J.H.C., Gerbrands J.J., Quantitative analysis of coronary occlusions from coronary cine-angiograms. *Proc. Comp. in Cardiol.* 1979, 177.
22. Rousseau M.F., Veriter C., Detry J.M.R., Brasseur L.A., Pouleur H., Impaired early left ventricular relaxation in coronary artery disease. Effects of intracoronary nifedipine. *Circulation* 62: 754, 1980.
23. Serruys P.W., Brand M. v.d., Effects of nifedipine on left ventricular isovolumic contraction following intravenous or intracoronary administration. *Circulation* 59 and 60, II: 82, 1979.

24. Serruys P.W., Brower R.W., Bom A.H., Katen H.J. ten, Hugenholtz P.G., Contractility relaxation and regional wall motion following intracoronary injection of a Ca^{++} antagonist. *Circulation* 59 and 60. II: 180, 1979.
25. Altieri P.L., Wilt S.M., Leighton R.F., Left ventricular wall motion during the isovolumic relaxation period. *Circulation* 48: 499, 1973.
26. Alam S.E., Tansey W.A., Cameron A., Kemp H.G., Asynchronous relaxation: an angiographic temporal analysis of asynchronous left ventricular relaxation in man. *Am. J. Cardiol.* 43: 4, 1979.
27. Gibson D.G., Doran J.H., Traill T.A., Brown D.J., Regional abnormalities of left ventricular wall movement during isovolumic relaxation in patients with ischemic heart disease. *Eur. J. Cardiol.* 7. (Suppl.): 251, 1978.
28. Ludbrook P.A., Byrne J.D., Influence of asynchronous early left ventricular relaxation on diastolic function. *Am. J. Cardiol.* 45: 399, 1980.
29. Dangman K.H., Hoffman B.F., Effects of nifedipine on electrical activity of cardiac cells. *Am. J. Cardiol.* 46: 1059, 1980.
30. Fleckenstein A., Tritthart H., Doering H.J., Byon K.Y., BAY a 1040 ein hochaktiver Ca^{++} -antagonistischer Inhibitor des elektromechanischen Koppelungsprozess in warmblueter Myokard. *Arzneim. Forsch.* 22: 22, 1972.
31. Grossman W., Serizawa T., Carabello B.A., Studies on the mechanism of altered left ventricular diastolic pressure-volume relations during ischaemia. *Europ. Heart J.* 1 (Suppl.): 1, 141, 1980.
32. Grossman W., Barry W.H., Diastolic pressure volume relations in the diseased heart. *Fed. Proc.* 39: 148, 1980.
33. Lewis M.J., Grey A.C., Henderson A.H., Determinants of hypoxic contracture in isolated heart muscle preparations. *Cardiovasc Res.* 13, 86, 1979.
34. Lorell B.H., Barry W.H., Effects of verapamil on myocardial systolic and diastolic function during calcium overload. *Circulation* 62, suppl. III: 293, 1980.
35. Bache R.J., McHale P.A., Greenfield J.C. Jr., Transmural myocardial perfusion during restricted coronary inflow in the awake dog. *Am. J. Physiol.* 232: H 645-H 651, 1977.
36. Lipscomb K., Gould K.L., Mechanism of the effect of coronary artery stenosis on coronary flow in the dog. *Am. Heart J.* 89: 60, 1975.
37. Gould K.L., Lipscomb K., Calvert C., Compensatory changes of the distal coronary vascular bed during progressive coronary constriction. *Circulation* 51: 1083, 1975.
38. Guyton R.A., McClenathan J.H., Newmen G.E., Michaelis L.L., Significance of sub-endocardial ST-segment elevation caused by coronary stenosis in the dog: epicardial ST-segment depression, local ischemia and subsequent necrosis. *Am. J. Cardiol.* 40: 373, 1977.
39. Nakamura M., Matsuguchi H., Mitsutake A., Kikuchi Y., Takeshita A., Nakagaki O., Kuroiwa A., The effect of graded coronary stenosis on myocardial blood flow and left ventricular wall motion. *Basic Res. Cardiol.* 72: 479, 1977.
40. Henry P.D., Shuchleib R., Clark R.E., Perez J.E., Effect of nifedipine on myocardial ischemia: analysis of collateral flow, pulsatile heat and regional muscle shortening. *Am. J. Cardiol.* 44: 817, 1979.
41. Weintraub W.S., Hattori S., Agarwal J., Bodenheimer M.M., Banka V.S., Helfant R.H., Variable effect of nifedipine on myocardial blood flow at three grades of coronary occlusion in the dog. *Circulation Research* 48: 937, 1981.
42. Schulz W., Kober G., Krauss G., Kaltenbach M., Influence of intracoronary and intravenous Nifedipine on diameters of coronary vessels and stenoses. In: *Unstable angina pectoris*, edited by Rafflenbeul W., Lichtlen P.R., Balcon R. Georg Thieme Verlag, Stuttgart, New York, 1981, p. 259.
43. Rafflenbeul W., Kaltenbach M., Engel H.J., Scherer D., Kober G., Lichtlen P., Mor-

- phological and functional criteria for a successful coronary angioplasty (PTCA). *Circulation* 64: Suppl. IV: 253, 1981.
44. Kaltenbach M., Schulz W., Kober G., Effects of nifedipine after intravenous and intracoronary administration. *Am. J. Cardiol.* 44: 832, 1979.
 45. Logan S.E., On the fluid mechanics of human coronary artery stenosis. *IEEE Trans. Biomed. Eng.* 22: 327, 1975.
 46. Walinsky P., Santamore W.P., Weiner L., Brest A.N., Dynamic changes in the hemodynamic severity of coronary artery stenosis in a canine model. *Cardiovasc. Res.* 13: 113, 1979.
 47. Santamore W.P., Walinsky P., Altered coronary flow response to vasoactive drugs due to coronary arterial stenosis in the dog. *Am. J. Cardiol.* 45: 276, 1980.
 48. Schwartz J.S., Carlyle P.F., Cohn J.N., Effect of dilation of the distal coronary bed on flow and resistance in severely stenotic coronary arteries in the dog. *Am. J. Cardiol.* 43: 219, 1979.
 49. Brown B.G., Bolson E., Frimer M., Dodge H.T., Angiographic distinction between variant angina and non vasospastic chest pain. *Circulation* 58: 122, 1978.
 50. Doerner T.C., Brown G.B., Bolson E., Frimer M., Dodge H.T., Vasodilatory effects of nitroglycerine and nitroprusside in coronary arteries — a comparative analysis. *Am. J. Cardiol.* 43: 416, 1979.
 51. Ovaretz R., Lee G., Baker L., Titus P., Joye J.A., Kaku R., Bogren H., Mason D.T., Prominent dilation of stenotic coronary artery lesions following sublingual nitroglycerine by quantitative arteriography. *Circulation* 58: 25, 1978.
 52. Gould K.L., Dynamic coronary stenosis. *Am. J. Cardiol.* 45: 286, 1980.

CHAPTER X

RECANALIZATION OF THE OCCLUDED CORONARY ARTERY IN PATIENTS WITH ACUTE MYOCARDIAL INFARCTION: INFLUENCE ON LEFT VENTRICULAR FUNCTION

Hooghoudt T.E.H., Serruys P.W., Reiber J.H.C., Slager C.J., Van den Brand M. (material contained in this chapter has been submitted in a modified form to *Am. J. Cardiol.*).

Abstract

In 25 patients with acute myocardial infarction a left ventriculogram was obtained within six hours after the onset of chest pain and during a follow-up study, 2 - 3 weeks later. In 12 patients the infarct related artery could be recanalized with selective intracoronary infusion of a thrombolytic agent and was still patent during the control study. In two cases the IRA was already patent during the first angiogram and remained so at the time of the follow-up study. The ejection fraction of these 14 patients with successful recanalization increased from 51 to 56 per cent ($p < 0.006$). In seven patients the infarct related artery could not be recanalized or was reoccluded at the time of the control study. The ejection fraction of these patients with unsuccessful recanalization decreased from 50 to 38 per cent ($p < 0.003$). In four cases attempts to recanalize the infarct related artery were unsuccessful, but the vessel appeared to be patent at the time of the follow-up study (spontaneous recanalization). Regional function analysis in five patients with anterior infarction and six patients with inferior infarction who had a successful recanalization and persistent patency of the infarct related vessel suggests that improvement of global ejection fraction is only partially due to improvement of regional pump function in the reperfused "infarct zone" but is also caused by enhancement of regional function in other wall regions.

Keywords: Regional pump function, coronary recanalization, thrombolytic agent, myocardial infarction.

INTRODUCTION

Coronary artery thrombosis is found in the majority of patients with an acute myocardial infarction (1 - 3). Recently it has been shown that acutely occluded

coronary arteries can be recanalized by intracoronary infusion of a fibrinolytic agent (4-7). Such intervention might prevent myocardium, made acutely ischemic by coronary occlusion, to progress to necrosis (8-10). Animal experiments have shown that restoration of coronary blood flow may save myocardium (11, 12) and improve survival (12), if the reperfusion is instituted within a few hours after coronary occlusion. On the other hand reperfusion of ischemic myocardium might be harmful because of the occurrence of serious arrhythmias (4, 5, 7, 13) and/or intramyocardial hemorrhage (14). To answer the question whether this new approach to the treatment of patients with acute myocardial infarction will be ultimately beneficial to most patients with acute myocardial infarction, a carefully designed randomized trial is needed (15). Such a study should include detailed analysis of the influence of myocardial reperfusion on left ventricular function before and after the procedure. Up to now, the assessment of global ejection fraction has mainly been used for this purpose (2, 5, 7, 16). However, improvement of global left ventricular function after successful recanalization of a coronary artery might be caused by salvage of jeopardized myocardium (16) or by compensatory action of other wall segments, or both. In an effort to dissect this problem, in this study the effect of myocardial reperfusion on regional left ventricular function has been quantitated.

MATERIAL AND METHODS

Between september 1980 and september 1981 sixty-six patients were catheterized within the first six hours after the onset of symptoms of acute myocardial infarction (AMI). The diagnosis of AMI was based on an anamnesis of typical chest pain, ECG-changes and serial CPK values. In all patients the ECG at admission showed changes compatible with acute myocardial ischemia. After informed consent was obtained coronary arteriography was performed via the retrograde brachial (17) or femoral (18) approach. In 53 patients injection of contrast medium into the infarct related artery (IRA) showed a total occlusion (figure 1). Thirty-four IRA's could be recanalized with 10 - 90 minutes intracoronary infusion of 2000 - 4000 U/min of streptokinase* or urokinase** (figure 2). In 25 patients two sequential left ventriculograms (during the acute event and during the follow-up study, 2 - 3 weeks later) of sufficient quality to permit automated analysis were obtained. The relatively small number of sequential angiograms was also due to:

- refusal of the patient to cooperate with the follow-up study.
- a left ventricular end diastolic pressure of ≥ 35 mmHg at the time of acute infarction: in such case left ventriculography was omitted.

* Behringwerke AG, Marburg, GBR.

** Abbott Laboratories, North Chicago, Illinois, U.S.A.

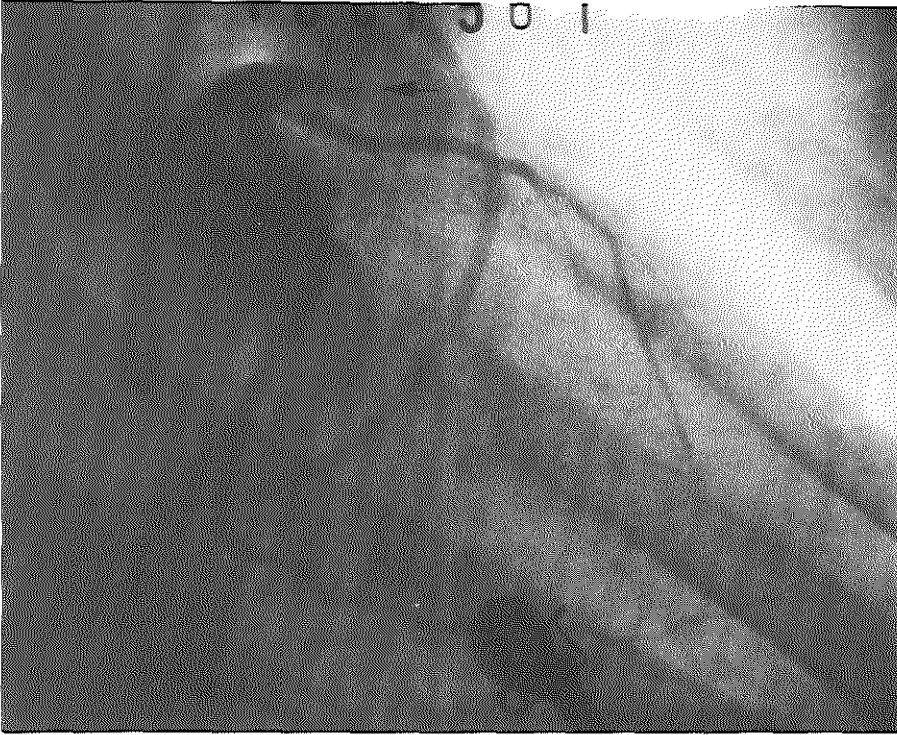


Figure 1. Left coronary artery in the right anterior oblique projection. The arrow indicates the occlusion of the left anterior descending coronary artery.

In 12 (of 25) patients the IRA could be recanalized and was still patent during the control study. Five patients had sustained an anterior myocardial infarction (IRA = left anterior descending coronary artery), six an inferior infarction (IRA = right coronary artery), one a lateral wall infarction (IRA = left circumflex coronary artery). In two other patients the IRA was already patent at the time of the first coronary angiogram and remained so during follow-up.

In seven patients the IRA could not be recanalized or was reoccluded at the time of the control study. In four other patients the IRA could not be recanalized with the thrombolytic agent, but appeared to be patent during follow-up.

The study groups consist of the seven patients with unsuccessful recanalization and the 14 patients with successful recanalization of the IRA. In the five patients with anterior infarction and six with inferior infarction with successful recanalization of the IRA, detailed analysis of regional left ventricular function was performed.

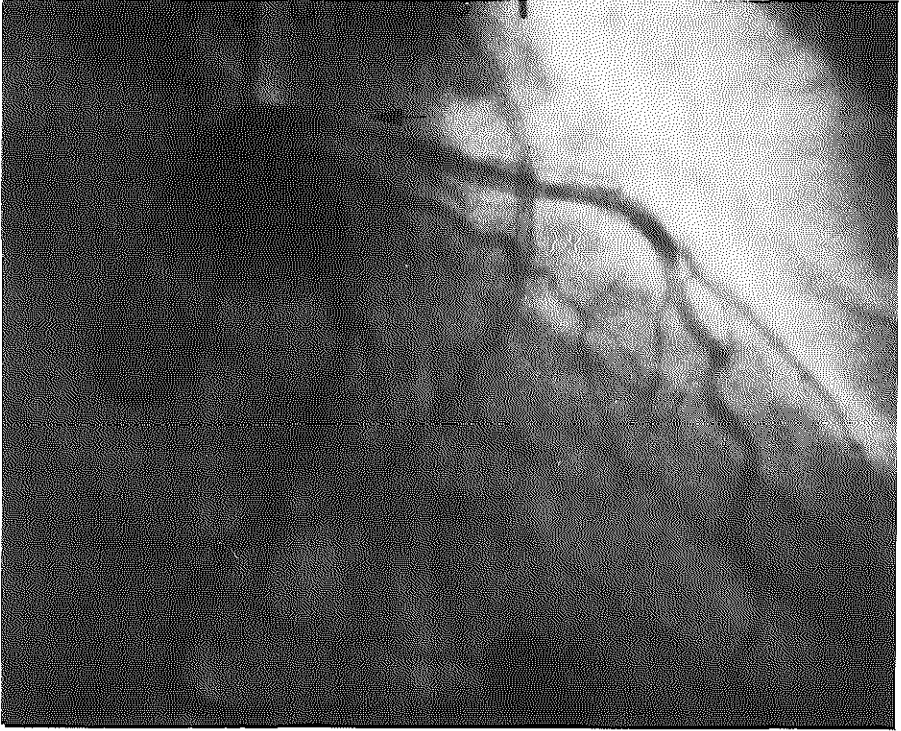


Figure 2. After 60 minutes of perfusion the entire left anterior descending coronary artery, as well as the diagonal branch are patent.

Regional left ventricular function was studied from the 30° right anterior oblique left ventricular cineangiogram with an automated hardwired endocardial contour detector (19) linked to a minicomputer. In figure 3 an example of the end diastolic (ED) and end systolic (ES) contours of the left ventriculogram, as displayed by the analysis system, are shown. Systolic regional wall displacement is determined along a system of 20 coordinates (figure 3), based on the pattern of actual endocardial wall motion in normal individuals (20). From the regional wall displacement values, the regional contribution to global ejection fraction (CREF) – a new regional pump function parameter which expresses the contribution of each segment to global ejection fraction – is computed for each segment (21). The crosshatched zones in figure 3 represent the segmental CREF values between the 10th (10) and 90th (90) percentile, as determined in 20 normal individuals. The segmental CREF values in the anterobasal (segments 1-5), anterolateral (segments 5-9), apical (segments 9, 10, 19 and 20), inferior

(segments 15-19) and posterobasal (segments 11-15) wall regions, before and 2 - 3 weeks after intervention with thrombolytic therapy, were compared with the paired t-test of Student.

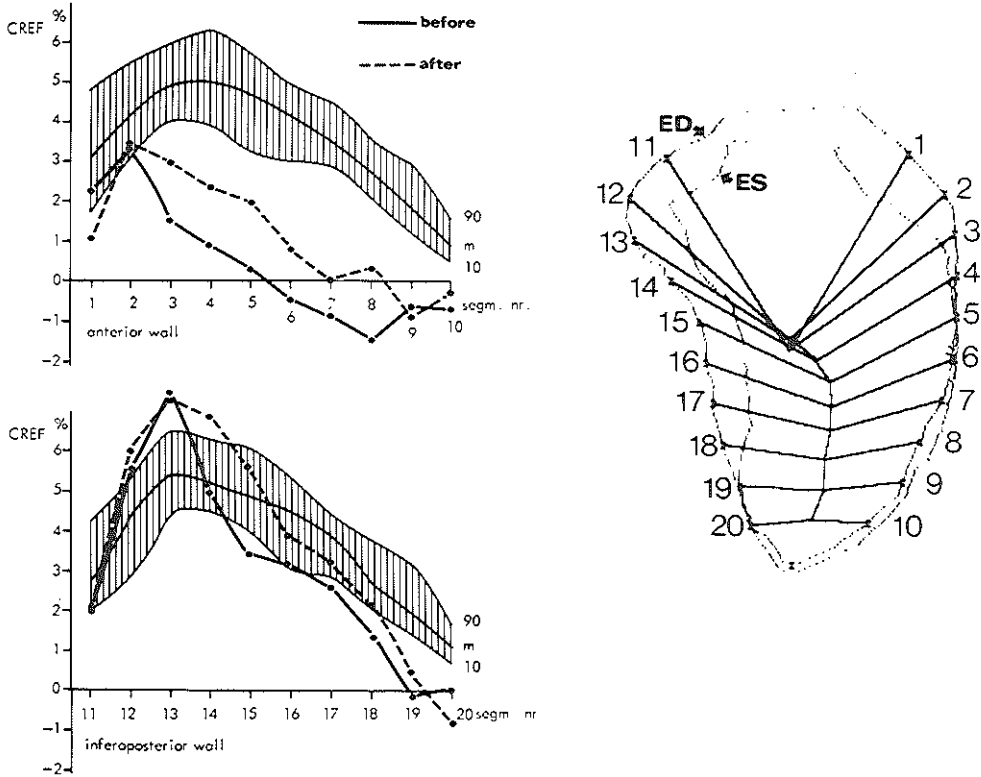


Figure 3. Regional wall motion and regional contribution to global ejection fraction (CREF) in 20 segments of the 30° right anterior oblique left ventriculogram, before (continuous line) and 2-3 weeks after (interrupted line) infusion of streptokinase. The end diastolic (ED) and end systolic (ES) contours of the pre-streptokinase ventriculogram are displayed with the system of coordinates along which regional wall displacement is determined. Wall motion is approximately normal in segments 1-2, and 11-18, but hypo-, a-, or dyskinetic in segments 3-10 and 19-20 (anterior and apical wall). Accordingly the corresponding CREF values show a severe depression in segments 3-10 and 19-20. Shaded areas represent CREF values in normals (10 : 10th percentile, 90 : 90th percentile, m : median). After intracoronary infusion of streptokinase, regional pump function improves not only in the anterior, but also in the inferior wall segments.

RESULTS

In table I the hemodynamic data obtained during the first catheterization (acute) and during the follow-up study (chronic) of seven patients with unsuccessful recanalization are shown. The most prominent data are the decrease in stroke volume (SV), cardiac index (CI) and ejection fraction (EF). In table II the hemodynamic data of 14 patients with successful opening and persistent patency of the IRA are shown. Global ejection fraction increases significantly ($p < 0.006$) from 51 to 56 per cent.

Tables I and II. *Hemodynamic data of seven patients with unsuccessful and 14 patients with successful recanalization of the infarct related artery, during acute infarction (acute) and during the follow-up study (chronic).*

	Unsuccessful Recanalization n: 7 (mean \pm SD)			Successful Recanalization n: 14 (mean \pm SD)		
	acute	chronic	p value	acute	chronic	p value
HR bpm	80 \pm 17	80 \pm 19	ns	79 \pm 17	70 \pm 13	<.02
mean AoP mmHg	84 \pm 21	91 \pm 14	ns	92 \pm 14	97 \pm 14	ns
EDP	16 \pm 7	23 \pm 9	ns	22 \pm 7	22 \pm 9	ns
CI l/m ²	3.9 \pm 1.3	2.9 \pm 1.5	<.05	3.1 \pm 0.7	3.1 \pm 0.6	ns
EDV ml/m ²	99 \pm 19	97 \pm 32	ns	85 \pm 26	88 \pm 25	ns
ESV ml/m ²	50 \pm 15	63 \pm 34	ns	43 \pm 21	37 \pm 11	ns
SV ml/m ²	49 \pm 15	35 \pm 13	<.008	41 \pm 11	46 \pm 10	ns
EF %	50 \pm 12	38 \pm 15	<.003	51 \pm 10	56 \pm 9	<.006

Abbreviations: HR: heartrate, AoP: aortic pressure, EDP: left ventricular end diastolic pressure, CI: cardiac index, EDV: left ventricular end diastolic volume, ESV: left ventricular end systolic volume, SV: stroke volume, EF: ejection fraction.

Values expressed as means \pm SD; p-value. Student's t-test (paired data).

The individual CREF data assessed in the 30° RAO ventriculogram of a patient with anterior infarction, during the acute event and during the follow-up study, are shown in figure 3. A few hours after the onset of infarction regional pump function is severely depressed in the anterior and apical wall segments (segments 3-10 and 19, 20), but is only slightly affected in the inferoposterior wall (segments 11-18). Three weeks after successful recanalization regional pump function is improved in both the anterior and the inferoposterior wall segments. In figure 4 the CREF values (mean \pm standard deviation) in five wall regions of five patients with an anterior infarction during the acute event (first bar) and after an interval of 2-3 weeks (second bar) are shown. The interrupted lines represent the 10th percentile (lower) border of regional pump function in normal individuals. In particular in the anterolateral and apical wall regions

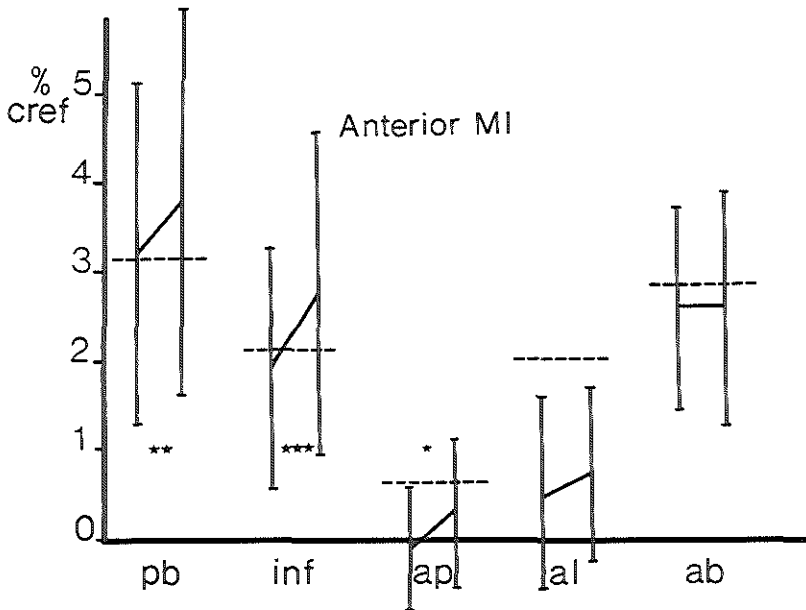


Figure 4. Mean CREF values \pm standard deviations (bars) of patients with acute anterior wall infarction, before (first bar) and 2-3 weeks after (second bar) recanalization of the left anterior descending coronary artery with a thrombolytic agent. Interrupted lines represent the 10th percentile border of CREF in normal individuals in the posterobasal (pb) inferior (inf), apical (ap), anterolateral (al), and anterobasal (ab) wall segments. Before recanalization, regional pump function is severely depressed in the anterior and apical wall segments. After recanalization a slight, but not significant improvement of pump function in the anterolateral wall and a significant improvement of pump function in the apical segments is accompanied by a significant compensatory improvement of pump function in the inferoposterior wall regions. * $p < 0.05$, ** $p < 0.01$, *** $p < 0.001$.

subnormal CREF values are observed, as would be expected in anterior infarction. Analysis with the paired t-test shows a slight, but not significant improvement of regional pump function in the anterolateral wall, and a significant ($p < 0.05$) improvement in the apical segments, which is accompanied by a significant increase of the CREF values in the inferior ($p < 0.001$) and posterobasal ($p < 0.01$) wall regions. In figure 5 the changes in regional pump function after recanalization of the right coronary artery are shown. At the time of acute inferior infarction a severe depression of pump function in the inferoposterior wall is observed, while CREF values in the anterior wall remain normal. After successful recanalization a significant ($p < 0.05$) increase of CREF is observed in the inferior wall, which is paralleled by a significant ($p < 0.05$) improvement of regional pump function in the apical segments.

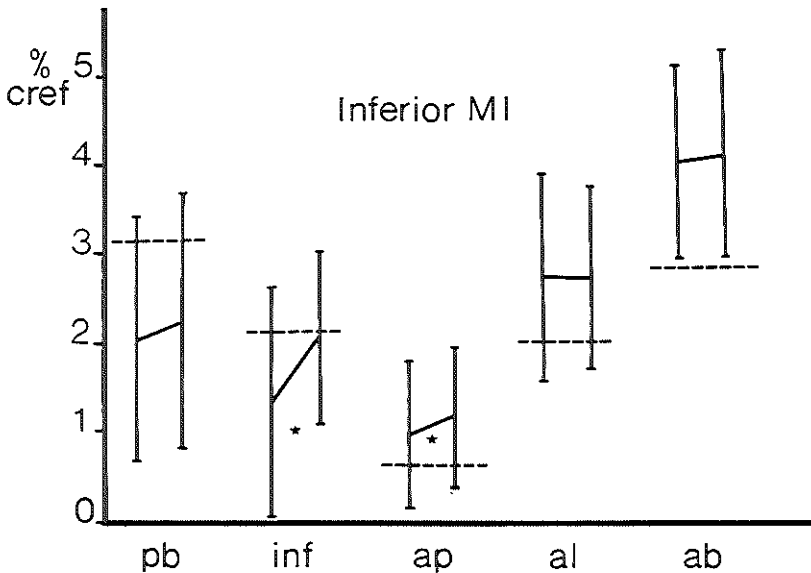


Figure 5. Mean CREF values \pm standard deviation (bars) of patients with acute inferior wall infarction, before (first bar) and 2-3 weeks after (second bar) recanalization of the right coronary artery with streptokinase. Before recanalization, regional pump function is severely depressed in the inferior and posterobasal wall and normal in the antero-apical wall segments. After recanalization a significant improvement of regional pump function in the inferior wall is accompanied by a significant improvement in the apical wall and a slight but not significant improvement in the posterobasal wall. * $p < 0.05$.

Abbreviations: see figure 4.

DISCUSSION

As shown in tables I and II, unsuccessful recanalization appears to be associated with depressed global left ventricular function, while successful recanalization and persistent patency of the IRA improves ejection fraction. This finding is in agreement with the results of similar studies by Rentrop et al. (2), Ganz et al. (5) and Mathey et al. (7). However, such improvement might be due not only to enhancement of regional function in the reperfused "infarct zone" but also by compensatory action of other wall segments. The results of this study suggest that, although some improvement of regional function in the infarct zone is observed, at least part of the increase of ejection fraction is caused by compensation of other wall regions.

However, these results must be interpreted with care, first of all because the number of patients studied is small and secondly because angiograms made during the first hours of myocardial infarction provide only one "snapshot" of

what must be a rapidly changing situation. Also, analysis of ejection fraction with conventional methods has proven to be subject to substantial variation (22), which makes any interpretation of small changes of ejection fraction in sequential angiograms a dubious affair. Computer assisted analysis of the angiograms reduces the variability significantly. In fact, with the system used in this study, intra- and inter-observer variability of repeated assessment of ejection fraction was only 1.6 - 2.3 per cent (23). Even so, variations of ejection fraction in sequential left ventriculograms may still be due to changes in pre- and after-load and in heartrate (24). While in this study no significant changes in left ventricular end diastolic pressure (EDP), volume (EDV) or mean aortic pressure (mean AoP) were observed, heartrate decreased slightly in the successfully recanalized group. It would have been interesting to perform a similar analysis of the angiograms of patients with unsuccessful recanalization. However, the heterogeneity of this small group with respect to localization of infarction and IRA's, would have made the interpretation very difficult.

These preliminary data suggest therefore, in our opinion, that improvement of ejection fraction after successful recanalization of an IRA is most likely due to some improvement (and no worsening) of regional function in the infarct zone, but must also be caused by compensatory action of other wall regions. Further study in more patients will be needed to provide a final conclusion. The data also indicate that efforts at early recanalization in appropriate patients are justified and may, in fact, lead to improved regional ventricular function.

REFERENCES

1. Chandler A.B., Chapman I., Erhardt L.R., Roberts W.C., Schwartz C.J., Sinapius D., Spain D.M., Sherry S., Ness P.M., Simon T.L., Coronary thrombosis in myocardial infarction. *Am. J. Cardiol.* 34: 823, 1974.
2. Rentrop P., Blanke H., Karsch K.R., Kaiser H., Kosterling H., Leitz K., Selective intracoronary thrombolysis in acute myocardial infarction and unstable angina pectoris. *Circulation* 63: 307, 1981.
3. DeWood M.A., Spores J., Notske R., Mouser L.T., Burroughs R., Golden M.S., Lang H.T., Prevalence of total coronary occlusion during the early hours of transmural myocardial infarction. *N. Engl. J. Med.* 303: 897, 1980.
4. Rentrop P., Blanke H., Karsch K.R., Kreuzer H., Initial experience with transluminal recanalization of the recently occluded infarct-related coronary artery in acute myocardial infarction - comparison with conventionally treated patients. *Clin. Cardiol.* 2: 92, 1979.
5. Ganz W., Buchbinder N., Marcus H., Mondkar A., Maddahi J., Charuzi Y., O'Connor L., Shell W., Fishbein M.C., Kass R., Miyamoto A., Swan H.J.C., Intracoronary thrombolysis in evolving myocardial infarction. *Am. Heart J.* 101: 4, 1981.
6. Leinbach R.C., Gold H.K., Regional streptokinase in myocardial infarction. *Circulation* 63: 498, 1981.
7. Mathey D.G., Kuck K-H., Tilsner V., Krebber H-J., Bleifeld W., Nonsurgical coronary artery recanalization in acute transmural myocardial infarction. *Circulation* 63: 489, 1981.

8. Maroko P.R., Braunwald E., Covell J.W., Ross J. Jr., Factors influencing the severity of myocardial ischemia following experimental coronary occlusion. *Circulation* 39 & 40: Suppl. 3: III-140. abstract, 1969.
9. Hillis L.D., Braunwald E., Myocardial ischemia. *N. Engl. J. Med.* 296: 971, 1034, 1093, 1977.
10. Kloner R.A., Braunwald E., Observations on experimental myocardial ischaemia. *Cardiovasc. Res.* 14: 371, 1980.
11. Reimer K.A., Lowe J.E., Rasmussen M.M., Jennings R.B., The wavefront phenomenon of ischemic cell death. 1. Myocardial infarct size vs. duration of coronary occlusion in dogs. *Circulation* 56: 786, 1977.
12. Baughman K.L., Maroko P.R., Vatner S.F., Effects of coronary artery reperfusion on myocardial infarct size and survival in conscious dogs. *Circulation* 63: 317, 1981.
13. Brand M. van den, Smissen H. van der, Serruys P.W., Hooghoudt T., Potential risks of intracoronary streptokinase during acute myocardial infarction. *Circulation* 64: Suppl. IV, 246. abstract, 1981.
14. Bresnahan G.F., Roberts R., Shell W.E., Ross J. Jr., Sobel B.E., Deleterious effects due to hemorrhage after myocardial reperfusion. *Am. J. Cardiol.* 33: 82, 1974.
15. Muller J.E., Stone P.H., Markis J.E., Braunwald E., Let's not let the genie escape from the bottle – again. *N. Engl. J. Med.* 304: 1294, 1981.
16. Rentrop P., Blanke H., Karsch K.R., Salvage of jeopardized myocardium by non-surgical reperfusion (NSR) in man. Abstracts of the 30th annual scientific session of the American College of Cardiology, San Francisco, California. *Am. J. Cardiol.*: 47, 493, 1981.
17. Sones F.M. Cine coronary angiography. *Mod. Concepts Cardiovasc. Dis.* 31: 735, 1962.
18. Judkins M.P., Selective coronary arteriography. Part I. A percutaneous transfemoral technique. *Radiology* 89: 815, 1967.
19. Slager C.J., Reiber J.H.C., Schuurbiers J.C.H., Meester G.T., Contouromat – A hard-wired left ventricular angio processing system. I. Design and application. *Comp. Bio-med. Res.* 11: 491, 1978.
20. Slager C.J., Hooghoudt T.E.H., Reiber J.H.C., Schuurbiers J.C.H., Booman F., Meester G.T., Left ventricular contour segmentation from anatomical landmark trajectories and its application to wall motion analysis. *Computers in Cardiology*, p. 347, IEEE Computer Society, 1979.
21. Hooghoudt T.E.H., Slager C.J., Reiber J.H.C., Serruys P.W., Schuurbiers J.C.H., Meester G.T., Regional contribution to global ejection fraction used to assess the applicability of a new wall motion model to the detection of regional wall motion in patients with asynergy. *Computers in Cardiology*, p. 253, IEEE Computer Society, 1980.
22. Cohn P.F., Levine J.A., Bergeron G.A., Gorlin R., Reproducibility of angiographic left ventricular ejection fraction in patients with coronary artery disease. *Am. Heart J.* 88: 713, 1974.
23. Hooghoudt T.E.H., Slager C.J., Reiber J.H.C., Brower R.W., Castellanos S., Zorn I.C.J., Hugenholtz P.G., Observer variability in the visual assessment of regional wall motion and in computer assisted analysis of regional left ventricular function. This thesis pp. 98-110.
24. Yang S.S., Bentivoglio L.G., Maranhao V., Goldberg H. eds. From cardiac catheterization data to hemodynamic parameters. F.A. Davis Company, Philadelphia, Pennsylvania, pg 264, 1978.

CURRICULUM VITAE

Ton Eric Hilco Hooghoudt was born at the 17th of Februari 1948 in Amsterdam. In 1966 he graduated at the Montessorilyceum in Rotterdam (gymnasium- α). In the same year he started his medical study at the just founded Medical Faculty in Rotterdam. During his medical study he was appointed at the Audio-visual Department of the Erasmus University, where he made a film on the immunological problems of organ transplantation. In 1972 he became a trainee of internal medicine at the St. Franciscus Gasthuis in Rotterdam. In 1977 he joined the Erasmus University to train in cardiology. His main interest is in invasive cardiology, with emphasis on the search for clinically useful parameters of regional left ventricular function. This thesis has been performed at the cardiac catheterization laboratory and the department of experimental hemodynamics of the Thoraxcenter, under supervision of Prof. P.G. Hugenholtz.

